

Master's Thesis  
석사 학위논문

A Design Method of Robust PID Control by Using  
Backstepping Control with Time Delay  
Estimation and Nonlinear Damping

Junyoung Lee (이 준 영 李 俊 榮)

Department of  
Robotics Engineering

**DGIST**

2013



Master's Thesis  
석사 학위논문

A Design Method of Robust PID Control by Using  
Backstepping Control with Time Delay  
Estimation and Nonlinear Damping

Junyoung Lee (이 준 영 李俊榮)

Department of  
Robotics Engineering

**DGIST**

2013



# A Design Method of Robust PID Control by Using Backstepping Control with Time Delay Estimation and Nonlinear Damping

Advisor : Professor Pyung Hun Chang

Co-advisor : Professor Jeon Il Moon

By

Jun Young Lee

Department of Robotics Engineering

DGIST

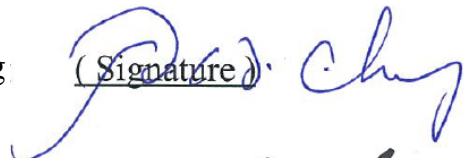
A thesis submitted to the faculty of DGIST in partial fulfillment of the requirements for the degree of Master of Science in the Department of Robotics Engineering. The study was conducted in accordance with Code of Research Ethics<sup>1</sup>

01. 04. 2013

Approved by

Professor Pyung Hun Chang  
(Advisor)

(Signature)



Professor Jeon Il Moon  
(Co-Advisor)

(Signature)



---

<sup>1</sup> Declaration of Ethical Conduct in Research: I, as a graduate student of DGIST, hereby declare that I have not committed any acts that may damage the credibility of my research. These include, but are not limited to: falsification, thesis written by someone else, distortion of research findings or plagiarism. I affirm that my thesis contains honest conclusions based on my own careful research under the guidance of my thesis advisor.



# A Design Method of Robust PID Control by Using Backstepping Control with Time Delay Estimation and Nonlinear Damping

Jun Young Lee

Accepted in partial fulfillment of the requirements for the degree of Master of  
Science.

12. 03. 2012

Head of Committee    Prof. Pyung Hun Chang



Committee Member    Prof. Jeon Il Moon



Committee Member    Prof. Jae Sung Hong







MS/RT  
201122004

이 준 영. Junyoung Lee. A Design Method of Robust PID Control by Using Backstepping Control with Time Delay Estimation and Nonlinear Damping. Department of Robotics Engineering. 2013. 81p. Advisors Prof. Chang, Pyung Hun, Co-Advisors Prof. Moon, Jeon Il.

## **ABSTRACT**

This thesis presents a design method of robust Proportional-integral-derivative (PID) control by using backstepping control with time delay estimation (TDE) and nonlinear damping. PID controllers are widely used as feedback control in many industrial control system fields. The structure of a PID control is simple and consists of three terms that include a proportional gain, an integral gain and a differential gain. The control makes its desired output by assigning PID gains that are required to control systems precisely after calculating the error between the desired input and output of systems.

Gains of PID control have definite physical meaning. If these gains are tuned carefully, acceptable performance can be obtained since steady-state error and transient response are improved simultaneously. To select PID gains, many previous studies investigated methods of tuning PID control gains to get good performance. Methods of tuning gains are selected on the analytical basis of closed-loop stability and performance. Since PID controllers are linear models and many studies deal with linear plants, it is very difficult to select PID gains for nonlinear plants. Although many previous studies have been conducted such

as Fuzzy control and optimal control, the methods proposed in these studies are very difficult and theoretically complex. As a result, PID gains are usually tuned heuristically.

A systematic method was proposed by Chang et al. to select gains of robust PID control for nonlinear plants by using second-order controller canonical forms in discrete PID controllers from the viewpoint of a sampled-data system. In that study, although the plant model was unknown, the method was enabled to determine robust PID gains by using time delay control (TDC) when the plant has second-order controller canonical form and when TDC and PID controls are conducted in discrete time domain. Due to the equivalence to TDC, the gains of PID control were determined.

TDC is a simple and effective technique for estimating system nonlinearities and uncertainties. This method uses the time delayed signal of system variables to estimate uncertainties of a system. While TDC has the advantage of requiring no prior knowledge of the system model, it also has the disadvantage of time delay estimation (TDE) error due to hard nonlinearities. It degrades the system stability and performance.

When PID gains are tuned by using TDC with a system that has hard nonlinearities, system stability and performance cannot be guaranteed. To overcome TDE error and guarantee the stability of a system, backstepping control with TDE and nonlinear damping was proposed.

Based on this method, in this paper, the equivalent relationship between PID control and backstepping

control with TDE, nonlinear damping will be presented to select PID gains efficiently. While general PID controllers have constant gains, the proposed PID controller has variable PID gains due to nonlinear damping that uses the feedback state. In addition, the gains of the proposed PID control will be analyzed to identify the characteristics of the purposed controller. Since the proposed PID control uses the equivalent control method by backstepping control with TDE and nonlinear damping, it has the enhanced control performance and stability with respect to the difficulties presented above.

**Keywords:** PID control, backstepping control, nonlinear damping, time delay estimation (TDE)



# Contents

Abstract .....	i
Contents .....	v
List of Tables .....	vii
List of Figures .....	viii
<b>I . INTRODUCTION</b>	
1.1 Motivations and objects.....	1
1.2 Dissertation structure.....	4
<b>II . Preliminaries</b>	
2.1 Target System and Control Objective .....	5
2.2 Preliminaries.....	6
2.2.1 Backstepping control.....	6
2.2.2 Time Delay Estimation (TDE) .....	7
2.2.3 Nonlinear damping .....	9
2.3 Backstepping control with TDE , nonlinear damping .....	11
2.3.1 Outline.....	11
2.3.2 Control design .....	12
2.3.3 Stability analysis .....	16
<b>III. The Design of Variable PID Control and Overviews</b>	
3.1 Introduction .....	21
3.2 The design of variable PID control.....	22
3.2.1 PID control in the discrete time domain.....	22
3.2.2 Backstepping control with TDE, nonlinear damping in discrete time domain ..	24
3.2.3 The Relationship between PID control with Backstepping control with TDE, nonlinear damping in discrete time domain.....	25
3.2.4. A constant dc-bias vector $\mathbf{u}_{DC}$ .....	27
3.3 Consideration of variable structure PID control .....	28
3.4 Comparison with the previous study .....	30
3.5 Simple method to design proposed PID control by the previous study.....	32
3.6 Conclusion.....	33

<b>IV. Simulation</b>	
4.1 Introduction	34
4.2 One-link robot manipulator	34
4.2.1 Simulation setup	34
4.2.2 Design of controllers	36
4.2.3 Simulation results	37
4.3. Two-link robot manipulator	43
4.3.1 Simulation setup	43
4.3.2 Design of controllers	45
4.3.3 Simulation results	47
4.4. Conclusion	58
<b>V. Experiment</b>	
5.1 Introduction	59
5.2 Experiment	59
5.2.1 Experimental setup	59
5.2.2 Design of controllers	61
5.2.3 Experimental results	64
5.3 Conclusion	77
<b>VI. Conclusion</b>	78

## List of Tables

3.1 Variation of PID gains .....	30
----------------------------------	----

## List of Figures

2.1 Black diagram of the backstepping control with TDE and nonlinear damping.....	15
3.1 Sequence of $\mathbf{x}_{(k)}$ and $\mathbf{u}_{(k)}$ .....	23
4.1 One-link manipulator .....	34
4.2 (a)Position trajectories and (b) Position errors by backstepping control with TDE, nonlinear damping and the proposed PID control .....	39
4.3 (a) Control inputs and (b) Difference of control inputs by backstepping control with TDE, nonlinear damping and the proposed PID control .....	40
4.4 (a) Gain $\mathbf{K}$ , (b) Gain $\mathbf{T}_I$ , and (c) Gain $\mathbf{T}_D$ of the proposed PID control .....	41
4.5 (a) Nonlinear damping component: $w$ , (b) Bounding Function: $\hat{F}$ (c) $ \hat{F} $ : $\rho$ , and (d) $ \dot{\alpha} $ : $\beta$ .....	42
4.6 Two-link manipulator.....	43
4.7 The desired trajectory of Joints .....	45
4.8 (a) Position trajectory of Joint 1, (b) Position trajectory of Joint 2, (c) Position error of Joint 1, and (d) Position error of Joint 2 by backstepping control with TDE, nonlinear damping and the proposed PID control.....	50
4.9 (a), (b) Control inputs, (c), (d) Control input difference of each joint by backstepping control with TDE, nonlinear damping and the proposed PID control .....	51
4.10 (a), (b) Gain $\mathbf{K}$ , (c), (d) Gain $\mathbf{T}_I$ , and (e), (f) Gain $\mathbf{T}_D$ of the proposed PID control .....	52
4.11 (a), (b) Gain $\mathbf{K}$ , (c), (d) Gain $\mathbf{T}_I$ , and (e), (f) Gain $\mathbf{T}_D$ of the proposed PID control without nonlinear damping .....	53
4.12 (a) Position trajectory of Joint 1, (b) Position trajectory of Joint 2, (c) Position errors of Joint 1, and (d) Position errors of Joint 2 by TDC and PID control without nonlinear damping .....	54
4.13 (a) Control inputs of Joint 1, (b) Control inputs of Joint 2, (c) Control input difference of Joint 1, and (d) Control input difference of Joint 2 by TDC and PID control without nonlinear damping .....	55
4.14 (a) Position trajectory of Joint 1, (b) Position trajectory of Joint 2, (c) Position errors of Joint 1, and (d)Position errors of Joint 2 by the proposed PID control (PID1) and the previous PID control (PID2) .....	56
4.15 (a) Control inputs of Joint 1, (b) Control inputs of Joint 2, (c) Control input difference of Joint 1, and (d) Control input difference of Joint 2 by the proposed PID control (PID1) and the previous PID control (PID2) .....	57
5.1 The 6 DOF PUMA robot (Samsung Faraman – AT2).....	60



5.2 The desired trajectory of Joints 1, 2, and 3.....	60
5.3 (a) Position trajectories of Joint 1, (b) Position errors of Joint 2, (c) Position trajectories of Joint 2, (d) Position errors of Joint 2, (e) Position trajectories of Joint 3, and (f) Position errors of Joint 3 by backstepping control with TDE, nonlinear damping and the proposed PID control .....	68
5.4 (a) Control inputs of Joint 1, (b) Control input difference of Joint 1, (c) Control inputs of Joint 2, (d) Control input difference of Joint 2, (e) Control inputs of Joint 3, and (f) Control input difference of Joint 2 by backstepping control with TDE, nonlinear damping and the proposed PID control in Time domain.....	69
5.5(a) Control inputs of Joint 1, (b) Control input difference of Joint 1, (c) Control inputs of Joint 2, (d) Control input difference of Joint 2, (e) Control inputs of Joint 3, and (f) Control input difference of Joint 2 by backstepping control with TDE, nonlinear damping and the proposed PID control in Frequency domain .....	70
5.6(a),(b), and (c) Gain $\mathbf{K}$ , (d),(e), and (f) Gain $\mathbf{T}_I$ , and (g), (h), and (i) Gain $\mathbf{T}_D$ of PID control .....	71
5.7(a), (b), and (c) $\hat{\mathbf{F}}$ , (d), (e), and (f) $\boldsymbol{\beta}$ , (g), (h), and (i) $\boldsymbol{\rho}$ , and (j), (k), and (l) $\mathbf{w}$ of the proposed PID control .....	72
5.8(a),(b), and (c) Gain $\mathbf{K}$ , (d),(e), and (f) Gain $\mathbf{T}_I$ , and (g), (h), and (i) Gain $\mathbf{T}_D$ of PID control without nonlinear damping .....	73
5.9(a) Position trajectories of Joint 1, (b) Position errors of Joint 2, (c) Position trajectories of Joint 2, (d) Position errors of Joint 2, (e) Position trajectories of Joint 3, and (f) Position errors of Joint 3 by TDC and the proposed PID control without nonlinear damping.....	74
5.10a) Control inputs of Joint 1, (b) Control input difference of Joint 1, (c) Control inputs of Joint 2, (d) Control input difference of Joint 2, (e) Control inputs of Joint 3, and (f) Control input difference of Joint 2 by TDC and PID control without nonlinear damping .....	75
5.11(a),(d), and (g) Position trajectories of Joint 1,2, and 3, (b), (e), and (h) Position errors of Joint 1, 2, and 3, (c), (f), and (i) Control inputs of Joint 1,2, and 3 by the proposed PID control (PID1) and the previous PID control (PID2) .....	76



# Chapter 1. Introduction

## 1.1 Motivations and objects

PID (Proportional-Integral-Derivation) control is widely used as feedback control in many industrial control system fields. A PID controller consists of three terms that include a proportional gain, an integral gain and a differential gain. The controller makes the desired output by assigning PID gains that are required to control systems precisely after it calculates the error between the desired input and output of systems [1].

PID controllers have simple structures and are easy to apply to general systems. In addition, the gains of PID control have definite physical meaning [4]. If these gains are well tuned, the desired performance can be obtained although there are nonlinear plants such as robot manipulators. But, in practice, tuning the gains is difficult due to problems such as stability of closed-loop systems and coupled gains with respect to system performance. That is, applying PID control to nonlinear systems is difficult. For example, if the number of joints is three in a robot manipulator, it is required to select nine gains since three gains are assigned to one joint. Since these gains are coupled each other and stability analysis is complicated, gain selection is very difficult.

There are many previous studies of tuning gains of PID control to get good response. For example, the Ziegler-

Nichols method is very well known in this field. Although this method is simple and easy to tune PID gains, its performance is insufficient in nonlinear systems. In general, while studies show good performance in linear systems [22], they have degraded performance in nonlinear systems. Thus, it is difficult to select PID gains for nonlinear plants [2], [3]. Although many previous studies have been implemented to select PID gains for nonlinear plants such as Fuzzy control [23]-[25] and optimal control [26]-[28], PID gains are usually tuned heuristically because the methods proposed in these studies are difficult and theoretically complex [4].

A systematic method was proposed by Chang et al. to select gains of robust PID control for nonlinear plants by using second-order controller canonical forms in discrete PID controllers from the viewpoint of a sampled-data system [4]. In that study, although the plant model was unknown, the method was enabled to determine robust PID gains by using time delay control (TDC) when the plant has second-order controller canonical form and when TDC and PID controls are conducted in discrete time domain [4]. Due to the equivalence to TDC, the gains of PID control were determined.

TDC is a simple and effective technique for estimating system nonlinearities and uncertainties [5], [29]. This method uses the time delayed signal of system variables to estimate uncertainties of the current system. While TDC has the advantage of requiring no prior knowledge of the system model, it also has the disadvantage of time delay estimation (TDE) error due to hard nonlinearities such as the Stiction and Coulomb friction. It

degrades the system stability and performance [5]. When PID gains are tuned by using TDC in the systems that have hard nonlinearities, system stability and performance cannot be guaranteed.

Many previous studies have investigated the disadvantages of TDE error. These studies concentrate on performance improvement by reducing TDE error. TDC with Sliding Mode Control [8], TDC with Internal Model Control [9] and TDC with ideal velocity feedback [10] were conducted by using an additional element in control input. However, an additional stability analysis of these controllers for nonlinear systems is required.

Backstepping control with TDE and nonlinear damping was introduced [7]. In this controller, TDE estimates system nonlinearity and uncertainty and, nonlinear damping guarantees the closed-loop stability by using the bounding functions. The advantage of this control is to make stability condition based on Lyapunov functions.

Based on this method, this paper presents, the equivalent relationship between PID control and backstepping control with TDE, nonlinear damping to consider selection of PID gains efficiently. Then, a PID control that is derived from equivalent relationship is satisfied with stability conditions since it has same properties of backstepping control with TDE, nonlinear damping.

The proposed PID control becomes a variable PID control due to nonlinear damping. Nonlinear damping uses the feedback state and, so changes according to time. In the industrial control, a PID control with constant gains is generally selected. Those controllers seldom meet desired performance criteria since system parameters

change when unknown disturbance or/and dynamics occur in the systems. For this reason, many studies have been conducted to tune PID gains automatically such as adaptive PID control method. In this process, there are some difficulties such as unknown disturbances, unmodeled dynamics and stability analysis. Since the proposed PID control is the equivalent control method by backstepping control with TDE and nonlinear damping [7], it has enhanced control performance and stability with respect to the difficulties presented above.

## **1.2 Dissertation structure**

Chapter 2 will describe the preliminaries needed to do this study including backstepping control, time delay estimation (TDE), nonlinear damping and introduce applicable systems. Chapter 3 will represent the design method of variable PID control by using backstepping control with TDE, nonlinear damping. After equivalence is derived from the relationship between variable PID control and backstepping control with TDE, nonlinear damping in discrete time domain, gains of variable PID control will be analyzed in the aspects of patterns and the range of gains. Chapters 4 and 5 will present simulation and experimentation to prove the proposed theory. Finally, Chapter 6 will summarize the findings of the paper.

# Chapter 2. Preliminaries

## 2.1 Target System and Control Objective

The target system is n-DOF nonlinear uncertain system as follows:

$$\dot{\mathbf{x}} = \mathbf{f}(\mathbf{x}, \dot{\mathbf{x}}) + \mathbf{G}(\mathbf{x})\mathbf{u} \quad (2.1)$$

where  $\mathbf{x} \in \mathfrak{R}^n$  and  $\dot{\mathbf{x}} \in \mathfrak{R}^n$  denote the state vectors of the system.  $\mathbf{u} \in \mathfrak{R}^n$  stands for the control input.

$\mathbf{f}(\mathbf{x}, \dot{\mathbf{x}}) \in \mathfrak{R}^n$  represents nonlinear function that includes uncertainty and disturbance.  $\mathbf{G}(\mathbf{x}) \in \mathfrak{R}^{n \times n}$

denotes the input matrix. The target system is represented as strict-feedback form. General physical systems

can be denoted as this form such as robot manipulator [11].

To design backstepping control with TDE and nonlinear damping, it is assumed that system (2.1) is satisfied

with the following assumptions [7]:

**Assumption 1.**  $\mathbf{G}(\mathbf{x})$  is positive-definite, and  $\|\mathbf{G}(\mathbf{x})\|$  is bounded such that

$$0 < G_a \leq \|\mathbf{G}(\mathbf{x})\| < G_b \quad (2.2)$$

where  $G_a$  and  $G_b$  are positive constants.

**Assumption 2.** There exist a finite positive, but not necessarily known constant  $N_f$  and a known positive-definite diagonal matrix function  $\hat{\mathbf{F}}(\mathbf{x}, \dot{\mathbf{x}}) \in \mathfrak{R}^{n \times n}$  such that the following inequalities hold for all  $(\mathbf{x}, \dot{\mathbf{x}})$  in the domain of interest:

$$\frac{|f_i|}{\hat{F}_i} \leq N_f \quad (2.3)$$

where  $1 \leq i \leq n, i \in N$ ;  $f_i$  denotes the  $i^{th}$  diagonal element of  $\mathbf{f}(\mathbf{x}, \dot{\mathbf{x}})$  and  $\hat{F}_i$  denotes the  $i^{th}$  diagonal element of  $\hat{\mathbf{F}}(\mathbf{x}, \dot{\mathbf{x}})$ . The bounding function  $\hat{\mathbf{F}}(\mathbf{x}, \dot{\mathbf{x}})$  will be used to construct nonlinear damping terms [12][13].

In this research, the control object is to track the known desired trajectory  $\mathbf{x}_d, \dot{\mathbf{x}}_d, \ddot{\mathbf{x}}_d \in \mathfrak{R}^n$  by using equivalent PID control that corresponds to backstepping control with TDE and nonlinear damping.

## 2.2 Preliminaries

### 2.2.1 Backstepping control

Backstepping method is a powerful way to control nonlinear systems [14]. The theory of backstepping control concentrates on guaranteeing the boundedness of state variables by stabilizing the system as well as tracking the reference input on the output of a system.

Backstepping control has a recursive procedure. Using this method, after the entire system is divided into each subsystem that is desired, each subsystem is designed as a top-down process. In addition, backstepping control



is based on Lyapunov functions. As Lyapunov functions are the method that prove the stability of systems, it is automatically made in the design process of backstepping control. Considering backstepping control with Lyapunov functions about the design of feedback control, control law is designed and satisfied with stability of the nonlinear system. Furthermore, nonlinear terms that are useful for a system are used in the design process of backstepping control.

### 2.2.2. Time delay estimation

Consider the following nonlinear differential equation [15].

$$\dot{\mathbf{x}} = \mathbf{f}(\mathbf{x}, t) + \mathbf{G}(\mathbf{x}, t)\mathbf{u} + \mathbf{d}(t) \quad (2.4)$$

where  $\mathbf{x} \in \mathfrak{R}^n$  denotes state vectors of the system.  $\mathbf{u} \in \mathfrak{R}^n$  stands for the input vector.  $\mathbf{f}(\mathbf{x}, t) \in \mathfrak{R}^n$  represents nonlinear function in companion form, which represents the plant dynamics and may be unknown yet bounded.  $\mathbf{G}(\mathbf{x}, t) \in \mathfrak{R}^{n \times r}$  denotes control distribution matrix, the range of which should be known.  $\mathbf{d}(t) \in \mathfrak{R}^n$  is unknown disturbances.

It is assumed that the states and their derivatives are measurable in this system. Introducing in (2.4) a constant matrix  $\widehat{\mathbf{G}}$  representing the known range of  $\mathbf{G}(\mathbf{x}, t)$ , (2.4) can be rearranged into the following equation :

$$\begin{aligned}
\dot{\mathbf{x}} &= \mathbf{f}(\mathbf{x}, t) + \mathbf{G}(\mathbf{x}, t)\mathbf{u} + \mathbf{d}(t) \\
&= \widehat{\mathbf{G}}\mathbf{u} + [\mathbf{f}(\mathbf{x}, t) + \{\mathbf{G}(\mathbf{x}, t) - \widehat{\mathbf{G}}\}\mathbf{u} + \mathbf{d}(t)] \\
&= \widehat{\mathbf{G}}\mathbf{u} + \mathbf{H}(t)
\end{aligned} \tag{2.5}$$

where  $\mathbf{H}(t)$  denotes the total uncertainty including the uncertainties in the plant and unknown disturbances, and is represented as

$$\mathbf{H}(t) = \mathbf{f}(\mathbf{x}, t) + \{\mathbf{G}(\mathbf{x}, t) - \widehat{\mathbf{G}}\}\mathbf{u} + \mathbf{d}(t) \tag{2.6}$$

The problem is to estimate the total uncertainty  $\mathbf{H}(t)$  of the system [5]. First, consider a sufficiently small time delay  $L$ .  $\mathbf{H}(t-L)$  can be used to estimate  $\mathbf{H}(t)$  by using the information of control input and state variables in former time. It means information of an accurate model is not required. If time delay  $L$  is very small, the following equation is denoted as

$$\mathbf{H}(t) \approx \mathbf{H}(t-L) = \widehat{\mathbf{H}}(t) = \dot{\mathbf{x}}(t-L) - \widehat{\mathbf{G}}\mathbf{u}(t-L) \tag{2.7}$$

This is referred to as time delay estimation [5] [29].

The robustness of control is decided by accuracy of estimating  $\mathbf{H}(t)$ . Effectiveness of time delay estimation (TDE) is affected by the time delay  $L$ . The time delay  $L$  needs to be selected such that the continuity assumption of  $\mathbf{H}(t)$  may be valid. That is, the time delay  $L$  must have faster bandwidth than bandwidth of disturbances and nonlinear dynamics of the system. In practice, the smallest achievable  $L$  is the sampling period in digital

implementation.

### 2.2.3 Nonlinear damping

Nonlinear damping is nonlinear design tool based on Lyapunov functions and a technique that guarantees the boundedness of trajectories when even no upper bound on the uncertainty is known [16]. Through an example from [16], we will show how it can be used to achieve stabilization [17].

Consider the scalar system

$$\dot{x} = x^4 + x^2 + x\delta_0(t) + u, \quad (2.8)$$

where  $\delta_0(t)$  is a bounded function with respect to time  $t$ , which is an unknown disturbance and  $u$  denotes the control input of the scalar system. It is assumed that  $\delta_0$  is uniformly bounded for all  $(t, x, u)$ . Although no upper bound on the term  $x\delta_0(t)$  in the above dynamics is known, the control component  $v(t)$  is designed as ensuring the boundedness of the trajectories of the closed-loop system.

The control input is designed as

$$u = \phi(x) + v(x), \quad (2.9)$$

where  $\phi(x)$  denotes the nominal stabilizing feedback control law and  $v(x)$  is the nonlinear damping component.

Considering the scalar system (2.8),  $\phi(x)$  and  $v(x)$  are designed as

$$\phi(x) = -x^4 - x^2 - x, \quad (2.10)$$

$$v(x) = -x^3 \quad (2.11)$$

With the control input designed above, the closed-loop dynamics can be obtained as

$$\begin{aligned} \dot{x} &= x^4 + x^2 + \phi + v + x\delta_0(t) \\ &= -x - x^3 + x\delta_0(t) \end{aligned} \quad (2.12)$$

Define the Lyapunov function as  $V(x) = \frac{1}{2}x^2$ , the derivative of  $V(x)$  is represented as

$$\begin{aligned} \dot{V} &= x\dot{x} \\ &= -x^2 - x^4 + x^2\delta_0 \\ &= -x^2 - x^2(x^2 - \delta_0). \end{aligned} \quad (2.13)$$

where  $\dot{V}$  is negative for any nonzero  $x$  satisfying  $x^2 > \delta_0$ .

That is, the above closed-loop dynamics has a bounded solution regardless of how large the bounded disturbance  $\delta_0$  is, due to the nonlinear damping term  $-x^3$ .

The design method of nonlinear damping is explained through the above example. Note that the design of nonlinear damping is not unique. For instance, if the nonlinear damping term is designed as  $-x^5$  or  $-x^7$ , the closed-loop system also can be stabilized. It means the design of nonlinear damping is flexible.

## 2.3 Backstepping control with Time delay estimation (TDE) , nonlinear damping

### 2.3.1 Outline

The general backstepping control method requires an accurate system model when the control input is designed. In the case of systems with uncertainties that include disturbances, modeling error except parameter uncertainties, backstepping control cannot be applied. Backstepping control using time delay estimation (TDE) was proposed to compensate for the above problems [21]. However, this control method is still subjected to TDE error. Applied TDE in the system, a sampling time  $L$  should be assumed as a very small value, but it is impossible in the case of a real system. Also, an estimated  $\hat{\mathbf{H}}(t)$  cannot estimate real  $\mathbf{H}(t)$  when there are hard nonlinearities in the system. This phenomenon is called TDE error.

Backstepping control with TDE and nonlinear damping was proposed [7]. The design of this method solved the above problems. Adding nonlinear damping [6] in backstepping control using TDE, two strong points were discovered. First, the closed-loop stability is guaranteed although there are time delayed terms and system uncertainties and nonlinearities. Second, the control performance is enhanced by dissipating the disturbing energy.

### 2.3.2 The controller design

Consider the target system

$$\ddot{\mathbf{x}} = \mathbf{f}(\mathbf{x}, \dot{\mathbf{x}}) + \mathbf{G}(\mathbf{x})\mathbf{u} \quad (2.14)$$

It is represented as second order dynamics of the state vector  $\mathbf{x}$ . According to backstepping method, the design of backstepping control with TDE, nonlinear damping is made up of two steps [7], [21]. In the first step, the whole system is divided into two subsystems. Each subsystem is expressed as a first-order state equation such as (2.15). Then, state vectors are used to make the tracking error. In addition, a state feedback control is designed for the subsystem 1. In the second step, TDE is used to estimate the system uncertainties and nonlinearities in the subsystem 2 and nonlinear damping term is applied to ensure the closed-loop stability [7].

#### Step one

Define  $\mathbf{x}_1 = \mathbf{x}$  and  $\mathbf{x}_2 = \dot{\mathbf{x}}$ , Then, the target system (2.14) can be transformed as

$$\begin{cases} \dot{\mathbf{x}}_1 = \mathbf{x}_2 \\ \dot{\mathbf{x}}_2 = \mathbf{f}(\mathbf{x}_1, \mathbf{x}_2) + \mathbf{G}(\mathbf{x}_1)\mathbf{u} \end{cases} \quad (2.15)$$

Define error vectors as

$$\begin{cases} \mathbf{z}_1 = \mathbf{x}_1 - \mathbf{x}_d \\ \mathbf{z}_2 = \mathbf{x}_2 - \boldsymbol{\alpha} \end{cases} \quad (2.16)$$

where  $\boldsymbol{\alpha}$  is a virtual input to stabilize the subsystem 1. Using (2.15), (2.16), subsystems are derived as

$$\begin{cases} \dot{\mathbf{z}}_1 = \mathbf{z}_2 + \boldsymbol{\alpha} - \dot{\mathbf{x}}_d & \text{(subsystem 1)} \\ \dot{\mathbf{z}}_2 = \mathbf{f}(\mathbf{x}_1, \mathbf{x}_2) + \mathbf{G}(\mathbf{x}_1)\mathbf{u} - \dot{\boldsymbol{\alpha}} & \text{(subsystem 2)} \end{cases} \quad (2.17)$$

The virtual input  $\boldsymbol{\alpha}$  is designed by a Lyapunov function as

$$\boldsymbol{\alpha} = \dot{\mathbf{x}}_d - \mathbf{c}_1 \mathbf{z}_1 \quad (2.18)$$

where  $\mathbf{c}_1 \in \mathfrak{R}^{n \times n}$  is a positive-definite diagonal gain matrix. The subsystem 1 is reformulated by using virtual input  $\boldsymbol{\alpha}$  as

$$\dot{\mathbf{z}}_1 = \mathbf{z}_2 - \mathbf{c}_1 \mathbf{z}_1 \quad (2.19)$$

Note that  $\mathbf{z}_2$  can be treated as the input forcing function of subsystem 1. It will be shown in a part of stability analysis.

### Step two

Let us reformulate subsystem 2 as

$$\mathbf{u} = \mathbf{G}^{-1}[\dot{\mathbf{z}}_2 - \mathbf{f} + \dot{\boldsymbol{\alpha}}] \quad (2.20)$$

where the function variables are omitted for simplicity.

To apply time delay estimation, let us define a positive-definite diagonal gain matrix,  $\bar{\mathbf{G}} \in \mathfrak{R}^{n \times n}$ . (2.20) is reformulated as

$$\mathbf{u} = \bar{\mathbf{G}}^{-1} \dot{\mathbf{z}}_2 + \mathbf{H} \quad (2.21)$$

where  $\mathbf{H} = (\mathbf{G}(\mathbf{x}_1)^{-1} - \bar{\mathbf{G}}^{-1}) \dot{\mathbf{z}}_2 + \mathbf{G}(\mathbf{x}_1)^{-1}(-\mathbf{f}(\mathbf{x}_1, \mathbf{x}_2) + \dot{\boldsymbol{\alpha}})$ . It includes all uncertainties and nonlinearities of the system.

(2.21) is denoted with respect to time  $t$  and reformulated in terms of  $\mathbf{H}$  as

$$\mathbf{H}_{(t)} = \mathbf{u}_{(t)} - \bar{\mathbf{G}}^{-1} \dot{\mathbf{z}}_{2(t)} \quad (2.22)$$

It is used to form the estimated  $\mathbf{H}_{(t)}$ .  $\hat{\mathbf{H}}$  is defined as the estimated  $\mathbf{H}_{(t)}$  and defined as

$$\hat{\mathbf{H}} \triangleq \mathbf{H}_{(t-L)} \quad (2.23)$$

where  $L$  denotes a constant time delay. Normally,  $L$  is expressed to the sampling time and is a sufficient small.

Then,  $\mathbf{H}_{(t-L)}$  means the value of  $\mathbf{H}_{(t)}$  in the former sampling time.

Thus, it is achieved as

$$\mathbf{u}_{\text{TDE}} = \hat{\mathbf{H}} = \mathbf{H}_{(t-L)} = \mathbf{u}_{(t-L)} - \bar{\mathbf{G}}^{-1} \dot{\mathbf{z}}_{2(t-L)} \quad (2.24)$$

To compensate TDE error called the estimation error ( $\hat{\mathbf{H}} - \mathbf{H}_{(t)}$ ), the nonlinear damping is applied in the

control input and the nonlinear damping is designed as

$$\begin{aligned} \mathbf{u}_{\text{ND}} &= -\bar{\mathbf{G}}^{-1} \mathbf{k} \mathbf{w} \mathbf{z}_{2(t)} \\ &= -\bar{\mathbf{G}}^{-1} \mathbf{k} (\hat{\mathbf{F}} + \boldsymbol{\beta} + \boldsymbol{\rho}) \mathbf{z}_{2(t)} \end{aligned} \quad (2.25)$$

where  $\mathbf{w}$  contains nonlinear damping components  $\hat{\mathbf{F}}, \boldsymbol{\beta}$ , and  $\boldsymbol{\rho}$ .  $\mathbf{k} \in \mathcal{R}^{n \times n}$  denotes a positive definite diagonal gain matrix.  $\hat{\mathbf{F}}$  is bounding function in assumption 2.  $\boldsymbol{\beta} \in \mathcal{R}^{n \times n}, \boldsymbol{\rho} \in \mathcal{R}^{n \times n}$  stand for positive-semidefinite diagonal matrix functions respectively.

$\boldsymbol{\beta}, \boldsymbol{\rho}$  are defined as

$$\begin{aligned} \boldsymbol{\beta} &= \text{diag}(|\dot{\alpha}_1|, |\dot{\alpha}_2|, \dots, |\dot{\alpha}_n|) \\ \boldsymbol{\rho} &= \text{diag}(|\hat{\mathbf{H}}_1|, |\hat{\mathbf{H}}_2|, \dots, |\hat{\mathbf{H}}_n|) \end{aligned} \quad (2.26)$$

where  $\dot{\alpha}_i, \hat{\mathbf{H}}_i$  ( $1 \leq i \leq n$ ) denote the elements of  $\dot{\boldsymbol{\alpha}}_{(t)}, \hat{\mathbf{H}}_{(t)}$ .

Considering TDE, to inject the desired error dynamics in (2.21), control input  $\mathbf{u}_{\text{INJ}}$  is designed as



$$\mathbf{u}_{\text{INJ}} = -\bar{\mathbf{G}}^{-1} \mathbf{c}_2 \mathbf{z}_2(t) \quad (2.27)$$

Therefore, the desired error dynamics is denoted as

$$\dot{\mathbf{z}}_2 + \mathbf{c}_2 \mathbf{z}_2 = 0 \quad (2.28)$$

where  $\mathbf{c}_2 \in \mathbb{R}^{n \times n}$  is a positive-definite diagonal gain matrix.

Consequently, the whole control input can be designed as

$$\begin{aligned} \mathbf{u}(t) &= \mathbf{u}_{\text{INJ}} + \mathbf{u}_{\text{TDE}} + \mathbf{u}_{\text{ND}} \\ &= -\bar{\mathbf{G}}^{-1} \mathbf{c}_2 \mathbf{z}_2(t) + \hat{\mathbf{H}}(t) - \bar{\mathbf{G}}^{-1} \mathbf{k} \mathbf{w} \mathbf{z}_2(t) \\ &= -\bar{\mathbf{G}}^{-1} \mathbf{c}_2 \mathbf{z}_2(t) + \mathbf{u}_{(t-L)} - \bar{\mathbf{G}}^{-1} \dot{\mathbf{z}}_2(t-L) - \bar{\mathbf{G}}^{-1} \mathbf{k} \mathbf{w} \mathbf{z}_2(t) \end{aligned} \quad (2.29)$$

The block diagram of backstepping control with TDE and nonlinear damping is shown in Fig. 2. 1.

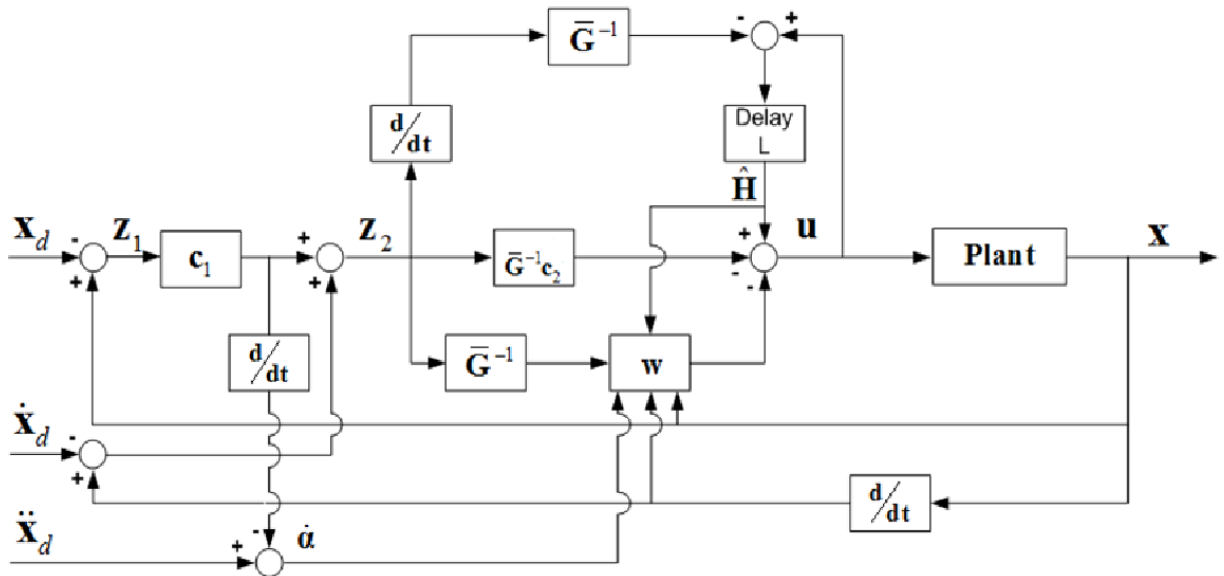


Fig. 2.1. Block diagram of backstepping control with TDE and nonlinear damping

### 2.3.3 Stability analysis

Backstepping method and nonlinear damping are based on the Lyapunov function. The Lyapunov function is a method for stability analysis in linear and nonlinear systems. It concludes stability without solving for the solution of the differential equation governing the system. Therefore stability analysis based on the Lyapunov function will be shown and the boundedness of the closed-loop tracking error will be proved. After two lemmas are expressed, the theorem will be shown [7].

#### Lemma 1

**Assumption:** If the virtual input  $\alpha$  is applied to subsystem 1 and if  $z_2$  is made uniformly bounded (as will be proved in Lemma 2), then  $z_1$  is uniformly bounded [7].

**Proof:** Define the Lyapunov function for subsystem 1 as

$$V_1 = \frac{1}{2} z_1^T z_1 \quad (2.30)$$

where  $z_1$  is positive for non-zero vector. The time variable  $t$  is omitted for simplicity. Substituting (2.19), the

time derivative of the Lyapunov function  $V_1$  is derived as

$$\begin{aligned} \dot{V}_1 &= z_1^T \dot{z}_1 \\ &= z_1^T (-c_1 z_1 + z_2) \end{aligned}$$

$$\begin{aligned}
&= -\mathbf{z}_1^T \mathbf{c}_1 \mathbf{z}_1 + \mathbf{z}_1^T \mathbf{z}_2 \\
&\leq -\mathbf{z}_1^T \mathbf{c}_1 \mathbf{z}_1 + |\mathbf{z}_1^T| |\mathbf{z}_2| \\
&= -|\mathbf{z}_1^T| \mathbf{c}_1 (|\mathbf{z}_1| - \mathbf{c}_1^{-1} |\mathbf{z}_2|)
\end{aligned} \tag{2.31}$$

where if  $|\mathbf{z}_1| > \mathbf{c}_1^{-1} |\mathbf{z}_2|$  and  $|\mathbf{z}_2|$  is bounded, the vector  $\dot{\mathbf{V}}_1$  is negative for any nonzero  $\mathbf{z}_1$ . Furthermore,  $|\mathbf{z}_1| - \mathbf{c}_1^{-1} |\mathbf{z}_2| > 0$ ,  $\mathbf{c}_1$  is a positive-definite diagonal matrix. Here, a vector is bounded if and only if each element of the vector is bounded. Thus  $\mathbf{z}_1$  will remain in the set  $(|\mathbf{z}_1| < \mathbf{c}_1^{-1} |\mathbf{z}_2|)$  as  $t \rightarrow +\infty$ . The boundedness of  $|\mathbf{z}_2|$  will be shown in Lemma 2.

## Lemma 2

**Assumption:** Assumption 1 and Assumption 2 are held. If the control input  $\mathbf{u}$  is applied to the subsystem 2,

then  $\mathbf{z}_2$  is uniformly bounded [7].

**Proof:** the closed-loop system is given from subsystem 2. Substituting the control input  $\mathbf{u}$  (2.29) into

subsystem 2, it derived as

$$\dot{\mathbf{z}}_2 = -\mathbf{G}\bar{\mathbf{G}}^{-1} \mathbf{c}_2 \mathbf{z}_2 + \mathbf{G}\hat{\mathbf{H}} - \mathbf{G}\bar{\mathbf{G}}^{-1} \mathbf{k} (\hat{\mathbf{F}} + \boldsymbol{\beta} + \boldsymbol{\rho}) \mathbf{z}_2 + \mathbf{f} - \dot{\boldsymbol{\alpha}} \tag{2.32}$$

Here, also the time variable  $t$  is omitted for simplicity. In the same manner in Lemma 1, the Lyapunov function

is defined as

$$\mathbf{V}_2 = \frac{1}{2} \mathbf{z}_2^T \mathbf{z}_2 \quad (2.33)$$

where  $\mathbf{z}_2$  is positive for none zero vector and  $\mathbf{V}_2$  is positive. By applying (2.32) to (2.33), the time derivative

of the Lyapunov function  $\mathbf{V}_2$  is derived as

$$\begin{aligned} \dot{\mathbf{V}}_2 &= \mathbf{z}_2^T \dot{\mathbf{z}}_2 \\ &= \mathbf{z}_2^T [-\mathbf{G}\bar{\mathbf{G}}^{-1}\mathbf{c}_2\mathbf{z}_2 - \mathbf{G}\bar{\mathbf{G}}^{-1}\mathbf{k}(\hat{\mathbf{F}} + \boldsymbol{\beta} + \boldsymbol{\rho})\mathbf{z}_2 + \mathbf{G}\hat{\mathbf{H}} + \mathbf{f} - \dot{\boldsymbol{\alpha}}] \\ &= -\mathbf{z}_2^T \mathbf{G}\bar{\mathbf{G}}^{-1}\mathbf{c}_2\mathbf{z}_2 - \mathbf{z}_2^T \mathbf{G}\bar{\mathbf{G}}^{-1}\mathbf{k}(\hat{\mathbf{F}} + \boldsymbol{\beta} + \boldsymbol{\rho})\mathbf{z}_2 + \mathbf{z}_2^T (\mathbf{f} + \mathbf{G}\hat{\mathbf{H}} - \dot{\boldsymbol{\alpha}}) \\ &\leq -\mathbf{z}_2^T \mathbf{G}\bar{\mathbf{G}}^{-1}\mathbf{c}_2\mathbf{z}_2 - \mathbf{z}_2^T \mathbf{G}\bar{\mathbf{G}}^{-1}\mathbf{k}(\hat{\mathbf{F}} + \boldsymbol{\beta} + \boldsymbol{\rho})\mathbf{z}_2 + |\mathbf{z}_2^T| (|\mathbf{f}| + \mathbf{G}|\hat{\mathbf{H}}| + |\dot{\boldsymbol{\alpha}}|) \\ &= -\mathbf{z}_2^T \mathbf{G}\bar{\mathbf{G}}^{-1}\mathbf{c}_2\mathbf{z}_2 - |\mathbf{z}_2^T| \boldsymbol{\Psi} [|\mathbf{z}_2| - \boldsymbol{\mu}] \end{aligned} \quad (2.34)$$

$$\text{where } \boldsymbol{\Psi} = \mathbf{G}\bar{\mathbf{G}}^{-1}\mathbf{k}(\hat{\mathbf{F}} + \boldsymbol{\beta} + \boldsymbol{\rho}), \quad (2.35)$$

$$\boldsymbol{\mu} = (\mathbf{k}(\hat{\mathbf{F}} + \boldsymbol{\beta} + \boldsymbol{\rho}))^{-1} \bar{\mathbf{G}}\mathbf{G}^{-1} (|\mathbf{f}| + \mathbf{G}|\hat{\mathbf{H}}| + |\dot{\boldsymbol{\alpha}}|) \quad (2.36)$$

$\boldsymbol{\Psi} \in \mathfrak{R}^{n \times n}$  is a diagonal matrix that includes nonlinear damping components and  $\boldsymbol{\mu} \in \mathfrak{R}^n$  is a vector.

$\mathbf{G}$ ,  $\bar{\mathbf{G}}$ ,  $\mathbf{c}_2$ , and  $\hat{\mathbf{F}}$  are positive-definite matrices.  $\boldsymbol{\beta}$ ,  $\boldsymbol{\rho}$  are positive-semidefinite matrices. Therefore,

$-\mathbf{z}_2^T \mathbf{G}\bar{\mathbf{G}}^{-1}\mathbf{c}_2\mathbf{z}_2$  is negative definite for any none zero vector  $\mathbf{z}_2$  and  $-|\mathbf{z}_2^T| \boldsymbol{\Psi} [|\mathbf{z}_2| - \boldsymbol{\mu}]$  has to be negative

definite. That is,  $\dot{\mathbf{V}}_2$  is negative for any nonzero vector  $\mathbf{z}_2$  satisfying

$$|\mathbf{z}_2| - \boldsymbol{\mu} \geq 0 \quad (2.37)$$

To prove (2.37), it is shown that  $\boldsymbol{\mu}$  is bounded for all  $t \in [0, \infty)$ . As  $(\mathbf{k}(\hat{\mathbf{F}} + \boldsymbol{\beta} + \boldsymbol{\rho}))^{-1}$  is a diagonal matrix,

$\boldsymbol{\mu}$  can be reformulated as

$$\begin{aligned}\boldsymbol{\mu} &= \bar{\mathbf{G}}\mathbf{G}^{-1}(\mathbf{k}(\hat{\mathbf{F}} + \boldsymbol{\beta} + \boldsymbol{\rho}))^{-1}(|\mathbf{f}| + \mathbf{G}|\hat{\mathbf{H}}| + |\dot{\boldsymbol{\alpha}}|) \\ &= \bar{\mathbf{G}}\mathbf{G}^{-1}\boldsymbol{\mu}_1 + \bar{\mathbf{G}}\boldsymbol{\mu}_2 + \bar{\mathbf{G}}\mathbf{G}^{-1}\boldsymbol{\mu}_3\end{aligned}\quad (2.38)$$

where  $\boldsymbol{\mu}_1 = (\mathbf{k}(\hat{\mathbf{F}} + \boldsymbol{\beta} + \boldsymbol{\rho}))^{-1} |\mathbf{f}|$ ,

$$\boldsymbol{\mu}_2 = (\mathbf{k}(\hat{\mathbf{F}} + \boldsymbol{\beta} + \boldsymbol{\rho}))^{-1} |\hat{\mathbf{H}}|,$$

$$\boldsymbol{\mu}_3 = (\mathbf{k}(\hat{\mathbf{F}} + \boldsymbol{\beta} + \boldsymbol{\rho}))^{-1} |\dot{\boldsymbol{\alpha}}|.\quad (2.39)$$

As  $\mathbf{k}$ ,  $\hat{\mathbf{F}}$ ,  $\boldsymbol{\beta}$ ,  $\boldsymbol{\rho}$  are all diagonal matrices and  $|\mathbf{f}|$ ,  $|\hat{\mathbf{H}}|$ ,  $|\dot{\boldsymbol{\alpha}}|$  are vectors, the  $i^{th}$  element of  $\boldsymbol{\mu}_1$ ,  $\boldsymbol{\mu}_2$ ,  $\boldsymbol{\mu}_3$  can

be respectively expressed as

$$\begin{cases} \mu_{1i} = (k_i(\hat{F}_i + \beta_i + \rho_i))^{-1} |f_i| \\ \mu_{2i} = (k_i(\hat{F}_i + \beta_i + \rho_i))^{-1} |\hat{H}_i| \\ \mu_{3i} = (k_i(\hat{F}_i + \beta_i + \rho_i))^{-1} |\dot{\alpha}_i| \end{cases}\quad (2.40)$$

Considering Assumption 1 and Assumption 2, the inequalities of (2.40) is obtained as

$$\begin{cases} \mu_{1i} = (k_i(\hat{F}_i + \beta_i + \rho_i))^{-1} |f_i| \leq \frac{|f_i|}{k_i \hat{F}_i} = \frac{N_f}{k_i} \\ \mu_{2i} = (k_i(\hat{F}_i + \beta_i + \rho_i))^{-1} |\hat{H}_i| \leq \frac{|\hat{H}_i|}{k_i \hat{F}_i + k_i \rho_i} < \frac{1}{k_i} \\ \mu_{3i} = (k_i(\hat{F}_i + \beta_i + \rho_i))^{-1} |\dot{\alpha}_i| \leq \frac{|\dot{\alpha}_i|}{k_i \hat{F}_i + k_i \beta_i} < \frac{1}{k_i} \end{cases}\quad (2.41)$$

Therefore, as (2.41) is applied to (2.38), the following inequalities are obtained as

$$\begin{aligned}\boldsymbol{\mu} &= \bar{\mathbf{G}}\mathbf{G}^{-1}\boldsymbol{\mu}_1 + \bar{\mathbf{G}}\boldsymbol{\mu}_2 + \bar{\mathbf{G}}\mathbf{G}^{-1}\boldsymbol{\mu}_3 \\ &< \bar{\mathbf{G}}\mathbf{G}^{-1}N_f\mathbf{k}^{-1} + \bar{\mathbf{G}}\mathbf{k}^{-1} + \bar{\mathbf{G}}\mathbf{G}^{-1}\mathbf{k}^{-1}\end{aligned}\quad (2.42)$$

Since  $\boldsymbol{\mu} > \mathbf{0}$ ,  $\bar{\mathbf{G}}\mathbf{G}^{-1}\mathbf{N}_f\mathbf{k}^{-1} > 0$ ,  $\bar{\mathbf{G}}\mathbf{k}^{-1} > 0$  and  $\bar{\mathbf{G}}\mathbf{G}^{-1}\mathbf{k}^{-1} > 0$ ,  $\boldsymbol{\mu}$  is expressed as

$$\begin{aligned}
\|\boldsymbol{\mu}\| &< \|\bar{\mathbf{G}}\mathbf{G}^{-1}\mathbf{N}_f\mathbf{k}^{-1} + \bar{\mathbf{G}}\mathbf{k}^{-1} + \bar{\mathbf{G}}\mathbf{G}^{-1}\mathbf{k}^{-1}\| \\
&\leq \|\bar{\mathbf{G}}\|(\mathbf{N}_f\|\mathbf{G}^{-1}\|\|\mathbf{k}^{-1}\| + \|\mathbf{k}^{-1}\| + \|\mathbf{G}^{-1}\|\|\mathbf{k}^{-1}\|) \\
&\leq \|\bar{\mathbf{G}}\|(\mathbf{N}_f\mathbf{G}_a^{-1}\|\mathbf{k}^{-1}\| + \|\mathbf{k}^{-1}\| + \mathbf{G}_a^{-1}\|\mathbf{k}^{-1}\|) \\
&\triangleq \mu_{\max}
\end{aligned} \tag{2.43}$$

where  $\mu_{\max}$  is a finite constant. Each element of  $\boldsymbol{\mu}$  is bounded by a finite constant  $\mu_{\max}$ .

That is,  $\dot{\mathbf{V}}_2$  is negative definite for any none zero vector  $\mathbf{z}_2$  satisfying  $|z_{2i}| \geq \mu_{\max}$ , for all  $1 \leq i \leq n$ ,  $i \in \mathbb{N}$ .

Therefore,  $\mathbf{z}_2$  is uniformly bounded.

### Theorem

**Assumption:** Assumption 1 and 2 are held. If the total control input  $\mathbf{u}$  is applied to the system (2.1), then the tracking error of the closed loop system is globally uniformly ultimately bounded.

**Proof:** In Lemma 1 and 2, it was proved that  $\dot{\mathbf{V}}_1 < 0$  for any nonzero vector  $\mathbf{z}_1$  satisfying  $|\mathbf{z}_1| > \mathbf{c}_1^{-1}\mu_{\max}$

Hence, the closed-loop tracking error  $|\mathbf{z}_1|$  with any initiate value is bounded by  $|\mathbf{z}_1| \leq \mathbf{c}_1^{-1}\mu_{\max}$ . According to the definition 4.6 in [16], the tracking error of the closed-loop system is globally uniformly ultimately bounded.

# Chapter 3. The Design of Variable PID Control and Overviews

## 3.1 Introduction

These days, many control systems are conducted by using digital devices such as computers, microprocessors in discrete time domain. Although many control systems are analyzed in continuous time domain, considering practical systems and the execution environment, these have to be analyzed in discrete time domain. In practice, many other control systems are interpreted in discrete time domains.

As was mentioned in Chapter 1, the relationship between the time delay control (TDC) and PID control was proved in discrete time domain [4]. PID control has robust properties by using TDC. However, inevitable problem called TDE error of TDC also is observed in equivalent PID control. Backstepping control with TDE and nonlinear damping was designed based on Lyapunov function that is used to analyze the stability of control systems, so it solved the problem of TDE error [7]. In this section, the relationship between PID control and backstepping control with TDE, nonlinear damping will be derived in the discrete time domain to design a PID controller.

## 3.2 The design of variable PID control

### 3.2.1 PID control in the discrete time domain [4]

Conventional PID control has three gains that are expressed as a proportional gain  $\mathbf{K}$ , an integral gain  $\mathbf{T}_I$ , a derivative gain  $\mathbf{T}_D$ . Considering the target system (2.1), PID control is denoted as

$$\mathbf{u}_{(t)} = \mathbf{K}[\mathbf{e}_{(t)} + \mathbf{T}_I^{-1} \int_0^t \mathbf{e}(\tau) d\tau + \mathbf{T}_D \dot{\mathbf{e}}_{(t)}] + \mathbf{u}_{DC} \quad (3.1)$$

$$\mathbf{e} = \mathbf{x}_d - \mathbf{x} \quad (3.2)$$

where  $\mathbf{e}$  is an error vector with respect to position  $\mathbf{x}$  and is denoted as (3.2).  $\mathbf{x}_d$  denotes the reference input vector.  $\mathbf{K}$  stands for the constant diagonal proportional gain matrix,  $\mathbf{T}_D$  denotes the constant diagonal derivative time matrix,  $\mathbf{T}_I$  the constant diagonal integral matrix and  $\mathbf{u}_{DC}$  a constant dc-bias vector, That is,

$$\mathbf{K} = \begin{bmatrix} K_1 & \dots & 0 \\ \vdots & \ddots & \vdots \\ 0 & \dots & K_n \end{bmatrix}, \mathbf{T}_I = \begin{bmatrix} T_{I_1} & \dots & 0 \\ \vdots & \ddots & \vdots \\ 0 & \dots & T_{I_n} \end{bmatrix}, \mathbf{T}_D = \begin{bmatrix} T_{D_1} & \dots & 0 \\ \vdots & \ddots & \vdots \\ 0 & \dots & T_{D_n} \end{bmatrix}, \mathbf{u}_{DC} = \begin{bmatrix} u_{DC_1} \\ \vdots \\ u_{DC_n} \end{bmatrix} \quad (3.3)$$

Note that the number of elements of PID gain matrices is  $3n$ .

To transfer continuous time domain to discrete time domain, causality relationship should be explained. The physical systems have causality with respect to time  $t$ . For example, the inputs are required to make output. In the case of system (3.1), variable  $\mathbf{x}$  and control input  $\mathbf{u}$  have sequence. It is shown in Fig. 3.1.



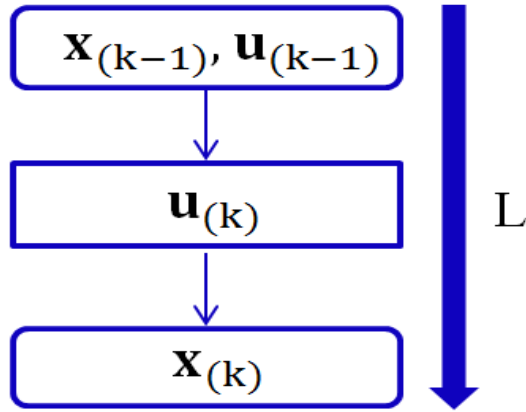


Fig. 3.1. Sequence of  $\mathbf{x}_{(k)}$  and  $\mathbf{u}_{(k)}$

where  $k$  denotes at  $k$ -th sampling instant ( $t=kL$ ) and  $L$  represents the sampling time of digital devices. As we can see in Fig. 3.1,  $\mathbf{x}_{(k-1)}$  and  $\mathbf{u}_{(k-1)}$  are used to get the control input  $\mathbf{u}_{(k)}$ . Similarly,  $\mathbf{x}_{(k)}$  is taken by using  $\mathbf{u}_{(k)}$ . Therefore, control input (3.1) of PID control is transferred to the following

$$\mathbf{u}_{(k)} = \mathbf{K}[\mathbf{e}_{(k-1)} + L\mathbf{T}_I^{-1} \sum_{i=0}^{k-1} \mathbf{e}_{(i)} + \mathbf{T}_D \dot{\mathbf{e}}_{(k-1)}] + \mathbf{u}_{DC} \quad (3.4)$$

(3.4) is transformed into another form to match backstepping control with TDE and nonlinear damping by follow procedure [4], [30]. Subtracting PID control input (3.5) at the discrete time  $(k-1)$  from PID control input (3.4) at the discrete time  $(k)$ ,

$$\mathbf{u}_{(k-1)} = \mathbf{K}[\mathbf{e}_{(k-2)} + L\mathbf{T}_I^{-1} \sum_{i=0}^{k-2} \mathbf{e}_{(i)} + \mathbf{T}_D \dot{\mathbf{e}}_{(k-2)}] + \mathbf{u}_{DC} \quad (3.5)$$

It is derived as

$$\mathbf{u}_{(k)} - \mathbf{u}_{(k-1)} = \mathbf{K}[(\mathbf{e}_{(k-1)} - \mathbf{e}_{(k-2)}) + \mathbf{T}_I^{-1} L \mathbf{e}_{(k-1)} + \mathbf{T}_D (\dot{\mathbf{e}}_{(k-1)} - \dot{\mathbf{e}}_{(k-2)})] \quad (3.6)$$

Considering (3.2), (3.6) is reformulated as

$$\begin{aligned} \mathbf{u}_{(k)} = \mathbf{u}_{(k-1)} + \mathbf{KL} \left[ \left( \frac{\mathbf{x}_{d(k-1)} - \mathbf{x}_{d(k-2)}}{L} - \frac{\mathbf{x}_{(k-1)} - \mathbf{x}_{(k-2)}}{L} \right) + \mathbf{T}_1^{-1} (\mathbf{x}_{d(k-1)} - \mathbf{x}_{(k-1)}) \right. \\ \left. + \mathbf{T}_D \left( \frac{\dot{\mathbf{x}}_{d(k-1)} - \dot{\mathbf{x}}_{d(k-2)}}{L} - \frac{\dot{\mathbf{x}}_{(k-1)} - \dot{\mathbf{x}}_{(k-2)}}{L} \right) \right] \end{aligned} \quad (3.7)$$

In addition, PID control is represented in discrete time domain as (3.7). The constant vector  $\mathbf{u}_{DC}$  will be explained after backstepping control with TDE and nonlinear damping is represented, since it is related with the backstepping method at the discrete time  $k = 1$ .

### 3.2.2. Backstepping control with TDE, nonlinear damping in discrete time domain

In Chapter 2, backstepping control with TDE and nonlinear damping was explained with respect to the control input and stability. The whole control input of that controller was formulated from (2.29) as

$$\mathbf{u}_{(t)} = \mathbf{u}_{(t-L)} - \bar{\mathbf{G}}^{-1} \mathbf{c}_2 \mathbf{z}_{2(t)} - \bar{\mathbf{G}}^{-1} \dot{\mathbf{z}}_{2(t-L)} - \bar{\mathbf{G}}^{-1} \mathbf{k} \mathbf{w} \mathbf{z}_{2(t)} \quad (3.8)$$

Backstepping control with TDE and nonlinear damping also are conducted in digital devices, so causality has to be considered. According to causality, (3.8) is reformulated with (2.19) as

$$\begin{aligned} \mathbf{u}_{(k)} = \mathbf{u}_{(k-1)} - \bar{\mathbf{G}}^{-1} [\dot{\mathbf{z}}_{1(k-1)} + \mathbf{c}_1 \dot{\mathbf{z}}_{1(k-1)} + (\mathbf{c}_2 + \mathbf{k} \mathbf{w})(\dot{\mathbf{z}}_{1(k-1)} + \mathbf{c}_1 \mathbf{z}_{1(k-1)})] \\ = \mathbf{u}_{(k-1)} - \bar{\mathbf{G}}^{-1} [\dot{\mathbf{z}}_{1(k-1)} + (\mathbf{c}_1 + \mathbf{c}_2 + \mathbf{k} \mathbf{w}) \dot{\mathbf{z}}_{1(k-1)} + (\mathbf{c}_2 + \mathbf{k} \mathbf{w}) \mathbf{c}_1 \mathbf{z}_{1(k-1)}] \end{aligned} \quad (3.9)$$

As  $\mathbf{c}_1$ ,  $\mathbf{c}_2$ ,  $\mathbf{k}$  and  $\mathbf{w}$  are a diagonal matrices, (3.9) is rearranged as

$$\mathbf{u}_{(k)} = \mathbf{u}_{(k-1)} - \bar{\mathbf{G}}^{-1}[\bar{\mathbf{z}}_{1(k-1)} + (\mathbf{c}_1 + \mathbf{c}_2 + \mathbf{k}\mathbf{w})\bar{\mathbf{z}}_{1(k-1)} + (\mathbf{c}_1\mathbf{c}_2 + \mathbf{c}_1\mathbf{k}\mathbf{w})\mathbf{z}_{1(k-1)}] \quad (3.10)$$

To match the form of PID control, (3.10) is transformed by using (2.16) as follows:

$$\begin{aligned} \mathbf{u}_{(k)} = & \mathbf{u}_{(k-1)} + \bar{\mathbf{G}}^{-1}[\ddot{\mathbf{x}}_{d(k-1)} - \ddot{\mathbf{x}}_{(k-1)} + (\mathbf{c}_1 + \mathbf{c}_2 + \mathbf{k}\mathbf{w})(\dot{\mathbf{x}}_{d(k-1)} - \dot{\mathbf{x}}_{(k-1)}) \\ & + (\mathbf{c}_1\mathbf{c}_2 + \mathbf{c}_1\mathbf{k}\mathbf{w})(\mathbf{x}_{d(k-1)} - \mathbf{x}_{(k-1)})] \end{aligned} \quad (3.11)$$

### 3.2.3. The Relationship between PID control with Backstepping control with TDE, nonlinear damping in discrete time domain

In the above parts, two control inputs were given from section 3.2.1 and 3.2.2 for the target system (2.1).

These are represented in discrete time domain as

**Control input of PID control:**

$$\begin{aligned} \mathbf{u}_{(k)} = & \mathbf{u}_{(k-1)} + \mathbf{K}\mathbf{L}\left[\left(\frac{\mathbf{x}_{d(k-1)} - \mathbf{x}_{d(k-2)}}{L} - \frac{\mathbf{x}_{(k-1)} - \mathbf{x}_{(k-2)}}{L}\right) + \mathbf{T}_I^{-1}(\mathbf{x}_{d(k-1)} - \mathbf{x}_{(k-1)})\right. \\ & \left. + \mathbf{T}_D\left(\frac{\dot{\mathbf{x}}_{d(k-1)} - \dot{\mathbf{x}}_{d(k-2)}}{L} - \frac{\dot{\mathbf{x}}_{(k-1)} - \dot{\mathbf{x}}_{(k-2)}}{L}\right)\right] \end{aligned} \quad (3.12)$$

**Control input of backstepping control with TDE and nonlinear damping:**

$$\begin{aligned} \mathbf{u}_{(k)} = & \mathbf{u}_{(k-1)} + \bar{\mathbf{G}}^{-1}[\ddot{\mathbf{x}}_{d(k-1)} - \ddot{\mathbf{x}}_{(k-1)} + (\mathbf{c}_1 + \mathbf{c}_2 + \mathbf{k}\mathbf{w})(\dot{\mathbf{x}}_{d(k-1)} - \dot{\mathbf{x}}_{(k-1)}) \\ & + (\mathbf{c}_1\mathbf{c}_2 + \mathbf{c}_1\mathbf{k}\mathbf{w})(\mathbf{x}_{d(k-1)} - \mathbf{x}_{(k-1)})] \end{aligned} \quad (3.13)$$

The above two control inputs must have similar forms to drive an equivalent relationship. To do this, numerical differentiation is used to solve the differential terms in each control input. In practice, many users in the control fields use numerical differentiation to get differential signals since they use digital devices. There are three kinds of numerical differentiation; forward method, center method, backward method [19]. In our case, the backward method will be used since others need to require a future value and do not satisfy causality of digital systems. The backward method is defined as

$$\dot{\mathbf{x}}_{(k)} = \frac{\mathbf{x}_{(k)} - \mathbf{x}_{(k-1)}}{L} \quad (3.14)$$

$\ddot{\mathbf{x}}_{(k)}$  is needed to resolve (3.13), it is considered as

$$\ddot{\mathbf{x}}_{(k)} = \frac{\mathbf{x}_{(k)} - 2\mathbf{x}_{(k-1)} + \mathbf{x}_{(k-2)}}{L^2} \quad (3.15)$$

Considering (3.14), (3.15), two control inputs are reformulated as

**Control input of PID control:**

$$\begin{aligned} \mathbf{u}_{(k)} = & \mathbf{u}_{(k-1)} + \mathbf{K}_L \left[ \left( \frac{\mathbf{x}_{d(k-1)} - \mathbf{x}_{d(k-2)}}{L} - \frac{\mathbf{x}_{(k-1)} - \mathbf{x}_{(k-2)}}{L} \right) + \mathbf{T}_I^{-1} (\mathbf{x}_{d(k-1)} - \mathbf{x}_{(k-1)}) \right. \\ & \left. + \mathbf{T}_D \left( \frac{\mathbf{x}_{d(k-1)} - 2\mathbf{x}_{d(k-2)} + \mathbf{x}_{d(k-3)}}{L^2} - \frac{\mathbf{x}_{(k-1)} - 2\mathbf{x}_{(k-2)} + \mathbf{x}_{(k-3)}}{L^2} \right) \right] \end{aligned} \quad (3.16)$$

**Control input of backstepping control with TDE and nonlinear damping:**

$$\begin{aligned}
\mathbf{u}_{(k)} = & \mathbf{u}_{(k-1)} + \bar{\mathbf{G}}^{-1} \left[ \frac{\mathbf{x}_{d(k)} - 2\mathbf{x}_{d(k-1)} + \mathbf{x}_{d(k-2)}}{L^2} - \frac{\mathbf{x}_{(k)} - 2\mathbf{x}_{(k-1)} + \mathbf{x}_{(k-2)}}{L^2} \right. \\
& + (\mathbf{c}_1 + \mathbf{c}_2 + \mathbf{k}\mathbf{w}) \left( \frac{\mathbf{x}_{d(k)} - \mathbf{x}_{d(k-1)}}{L} - \frac{\mathbf{x}_{(k)} - \mathbf{x}_{(k-1)}}{L} \right) \\
& \left. + (\mathbf{c}_1\mathbf{c}_2 + \mathbf{c}_1\mathbf{k}\mathbf{w}) (\mathbf{x}_{d(k-1)} - \mathbf{x}_{(k-1)}) \right]
\end{aligned} \tag{3.17}$$

As comparing (3.16) and (3.17), **the equivalent relationship** is found as

$$\begin{aligned}
\mathbf{K} &= \frac{\bar{\mathbf{G}}^{-1}(\mathbf{c}_1 + \mathbf{c}_2 + \mathbf{k}\mathbf{w})}{L}, \\
\mathbf{T}_1 &= (\mathbf{c}_1 + \mathbf{c}_2 + \mathbf{k}\mathbf{w})(\mathbf{c}_1\mathbf{c}_2 + \mathbf{c}_1\mathbf{k}\mathbf{w})^{-1}, \\
\mathbf{T}_D &= (\mathbf{c}_1 + \mathbf{c}_2 + \mathbf{k}\mathbf{w})^{-1}
\end{aligned} \tag{3.18}$$

where  $\mathbf{w}$  denotes a nonlinear damping component and is changing with respect to time by using feedback states. Therefore, it becomes variable PID control due to  $\mathbf{w}$ .

### 3.2.4. A constant dc-bias vector $\mathbf{u}_{DC}$

In the PID control,  $\mathbf{u}_{DC}$  already is mentioned briefly in section 3.2.1 and denotes a  $n \times 1$  constant vector representing a dc-bias decided by initial conditions [4].  $\mathbf{u}_{DC}$  is derived from the equivalence between PID control and backstepping control with TDE, nonlinear damping at a discrete time  $k=1$ .

When a discrete time  $k=1$ , the control input of backstepping control with TDE, nonlinear damping is denoted from (3.11) as

$$\mathbf{u}_{(1)\text{Back}} = \mathbf{u}_{(0)} + \bar{\mathbf{G}}^{-1}[\ddot{\mathbf{e}}_{(0)} + (\mathbf{c}_1 + \mathbf{c}_2 + \mathbf{k}\mathbf{w})\dot{\mathbf{e}}_{(0)} + (\mathbf{c}_1\mathbf{c}_2 + \mathbf{c}_1\mathbf{k}\mathbf{w})\mathbf{e}_{(0)}] \quad (3.19)$$

where  $\mathbf{e} = \mathbf{x}_d - \mathbf{x}$ ,  $\mathbf{e}_{(0)}$  denotes an initial error,  $\mathbf{u}_{(0)}$  stands for initial control input.

With a discrete time  $k=1$ , the control input of the variable PID control is represented from (3.4) as

$$\mathbf{u}_{(1)\text{PID}} = \mathbf{K}[\mathbf{e}_{(0)} + \mathbf{L}\mathbf{T}_I^{-1}\mathbf{e}_{(0)} + \mathbf{T}_D\dot{\mathbf{e}}_{(0)}] + \mathbf{u}_{\text{DC}} \quad (3.20)$$

Considering  $\mathbf{u}_{(1)\text{Back}} = \mathbf{u}_{(1)\text{PID}}$ ,  $\mathbf{u}_{\text{DC}}$  is derived by using (3.18) as

$$\mathbf{u}_{\text{DC}} = \bar{\mathbf{G}}^{-1}[(\ddot{\mathbf{e}}_{(0)} + (\mathbf{c}_1 + \mathbf{c}_2 + \mathbf{k}\mathbf{w})\dot{\mathbf{e}}_{(0)}) - \mathbf{L}^{-1}(\dot{\mathbf{e}}_{(0)} + (\mathbf{c}_1 + \mathbf{c}_2 + \mathbf{k}\mathbf{w})\mathbf{e}_{(0)})] \quad (3.21)$$

### 3.3 Consideration of variable PID control

In the previous research, gains of original time delay control (TDC) are transferred constant gains of PID control by using equivalent relationship between the two controls [4]. But, in this paper, gains of PID control are changed with variation of time due to nonlinear damping.

From (3.18), the equivalent relationship was expressed as

$$\mathbf{K} = \frac{\bar{\mathbf{G}}^{-1}(\mathbf{c}_1 + \mathbf{c}_2 + \mathbf{k}\mathbf{w})}{\mathbf{L}}$$

$$\mathbf{T}_I = (\mathbf{c}_1 + \mathbf{c}_2 + \mathbf{k}\mathbf{w})(\mathbf{c}_1\mathbf{c}_2 + \mathbf{c}_1\mathbf{k}\mathbf{w})^{-1},$$

$$\mathbf{T}_D = (\mathbf{c}_1 + \mathbf{c}_2 + \mathbf{k}\mathbf{w})^{-1}$$

(3.22)

where others are constant diagonal matrices without nonlinear damping component  $\mathbf{w}$ . As  $\mathbf{w}$  is a variable positive-definite diagonal matrix, gains of PID control are changed according to the size of nonlinear damping component  $\mathbf{w}$ . To get the range of gains, (3.22) is rearranged as

$$\mathbf{K} = \frac{\bar{\mathbf{G}}^{-1}(\mathbf{c}_1 + \mathbf{c}_2)}{L} + \frac{\bar{\mathbf{G}}^{-1}\mathbf{k}\mathbf{w}}{L}$$

$$\mathbf{T}_I = \mathbf{c}_1^{-1} + (\mathbf{c}_2 + \mathbf{k}\mathbf{w})^{-1}$$

$$\mathbf{T}_D = (\mathbf{c}_1 + \mathbf{c}_2 + \mathbf{k}\mathbf{w})^{-1}$$
(3.23)

where a gain  $\mathbf{T}_I$  is derived by a partial-fraction expansion. As each gain consists of diagonal matrices, gains can be expressed such as (3.23).

Considering a size of nonlinear damping component  $\mathbf{w}$ , it is assumed that  $\text{diag}(0, \dots, 0) < \mathbf{w} \leq \text{diag}(\infty, \dots, \infty)$ . Then, the range of PID gains is determined as

$$\frac{\bar{\mathbf{G}}^{-1}(\mathbf{c}_1 + \mathbf{c}_2)}{L} < \mathbf{K} \leq \frac{\bar{\mathbf{G}}^{-1}(\mathbf{c}_1 + \mathbf{c}_2)}{L} + \frac{\bar{\mathbf{G}}^{-1}\mathbf{k}\mathbf{w}}{L}$$

$$\mathbf{c}_1^{-1} \leq \mathbf{T}_I < \mathbf{c}_1^{-1} + \mathbf{c}_2^{-1}$$

$$\text{diag}(0, \dots, 0) \leq \mathbf{T}_D < (\mathbf{c}_1 + \mathbf{c}_2)^{-1}$$
(3.24)

$\bar{\mathbf{G}}^{-1}$ ,  $\mathbf{c}_1$ ,  $\mathbf{c}_2$  and  $\mathbf{k}$  are constant diagonal matrices and  $L$  is constant. If  $\mathbf{w}$  is removed, each gain has constant

value. That is, since gains of a PID controller depend on the variation of nonlinear damping component  $w$ , patterns and ranges of gains can be anticipated.

According to the size of  $w$ , the variation of each gain is represented in Table.3.1

Gains \ $w$	Increase	Decrease
<b>K</b>	Increase	Decrease
<b>T<sub>I</sub></b>	Decrease	Increase
<b>T<sub>D</sub></b>	Decrease	Increase

Table.3.1. Variation of PID gains

Note that gain **K** is proportional to nonlinear damping component  $w$ , **T<sub>I</sub>** and **T<sub>D</sub>** are inversely proportional to  $w$ . It means that characteristics of system response are changed by variation of gains.

### 3.4 Comparison with the previous study

As was mentioned in Chapter 1, a systematic method was proposed to select PID gains [4]. That method makes PID gains constant by using TDC. In this paper, the proposed PID control has variable gains by using backstepping control with TDE and nonlinear damping. Both controllers use TDE equally. To compare two methods, closed-loop dynamics are shown as follows:

$$\ddot{e}_{(t)} + k_v \dot{e}_{(t)} + k_p e_{(t)} = \bar{G}(H_{(t)} - \hat{H}_{(t)}) \quad (3.25)$$



$$\ddot{\mathbf{z}}_{1(t)} + (\mathbf{c}_1 + \mathbf{c}_2)\dot{\mathbf{z}}_{1(t)} + \mathbf{c}_1\mathbf{c}_2\mathbf{z}_{1(t)} = \bar{\mathbf{G}}(\hat{\mathbf{H}}_{(t)} - \mathbf{H}_{(t)}) - \mathbf{k}\mathbf{w}\mathbf{z}_{2(t)} \quad (3.26)$$

where  $\mathbf{e} = \mathbf{x}_d - \mathbf{x}$ ,  $\mathbf{z}_1 = \mathbf{x} - \mathbf{x}_d$  and  $\mathbf{z}_2 = \dot{\mathbf{z}}_1 + \mathbf{c}_1\mathbf{z}_1$ .

(3.25) is from TDC and (3.26) is from backstepping control with TDE and nonlinear damping. Note that the proposed PID control is theoretically equal to backstepping control with TDE, nonlinear damping. (3.26) is reformulated as the follow.

$$\ddot{\mathbf{e}}_{(t)} + \mathbf{k}_v\dot{\mathbf{e}}_{(t)} + \mathbf{k}_p\mathbf{e}_{(t)} = \bar{\mathbf{G}}(\mathbf{H}_{(t)} - \hat{\mathbf{H}}_{(t)}) + \mathbf{k}\mathbf{w}(\dot{\mathbf{e}}_{1(t)} + \mathbf{c}_1\mathbf{e}_1) \quad (3.27)$$

Note that  $\mathbf{H}_{(t)}$ ,  $\hat{\mathbf{H}}_{(t)}$  from (3.25) are a little different with  $\mathbf{H}_{(t)}$ ,  $\hat{\mathbf{H}}_{(t)}$  from (3.27) but these are similar each other. If nonlinear damping component  $\mathbf{w}$  is removed from (3.27), (3.25) is almost similar with (3.27).

$\mathbf{k}_v$ ,  $\mathbf{k}_p$ ,  $\mathbf{c}_1$ , and  $\mathbf{c}_2$  are determined by desired error dynamics. Damping ratio  $\xi = 1$  was used and desired error dynamics from the two controls are shown as

$$\ddot{\mathbf{e}} + \mathbf{k}_D\dot{\mathbf{e}} + \mathbf{k}_P\mathbf{e} = 0 \quad (3.28)$$

$$\ddot{\mathbf{e}} + (\mathbf{c}_1 + \mathbf{c}_2)\dot{\mathbf{e}} + \mathbf{c}_1\mathbf{c}_2\mathbf{e} = 0 \quad (3.29)$$

Then, to match each other,  $\mathbf{k}_v, \mathbf{k}_p$  is represented as

$$\mathbf{k}_v = \mathbf{c}_1 + \mathbf{c}_2 ,$$

$$\mathbf{k}_p = \mathbf{c}_1\mathbf{c}_2 \quad (3.30)$$

In practice, (3.30) has to be satisfied when considering a same system. Thus, if nonlinear damping is removed in

the proposed PID control, the control has same relationship with the previous study and each gain is represented

as

$$\mathbf{K} = \frac{\bar{\mathbf{G}}^{-1}(\mathbf{c}_1 + \mathbf{c}_2)}{\mathbf{L}},$$

$$\mathbf{T}_I = (\mathbf{c}_1 + \mathbf{c}_2)(\mathbf{c}_1\mathbf{c}_2)^{-1},$$

$$\mathbf{T}_D = (\mathbf{c}_1 + \mathbf{c}_2)^{-1}. \quad (3.31)$$

Considering (3.30), the above is same with the previous study that dealt with relationship between TDC and

PID control. It will be proved in simulation and experiment.

### 3.5 Simple method to design proposed PID control by the previous study

Considering the relationship between TDC and previous PID control in the previous study [4], the proposed

PID control can be designed easily. The relationship in the previous study was denoted as follows:

$$\mathbf{K} = \frac{\bar{\mathbf{G}}^{-1}\mathbf{k}_v}{\mathbf{L}},$$

$$\mathbf{T}_I = \mathbf{k}_v\mathbf{k}_p^{-1},$$

$$\mathbf{T}_D = \mathbf{k}_v^{-1} \quad (3.32)$$

As was mentioned in the section 3.4, (3.32) can be reformulated as

$$\mathbf{K} = \frac{\bar{\mathbf{G}}^{-1}(\mathbf{c}_1 + \mathbf{c}_2)}{\mathbf{L}},$$

$$\begin{aligned} \mathbf{T}_1 &= (\mathbf{c}_1 + \mathbf{c}_2)(\mathbf{c}_1 \mathbf{c}_2)^{-1}, \\ \mathbf{T}_D &= (\mathbf{c}_1 + \mathbf{c}_2)^{-1} \end{aligned} \quad (3.33)$$

Substituting  $\mathbf{c}_2$  with  $\mathbf{c}_2 + \mathbf{k}\mathbf{w}$  in (3.33), PID gains are given as

$$\begin{aligned} \mathbf{K} &= \frac{\bar{\mathbf{G}}^{-1}(\mathbf{c}_1 + \mathbf{c}_2 + \mathbf{k}\mathbf{w})}{L}, \\ \mathbf{T}_1 &= (\mathbf{c}_1 + \mathbf{c}_2 + \mathbf{k}\mathbf{w})(\mathbf{c}_1 \mathbf{c}_2 + \mathbf{c}_1 \mathbf{k}\mathbf{w})^{-1}, \\ \mathbf{T}_D &= (\mathbf{c}_1 + \mathbf{c}_2 + \mathbf{k}\mathbf{w})^{-1} \end{aligned} \quad (3.34)$$

The proposed PID gains are simply derived.

### 3.6 Conclusion

In this chapter, the equivalent relationship between PID control and backstepping control with TDE, nonlinear damping was proved in the discrete time domain. Considering this relationship, each PID gain was expressed as a variable gain. That is, the equivalent control becomes variable PID control. As nonlinear damping terms were considered, a range and patterns of PID gains can be anticipated. In addition, the proposed PID control is the same as PID control by TDC when nonlinear damping is removed in the proposed PID control. In the later chapters, these will be proved through simulations and experiments.

# Chapter 4. Simulation

## 4.1 Introduction

In the previous chapter, the equivalent relationship between variable PID control and backstepping control with TDE, nonlinear damping was introduced. PID gains are obtained by that relationship. In this chapter, the simulation with respect to 1-DOF and 2-DOF robot manipulators will be shown to prove the equivalent relationship.

## 4.2 One-link robot manipulator

### 4.2.1. Simulation Setup

A one-DOF robot manipulator is adopted in the simulation as shown in Fig. 4.1.

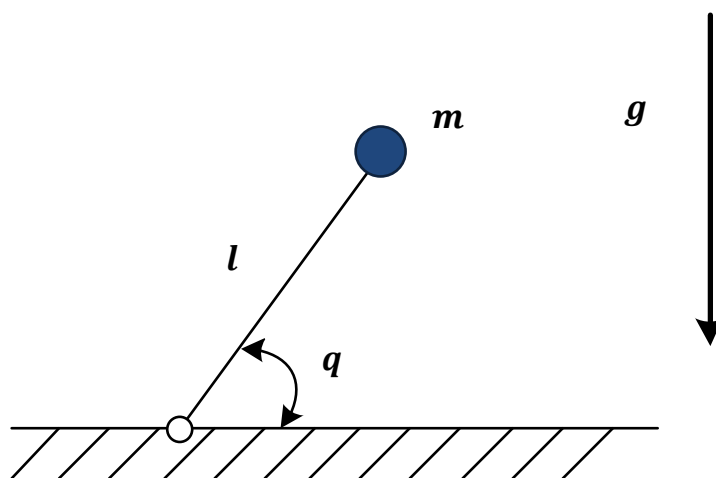


Fig. 4.1. One-link manipulator

where  $l$  stands for length of link 1.  $m$  denotes the mass of link 1.  $g$  stands for the acceleration of gravity.  $q$  denotes the joint angle of link 1.

The robot dynamics is written in the form as

$$M(q)\ddot{q} + C(q, \dot{q}) + G(q) + F(q, \dot{q}) + \tau_d = \tau \quad (4.1)$$

The functions in robot dynamics are expressed as

$$M(q) = ml_2^2,$$

$$C(q, \dot{q}) = 0,$$

$$G(q) = mgl\cos(q),$$

$$F(q, \dot{q}) = f_v\dot{q} + f_c\text{sgn}(\dot{q}),$$

$$\tau_d = \sin(4\pi t).$$

(4.2)

where  $q, \dot{q}$  represents the position and velocity of the joints, respectively.  $M(q)$  stands for the generalized inertia,  $C(q, \dot{q})$  coriolis and centripetal force,  $G(q)$  the gravity,  $F(q, \dot{q})$  the friction forces,  $\tau_d$  the unknown disturbance torque and  $\tau$  the joint torque.  $f_c, f_v$  denote the Coulomb friction coefficient and the viscous friction coefficient.

The initial  $q, \dot{q}$  and control input are set to zeros in the time  $t=0$ . The parameters of the robot dynamics are

$m=1.0\text{kg}$ ,  $l = 1.0 \text{ m}$ ,  $f_v= 5.0\text{Nm}$ ,  $f_c=5.0 \text{ Nm}$ ,  $g = 9.8\text{m/s}^2$ . The reference trajectory of position is adopted as

$$q_d(t) = 10 \sin\left(\frac{\pi}{2}t\right) [\text{deg}]. \quad (4.3)$$

A sampling time is adopted as  $L=0.002 \text{ sec}$  in the simulation. The simulation is implemented for 6 sec.

#### 4.2.2. Design of Controllers

To prove the equivalent relationship between variable PID control and backstepping control with TDE, nonlinear damping, each control is compared. After designing backstepping control with TDE and nonlinear damping, the equivalent PID control is designed by using backstepping control with TDE, nonlinear damping such as (3.22)

The desired error dynamics are determined by considering damping ratio  $\xi = 1$  and natural frequency  $w= 10$ .

According to design method in [7],  $c_1$  and  $c_2$  are calculated as

$$c_1 = 10, c_2 = 10 \quad (4.4)$$

Nonlinear damping  $w$  is designed as

$$w = \hat{F} + \beta + \rho \quad (4.5)$$

where the bounding function  $\hat{F}$  is determined as  $\hat{F} = \dot{q}^2 + 1.0 \times 10^{-6}$  by using nominal model that is given as  $M(q)^{-1}(C(q, \dot{q}) + G(q) + F(q, \dot{q}) + \tau_d)$ .  $1.0 \times 10^{-6}$  was used to keep  $\hat{F}$  positive definite.  $\beta$  and  $\rho$  are determined as  $\beta = |\dot{\alpha}|$ ,  $\rho = |\hat{H}|$ . Note that nonlinear damping component  $w$  is flexible. Thus, it can be

changed. Gains  $\bar{G}$ ,  $k$  are tuned as

$$\bar{G} = 1, k = 20 \quad (4.6)$$

Considering PID control, the control input of PID control is denoted by the equivalent relationship (3.18). Each gain is expressed as

$$K = 10000(1+w),$$

$$T_I = \frac{1+w}{5(1+w)},$$

$$T_D = \frac{1}{20(1+w)}$$

(4.7)

### 4.2.3. Simulation Result

The position trajectories of backstepping control with TDE, nonlinear damping and the proposed PID control are shown with the desired trajectory in Fig. 4.2 (a). The result seems to be one line, but is actually two lines, one on top of the other. The position trajectories of each control follow the desired trajectory well. In Fig. 4.2 (b), each position error is compared to confirm the equivalent relationship between the two controls. Above all, to make certain of the equivalent relationship of the two control input, the control inputs are shown in Fig. 4.3 (a). As these look like similar, the difference between the two control inputs is calculated as defining difference of control inputs ( $u_{\text{Back}} - u_{\text{PID}}$ ) and shown in Fig. 4.3 (b) to give more detail. The range of difference is small.

This result means the equivalent relationship between the proposed PID control and backstepping control with TDE, nonlinear damping has been achieved.

Considering a range of gains with (3.24) in PID control, the range of each gain is arranged as

$$10000 < K \leq 10000(1 + w)$$

$$\frac{1}{10} \leq T_I < \frac{1}{5}$$

$$0 \leq T_D < \frac{1}{20}$$

(4.8)

These ranges are identified in Fig. 4.4. To understand the patterns of PID gains, Fig. 4.5 is shown. The gains of the proposed PID control depend on nonlinear damping component  $w$ . In the case of this simulation, nonlinear damping component  $w$  is affected by  $\rho$  that is an absolute value of an estimated  $H$ . Since  $\rho$  is larger than others relatively in nonlinear damping component  $w$ , the pattern of nonlinear damping is similar with the control input when considering (2.24). That is, when a control input is sufficiently large, the patterns of PID control can be anticipated by a control input. In general, the patterns and ranges of PID gains depend on nonlinear damping that is proportional to gain  $K$ , and inversely proportional to gains  $T_I$  and  $T_D$ .



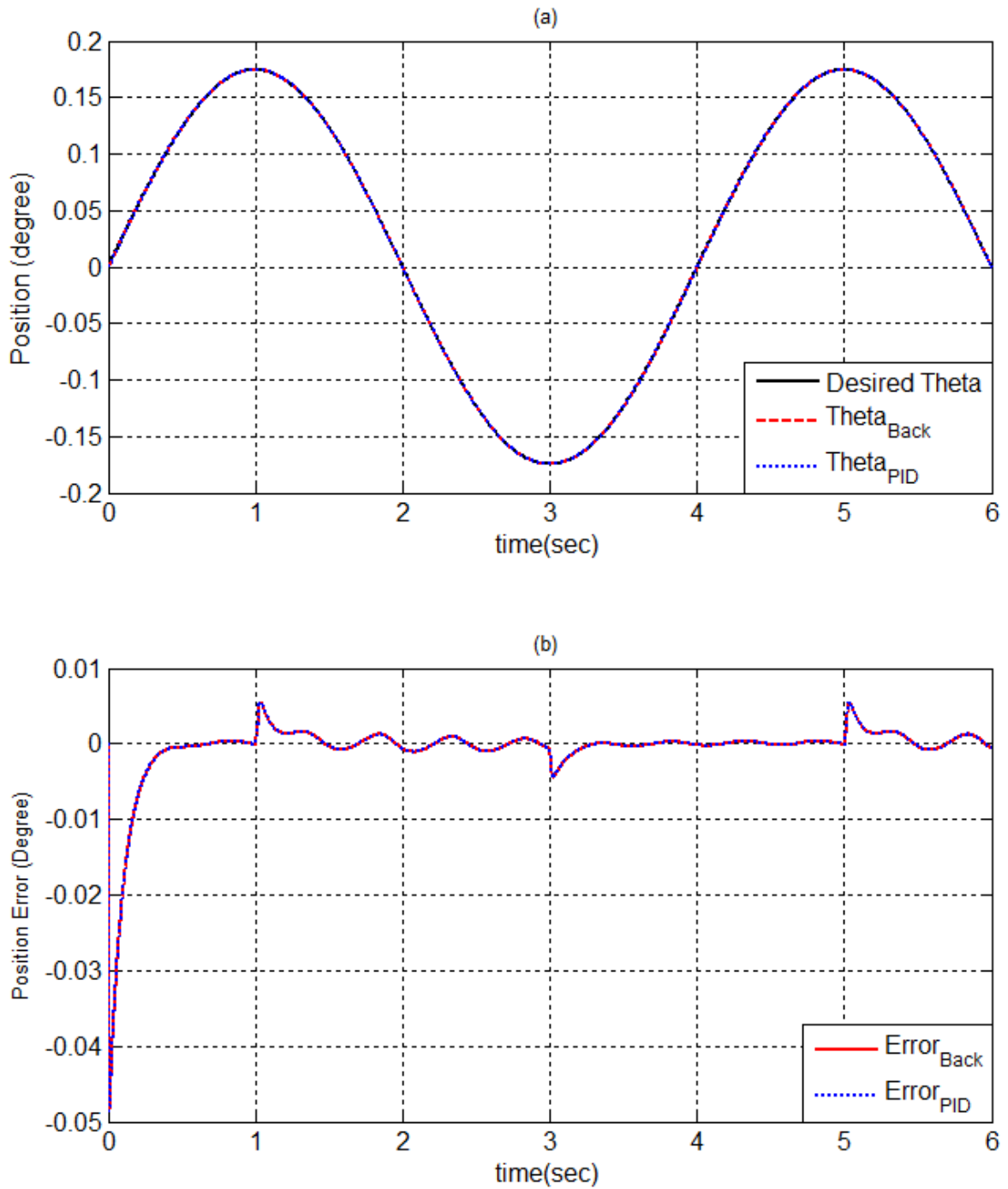


Fig. 4.2. (a)Position trajectories and (b) Position errors by backstepping control with TDE, nonlinear damping

and the proposed PID control

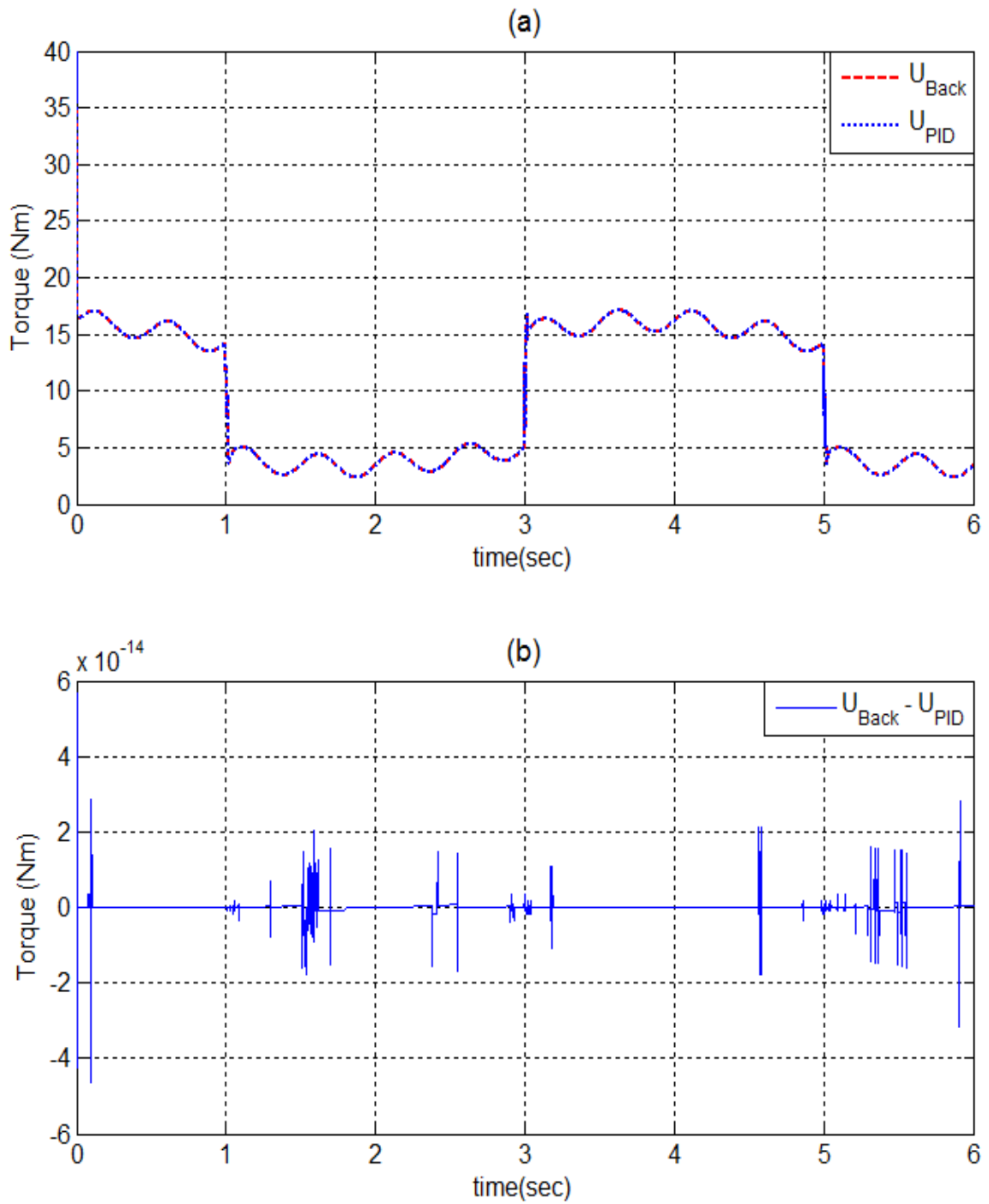


Fig. 4.3. (a) Control inputs and (b) Difference of control inputs by backstepping control with TDE, nonlinear

damping and the proposed PID control

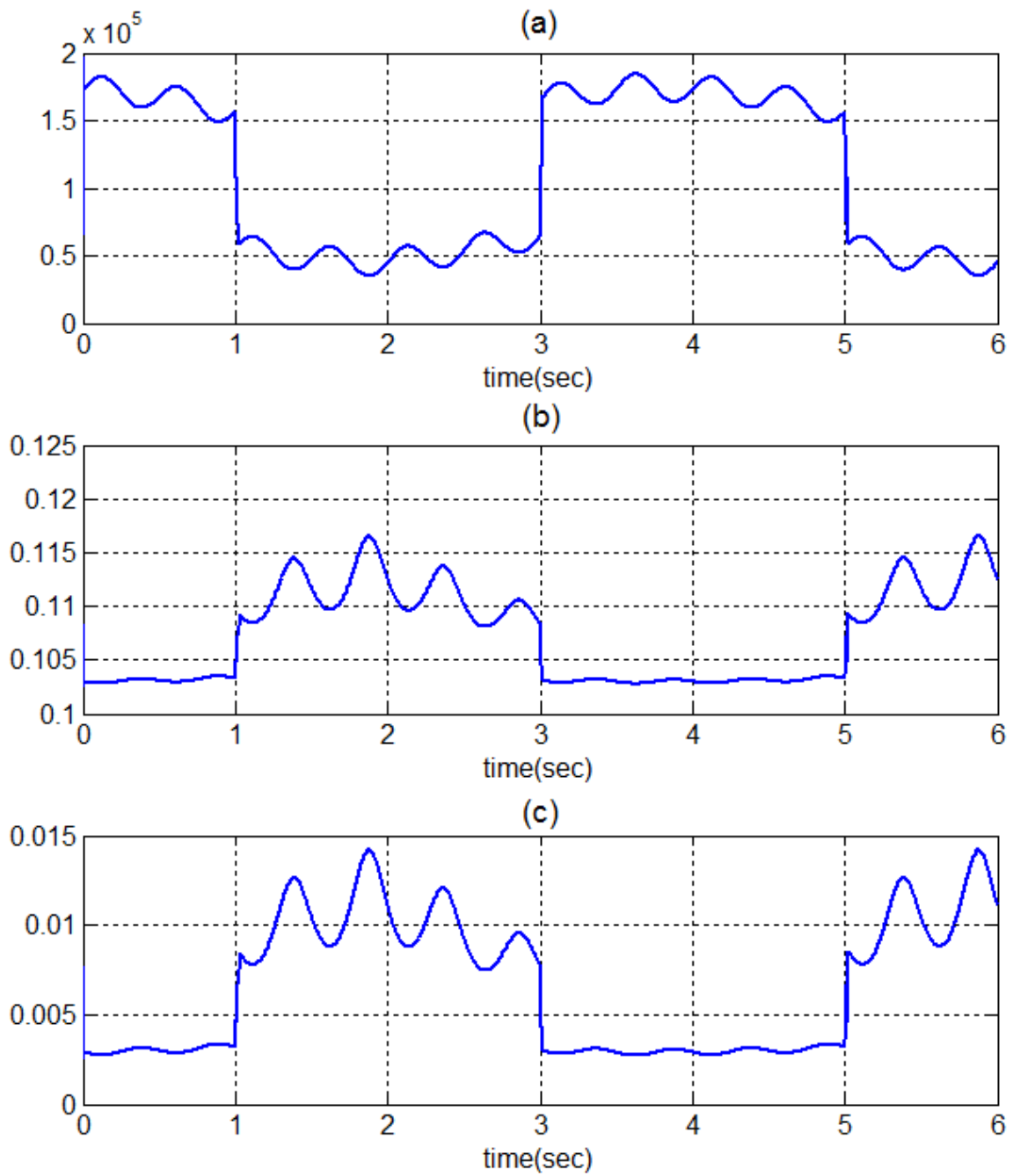


Fig. 4.4. (a) Gain  $K$ , (b) Gain  $T_I$ , and (c) Gain  $T_D$  of the proposed PID control

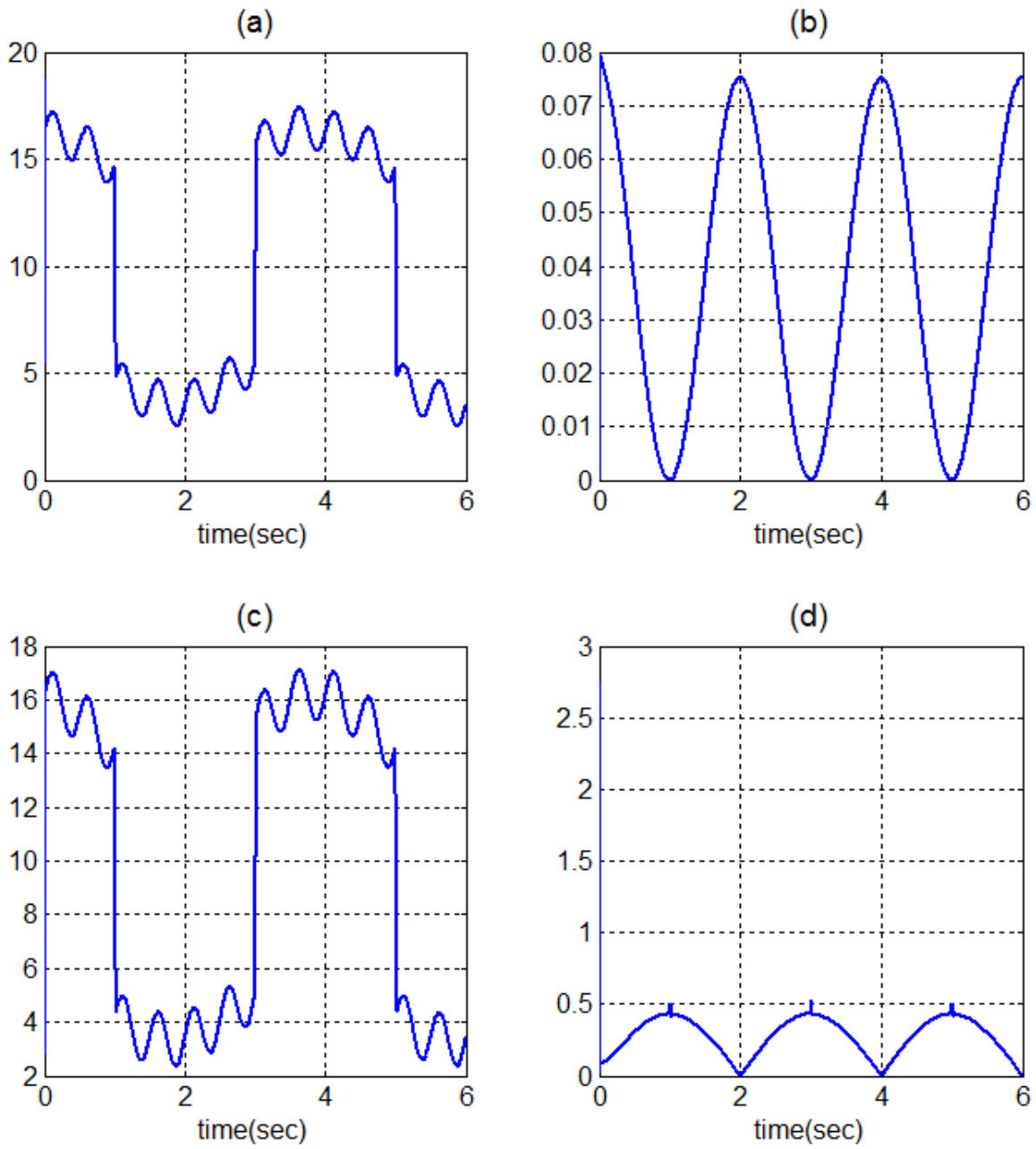


Fig. 4.5. (a) Nonlinear damping component:  $w$ , (b) Bounding function:  $\hat{F}$  (c)  $\rho$ , and (d)  $|\dot{\alpha}|/\beta$

## 4.3 Two-link robot manipulator

### 4.3.1. Simulation Setup

A two-link robot manipulator is used to prove the equivalent relationship between the two controllers and has the viscous friction and the Coulomb friction. The target plant is shown as Fig. 4.6.

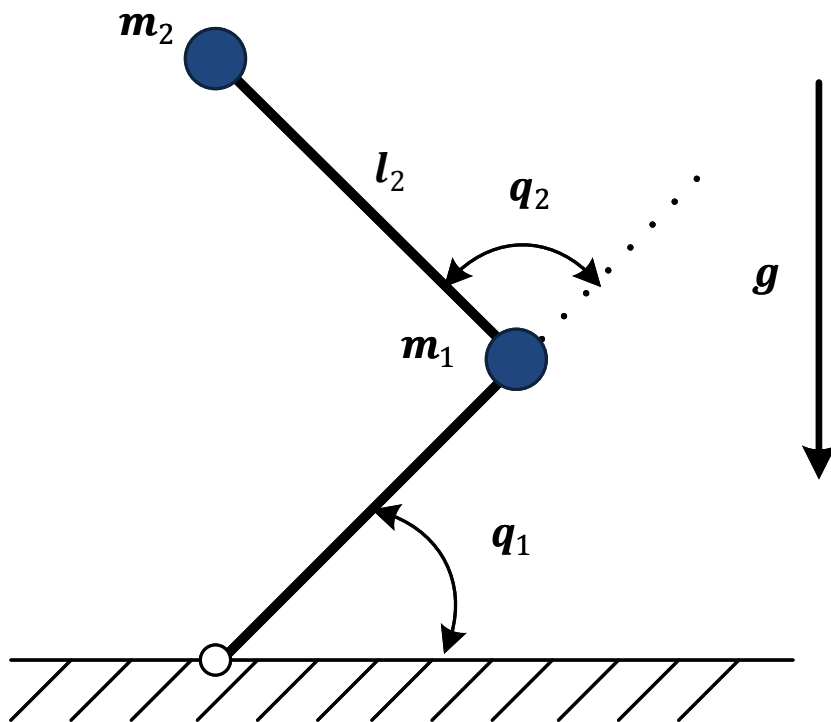


Fig. 4.6. Two-link manipulator

where  $l_1, l_2$  stand for length of link 1, link 2.  $m_1, m_2$  denote mass of link 1, link 2 respectively.  $g$  stands for the local acceleration of gravity.  $q_1, q_2$  denote joint angles of link 1 and link 2 respectively.

Let  $\mathbf{x} = [q_1 \ q_2]^T$ . Then, a dynamic equation of 2-link robot manipulator is given as

$$\mathbf{M}(\mathbf{x})\ddot{\mathbf{x}} + \mathbf{C}(\mathbf{x}, \dot{\mathbf{x}}) + \mathbf{G}(\mathbf{x}) + \mathbf{F}(\mathbf{x}, \dot{\mathbf{x}}) + \boldsymbol{\tau}_d = \boldsymbol{\tau} \quad (4.9)$$

where  $\mathbf{x}, \dot{\mathbf{x}}, \ddot{\mathbf{x}} \in \mathfrak{R}^n$  represents the position, velocity, and acceleration of the joints, respectively.

$$\mathbf{M}(\mathbf{x}) = \begin{bmatrix} m_1 l_2^2 + 2m_2 l_1 l_2 \cos(q_2) + (m_1 + m_2) l_1^2 & m_2 l_2^2 + m_2 l_1 l_2 \cos(q_2) \\ m_2 l_2^2 + m_2 l_1 l_2 \cos(q_2) & m_2 l_2^2 \end{bmatrix}$$

$$\mathbf{C}(\mathbf{x}, \dot{\mathbf{x}}) = \begin{bmatrix} -2\dot{q}_1 \dot{q}_2 m_2 l_1 l_2 \sin(q_2) - \dot{q}_2^2 m_2 l_1 l_2 \sin(q_2) \\ \dot{q}_2^2 m_2 l_1 l_2 \sin(q_2) \end{bmatrix}$$

$$\mathbf{G}(\mathbf{x}) = \begin{bmatrix} m_2 l_2 g \cos(q_1 + q_2) + (m_1 + m_2) l_1 g \cos(q_1) \\ m_2 l_2 g \cos(q_1 + q_2) \end{bmatrix}$$

$$\mathbf{F}(\mathbf{x}, \dot{\mathbf{x}}) = \begin{bmatrix} f_{v1} \dot{q}_1 + f_{c1} \text{sgn}(\dot{q}_1) \\ f_{v2} \dot{q}_2 + f_{c2} \text{sgn}(\dot{q}_2) \end{bmatrix}$$

$$\boldsymbol{\tau}_d = \begin{bmatrix} \sin(2\pi t) \\ \sin(2\pi t) \end{bmatrix}$$

(4.10)

where  $\mathbf{M}(\mathbf{x}) \in \mathfrak{R}^{n \times n}$  stands for the generalized inertia matrix.  $\mathbf{C}(\mathbf{x}, \dot{\mathbf{x}}) \in \mathfrak{R}^n$  coriolis and centripetal matrix,

$\mathbf{G}(\mathbf{x}) \in \mathfrak{R}^n$  the gravitational vector,  $\mathbf{F}(\mathbf{x}, \dot{\mathbf{x}}) \in \mathfrak{R}^n$  the friction forces,  $\boldsymbol{\tau}_d \in \mathfrak{R}^n$  the unknown disturbance

torque and  $\boldsymbol{\tau} \in \mathfrak{R}^n$  the joint torque.  $f_c$  and  $f_v$  are the Coulomb friction coefficient and the viscous friction coefficient.

The initial  $\mathbf{x}, \dot{\mathbf{x}}$  and control input are set to zeros in the time  $t=0$ . The parameters of the robot dynamics are

$m_1 = 1.0\text{kg}$ ,  $m_2 = 1.0\text{kg}$ ,  $l_1 = 1.0 \text{ m}$ ,  $l_2 = 1.0 \text{ m}$ ,  $f_{v1} = 5.0\text{Nm}$ ,  $f_{v2} = 5.0\text{Nm}$ ,  $f_{c1} = 5.0 \text{ Nm}$ ,  $f_{c2} = 5.0 \text{ Nm}$ ,  $g =$

9.8m/s<sup>2</sup>. A fifth-order polynomial trajectory is used as the desired trajectory and is shown in Fig. 4.7. A

sampling time is adopted as L=0.001 sec in the simulation. The simulation is implemented for 20 sec.

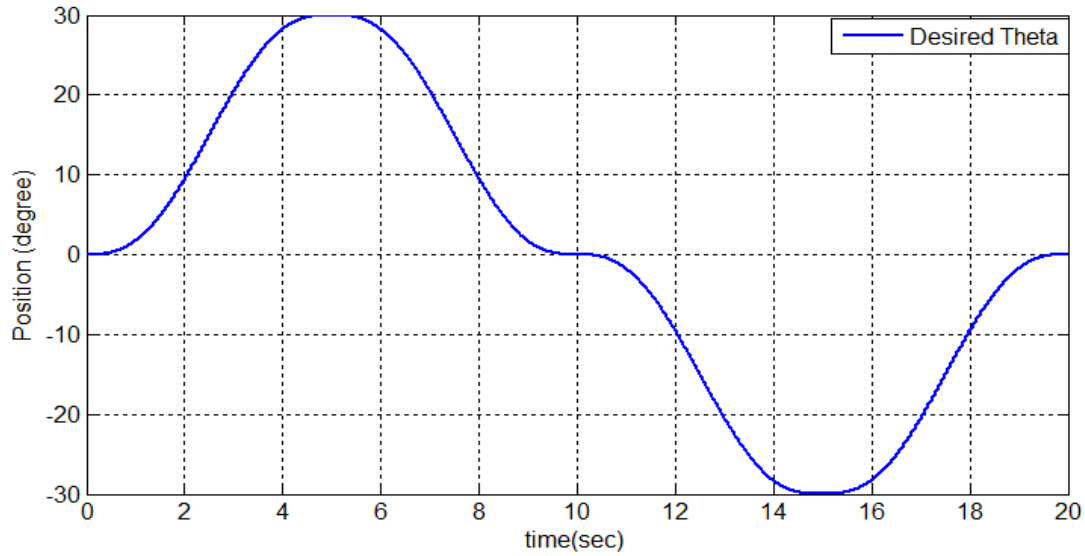


Fig. 4.7.The desired trajectory of Joints

### 4.3.2 Design of Controllers

The equivalent relationship between proposed PID control and backstepping control with TDE, nonlinear damping will be proved through this simulation in the same manner with the previous simulation.

First, backstepping control with TDE, nonlinear damping is designed to make the equivalent PID control. The desired error dynamics is adopted as considering damping ratio  $\xi = 1$  and natural frequency  $w = 5$ . According to the design method in [7],  $\mathbf{c}_1$  and  $\mathbf{c}_2$  are calculated as

$$\mathbf{c}_1 = \begin{bmatrix} 5 & 0 \\ 0 & 5 \end{bmatrix}, \quad \mathbf{c}_2 = \begin{bmatrix} 5 & 0 \\ 0 & 5 \end{bmatrix} \quad (4.11)$$

and nonlinear damping component  $\mathbf{w}$  is designed as

$$\mathbf{w} = \hat{\mathbf{F}} + \boldsymbol{\beta} + \boldsymbol{\rho} \quad (4.12)$$

where

$$\hat{\mathbf{F}} = \begin{bmatrix} \dot{q}_1^2 + \dot{q}_2^2 + 1.0 \times 10^{-5} & 0 \\ 0 & \dot{q}_1^2 + \dot{q}_2^2 + 1.0 \times 10^{-5} \end{bmatrix},$$

$$\boldsymbol{\beta} = \begin{bmatrix} |\dot{\alpha}_1| & 0 \\ 0 & |\dot{\alpha}_2| \end{bmatrix},$$

$$\boldsymbol{\rho} = \begin{bmatrix} |\hat{H}_1| & 0 \\ 0 & |\hat{H}_2| \end{bmatrix} \quad (4.13)$$

The bounding function  $\hat{\mathbf{F}}$  is determined by using nominal model.  $1.0 \times 10^{-5}$  of  $\hat{\mathbf{F}}$  was used to keep  $\hat{\mathbf{F}}$  positive definite.

Gains  $\bar{\mathbf{G}}, \mathbf{k}$  are tuned as

$$\bar{\mathbf{G}}^{-1} = \begin{bmatrix} 0.5 & 0 \\ 0 & 0.2 \end{bmatrix}, \mathbf{k} = \begin{bmatrix} 5 & 0 \\ 0 & 10 \end{bmatrix} \quad (4.14)$$

Second, considering PID control, the control input of PID control can be designed by the equivalent relationship. PID control gains are denoted as

$$\mathbf{K} = \begin{bmatrix} 5000 & 0 \\ 0 & 2000 \end{bmatrix} + \begin{bmatrix} 2500 & 0 \\ 0 & 2000 \end{bmatrix} \mathbf{w}$$

$$\mathbf{T}_I = \begin{bmatrix} \frac{10 + 5w_{11}}{25(1 + w_{11})} & 0 \\ 0 & \frac{10 + 10w_{22}}{(25 + 50w_{22})} \end{bmatrix}$$

$$\mathbf{T}_D = \begin{bmatrix} \frac{1}{5(2 + w_{11})} & 0 \\ 0 & \frac{1}{10(1 + w_{22})} \end{bmatrix}$$

(4.15)



where  $\mathbf{w} = \begin{bmatrix} w_{11} & 0 \\ 0 & w_{22} \end{bmatrix}$  and  $\mathbf{w}$  is a positive definite diagonal matrix.

Third, time delay control (TDC) is designed to compare the proposed method. Relationship between proposed method and the previous study of [4] will be found through this step. Considering desired error dynamics and (3.30),  $\mathbf{k}_v$  and  $\mathbf{k}_p$  are calculated as

$$\mathbf{k}_v = \begin{bmatrix} 10 & 0 \\ 0 & 10 \end{bmatrix}, \quad \mathbf{k}_p = \begin{bmatrix} 25 & 0 \\ 0 & 25 \end{bmatrix} \quad (4.16)$$

Gains  $\bar{\mathbf{G}}$  is determined as

$$\bar{\mathbf{G}}^{-1} = \begin{bmatrix} 0.5 & 0 \\ 0 & 0.2 \end{bmatrix} \quad (4.17)$$

Fourth, PID control of the previous study is designed by considering TDC. Then, PID gains are denoted as

$$\mathbf{K} = \begin{bmatrix} 5000 & 0 \\ 0 & 2000 \end{bmatrix}$$

$$\mathbf{T}_I = \begin{bmatrix} 0.4 & 0 \\ 0 & 0.4 \end{bmatrix}$$

$$\mathbf{T}_D = \begin{bmatrix} 0.1 & 0 \\ 0 & 0.1 \end{bmatrix}$$

(4.18)

### 4.3.3 Simulation Result

Position trajectories of backstepping control with TDE, nonlinear damping and the proposed PID control are shown in Fig. 4.8 (a), (b). Each position trajectory seems to be one line, but is actually two lines, one on top of the other. The position trajectories of the controllers follow the desired trajectory well as shown in Fig. 4.8 (a),

(b). Each position error is compared to confirm the equivalent relationship between the two controllers in Fig. 4.8 (c), (d).

To prove the equivalent relationship of the two controllers, the control inputs of joints were compared and are shown in Fig. 4.9 (a), (b). As these look similar, the difference between two control inputs is calculated as defining the difference of control inputs ( $\mathbf{u}_{Back} - \mathbf{u}_{PID}$ ) and is shown in Fig. 4.9 (c), (d) to give more detail. The ranges of difference are small. As was already mentioned in the above simulation, this result means the equivalent relationship between backstepping control with TDE, nonlinear damping and the proposed PID control has been achieved.

Considering the ranges of gains with (3.24), the ranges of PID gains are arranged as

$$\begin{aligned} \begin{bmatrix} 5000 & 0 \\ 0 & 2000 \end{bmatrix} < \mathbf{K} \leq \begin{bmatrix} 5000 + 2500w_{11} & 0 \\ 0 & 2000 + 2000w_{22} \end{bmatrix}, \\ \begin{bmatrix} 0.2 & 0 \\ 0 & 0.2 \end{bmatrix} \leq \mathbf{T}_I < \begin{bmatrix} 0.4 & 0 \\ 0 & 0.4 \end{bmatrix}, \\ \text{diag}(0, \dots, 0) \leq \mathbf{T}_D < \begin{bmatrix} 0.1 & 0 \\ 0 & 0.1 \end{bmatrix}. \end{aligned} \quad (4.19)$$

With (4.19), the ranges and patterns of the proposed PID gains are shown in Fig. 4.10. In addition, each range and pattern of each gain can be anticipated as was mentioned in the above simulation. In Fig. 4.10, diagonal elements of PID gains are only shown since other elements are zero.

To analyze PID gains in detail, nonlinear damping component  $\mathbf{w}$  is removed from the proposed PID control.

Then, PID gains are shown in Fig. 4.11 and represented as

$$\mathbf{K} = \begin{bmatrix} 5000 & 0 \\ 0 & 2000 \end{bmatrix}$$

$$\mathbf{T}_I = \begin{bmatrix} 0.4 & 0 \\ 0 & 0.4 \end{bmatrix}$$

$$\mathbf{T}_D = \begin{bmatrix} 0.1 & 0 \\ 0 & 0.1 \end{bmatrix}$$

(4.20)

where each gain is expressed as a constant diagonal matrix.

The constant gain  $\mathbf{K}$  is smaller than the variable gain  $\mathbf{K}$  and the constant gain  $\mathbf{T}_I$  and  $\mathbf{T}_D$  are larger than the variable gain  $\mathbf{T}_I$  and  $\mathbf{T}_D$ . That is, gain  $\mathbf{K}$  increases and the gain  $\mathbf{T}_I$  and  $\mathbf{T}_D$  decreases by applying nonlinear damping. Note that results of (4.20) are the same as (4.18).

In Section 3.4, the proposed PID control without nonlinear damping was compared with the previous study [4].

The results show that if nonlinear damping is removed, the relationship between backstepping control with TDE, nonlinear damping and the proposed PID control has the same relationship between TDC and PID control.

To prove this result, when there is no nonlinear damping, the PID control and original TDC are compared in the same manner. These results are shown in Fig. 4.12 and Fig. 4.13 respectively. That is, the proposed PID control without nonlinear damping is considered as TDC. In addition, performance of the proposed PID control and a previous PID control are compared in Fig. 4.14 and Fig. 4. 15.

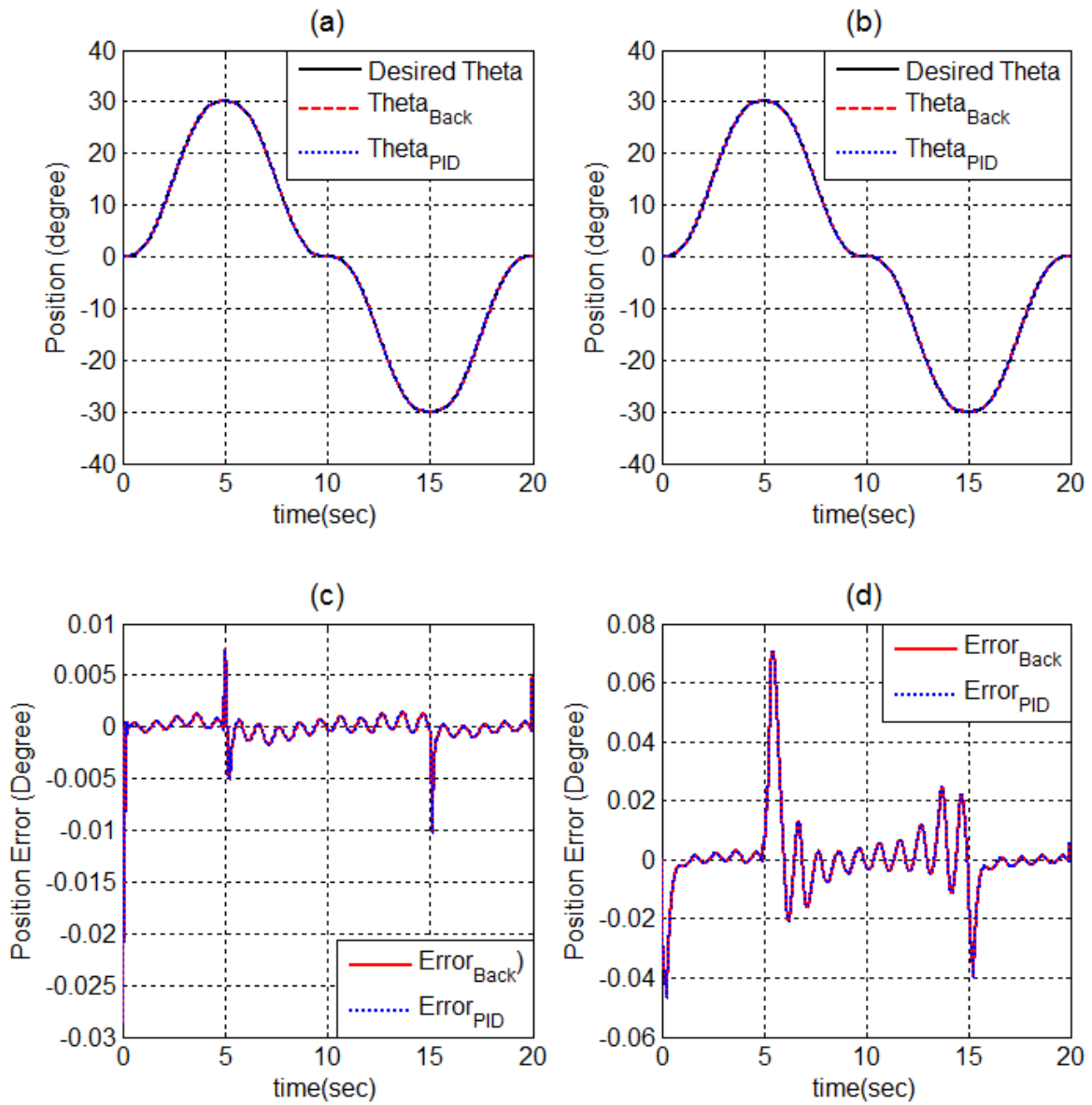


Fig. 4.8. (a) Position trajectory of Joint 1, (b) Position trajectory of Joint 2, (c) Position error of Joint 1, and (d)

Position error of Joint 2 by backstepping control with TDE, nonlinear damping and the proposed PID control.

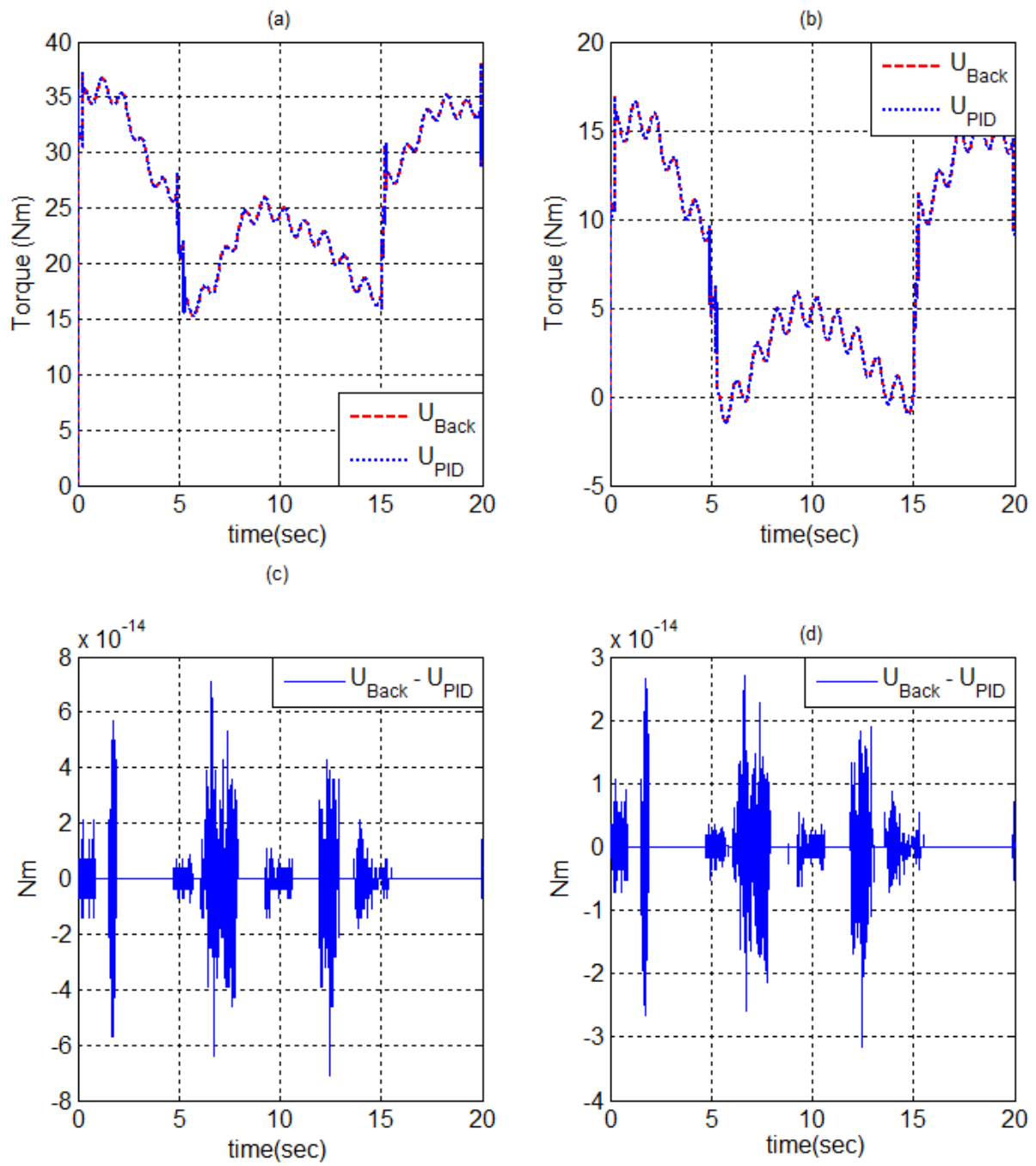


Fig. 4.9. (a), (b) Control inputs, (c), (d) Control input difference of each joint by backstepping control with TDE,

nonlinear damping and the proposed PID control

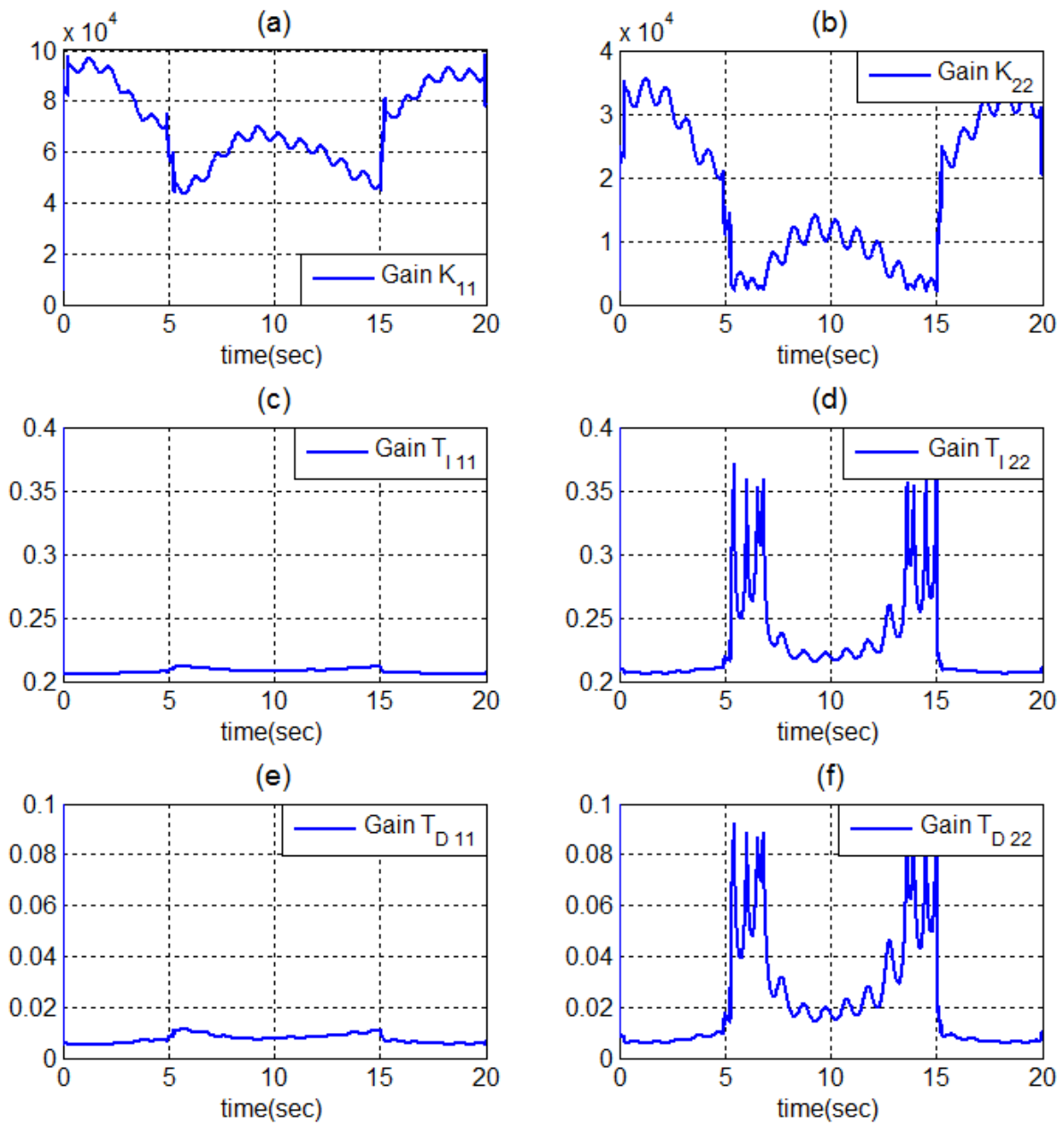


Fig. 4.10. (a), (b) Gain  $\mathbf{K}$ , (c), (d) Gain  $\mathbf{T}_I$ , and (e), (f) Gain  $\mathbf{T}_D$  of the proposed PID control.

The diagonal elements are only shown.

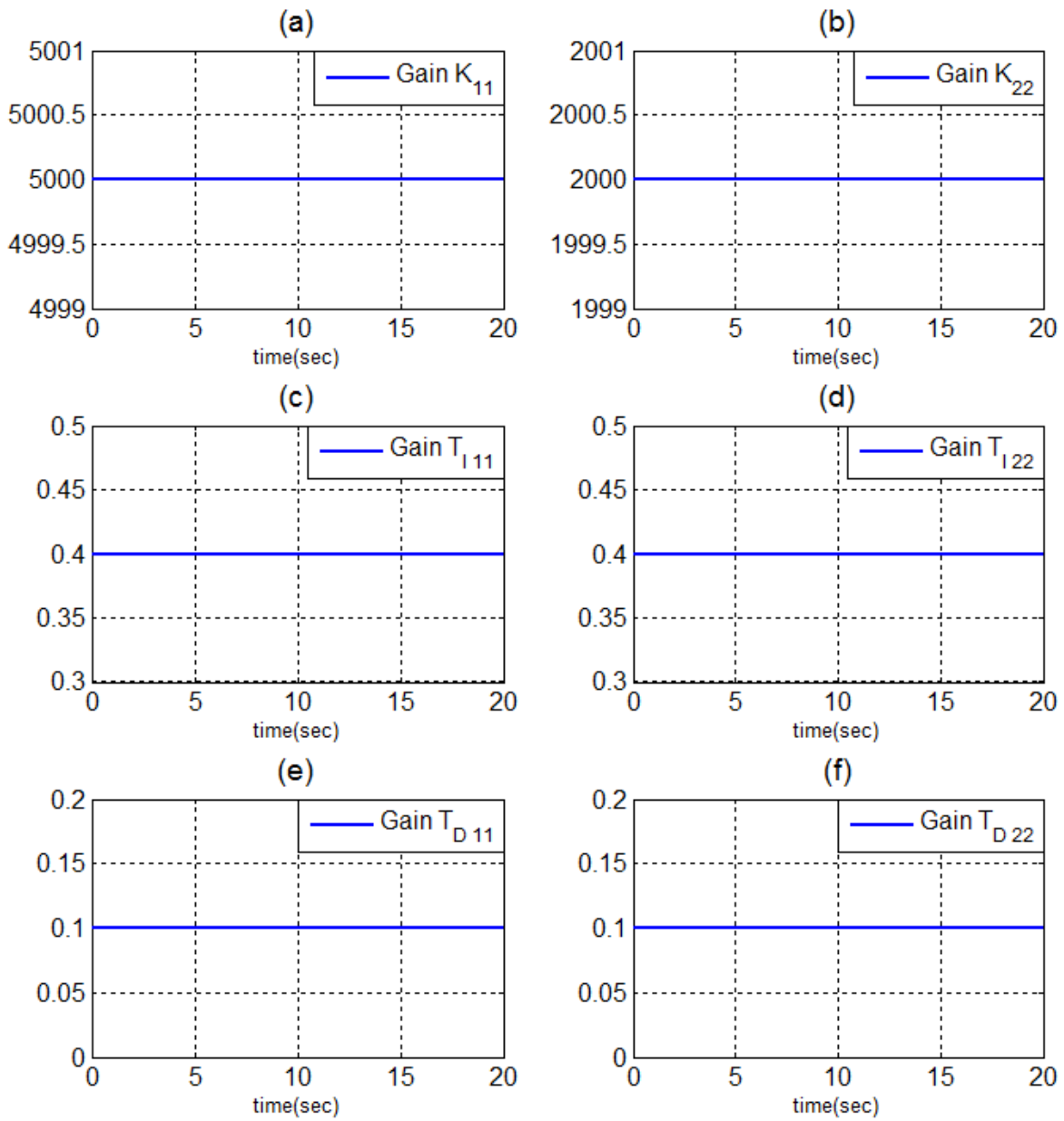


Fig. 4.11. (a), (b) Gain  $\mathbf{K}$ , (c), (d) Gain  $\mathbf{T}_I$ , and (e), (f) Gain  $\mathbf{T}_D$  of the proposed PID control without nonlinear

damping. The diagonal elements are only shown.

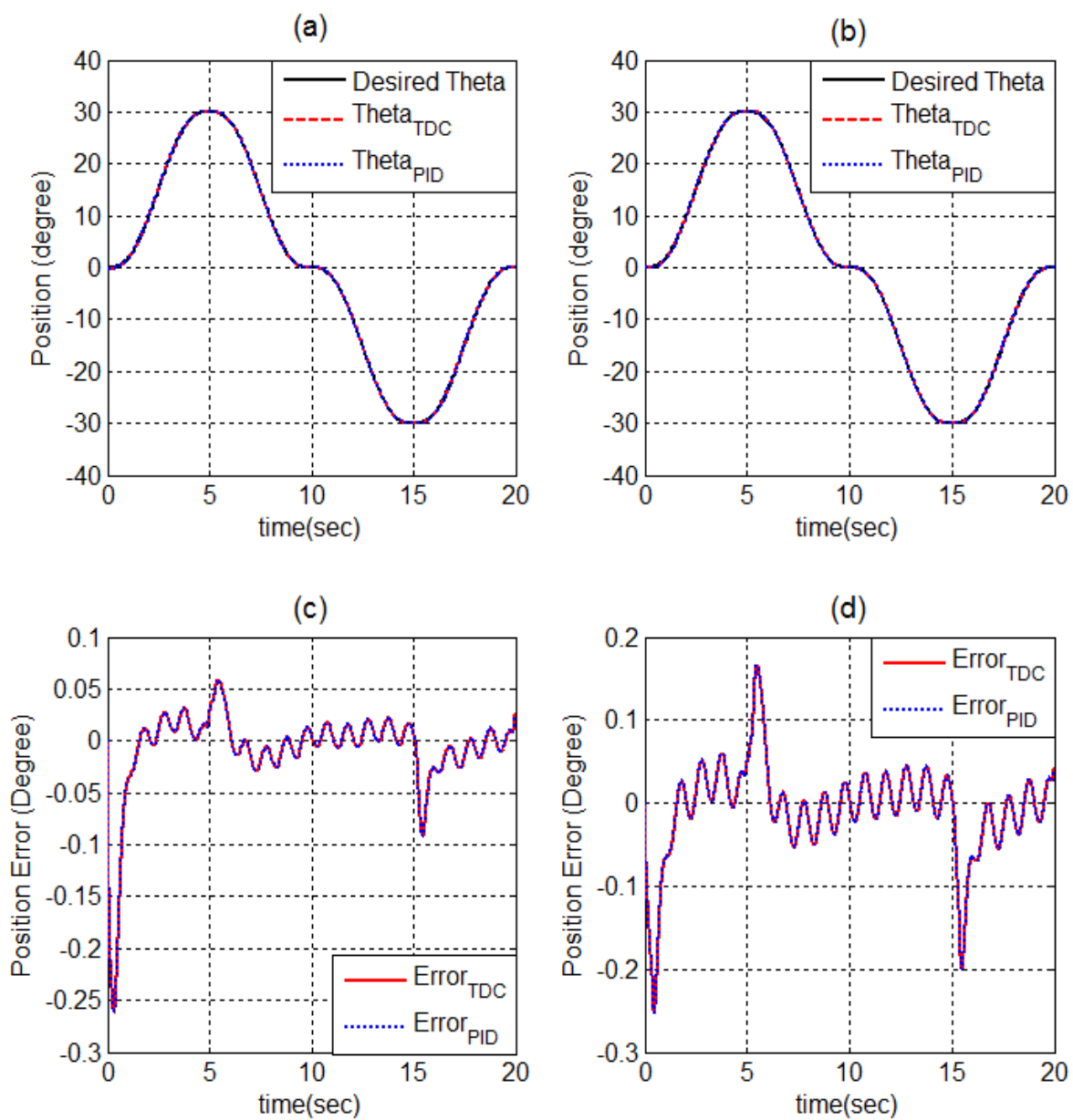


Fig. 4.12. (a) Position trajectory of Joint 1, (b) Position trajectory of Joint 2, (c) Position errors of Joint 1, and (d) Position errors of Joint 2 by TDC and PID control without nonlinear damping



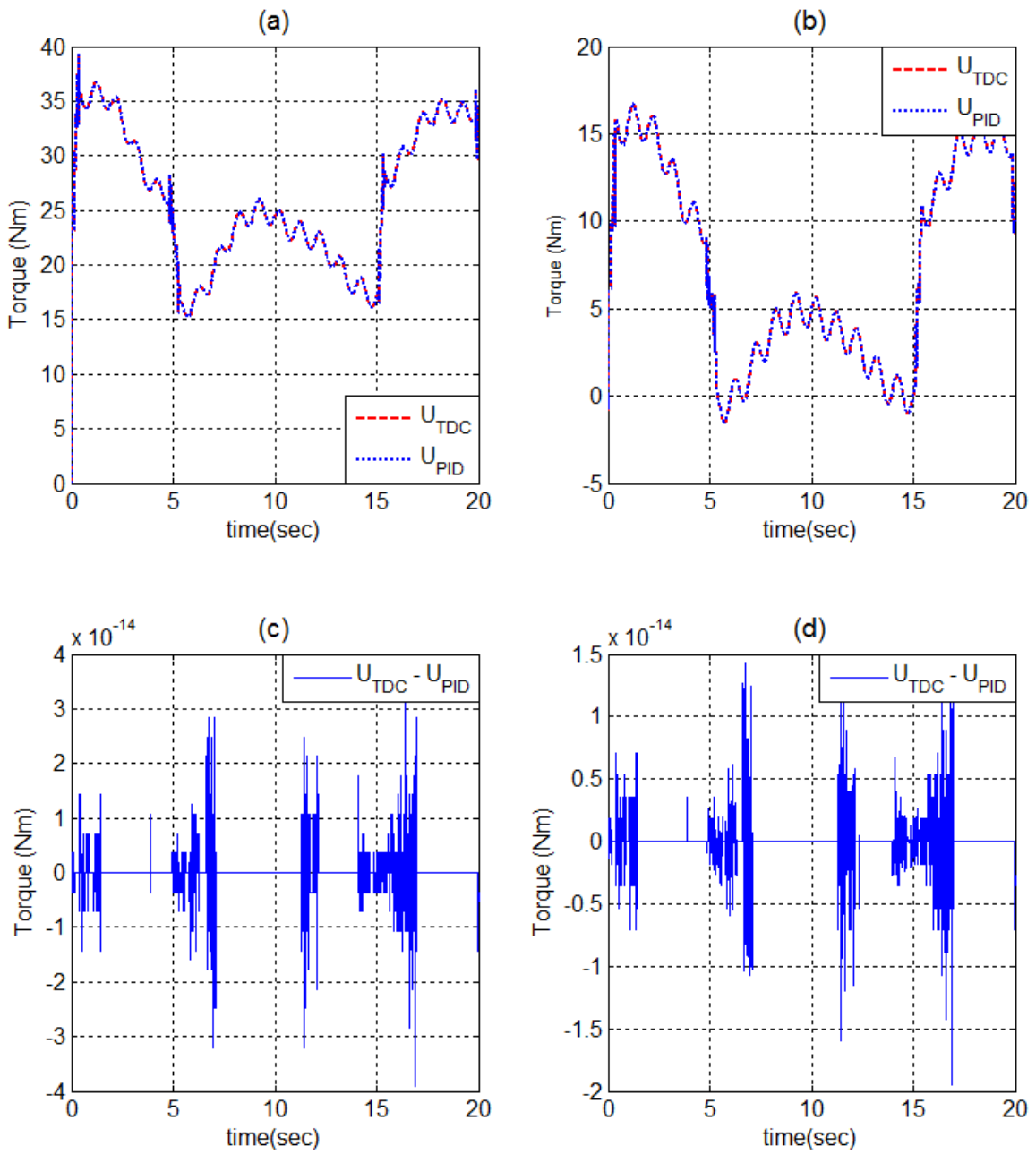


Fig. 4.13. (a) Control inputs of Joint 1, (b) Control inputs of Joint 2, (c) Control input difference of Joint 1, and

(d) Control input difference of Joint 2 by TDC and PID control without nonlinear damping

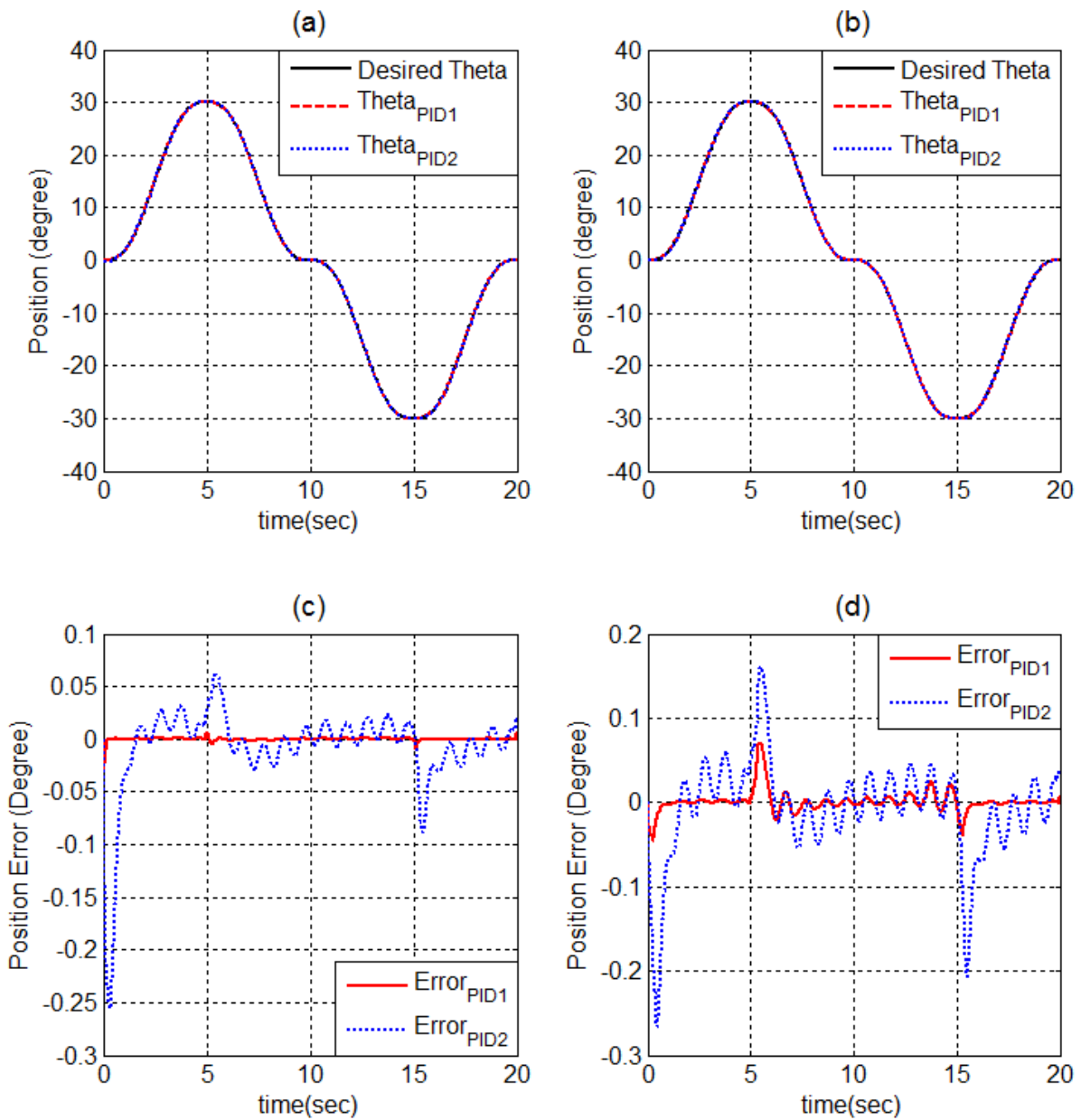


Fig. 4.14. (a) Position trajectory of Joint 1, (b) Position trajectory of Joint 2, (c) Position errors of Joint 1, and

(d) Position errors of Joint 2 by the proposed PID control (PID1) and the previous PID control (PID2)

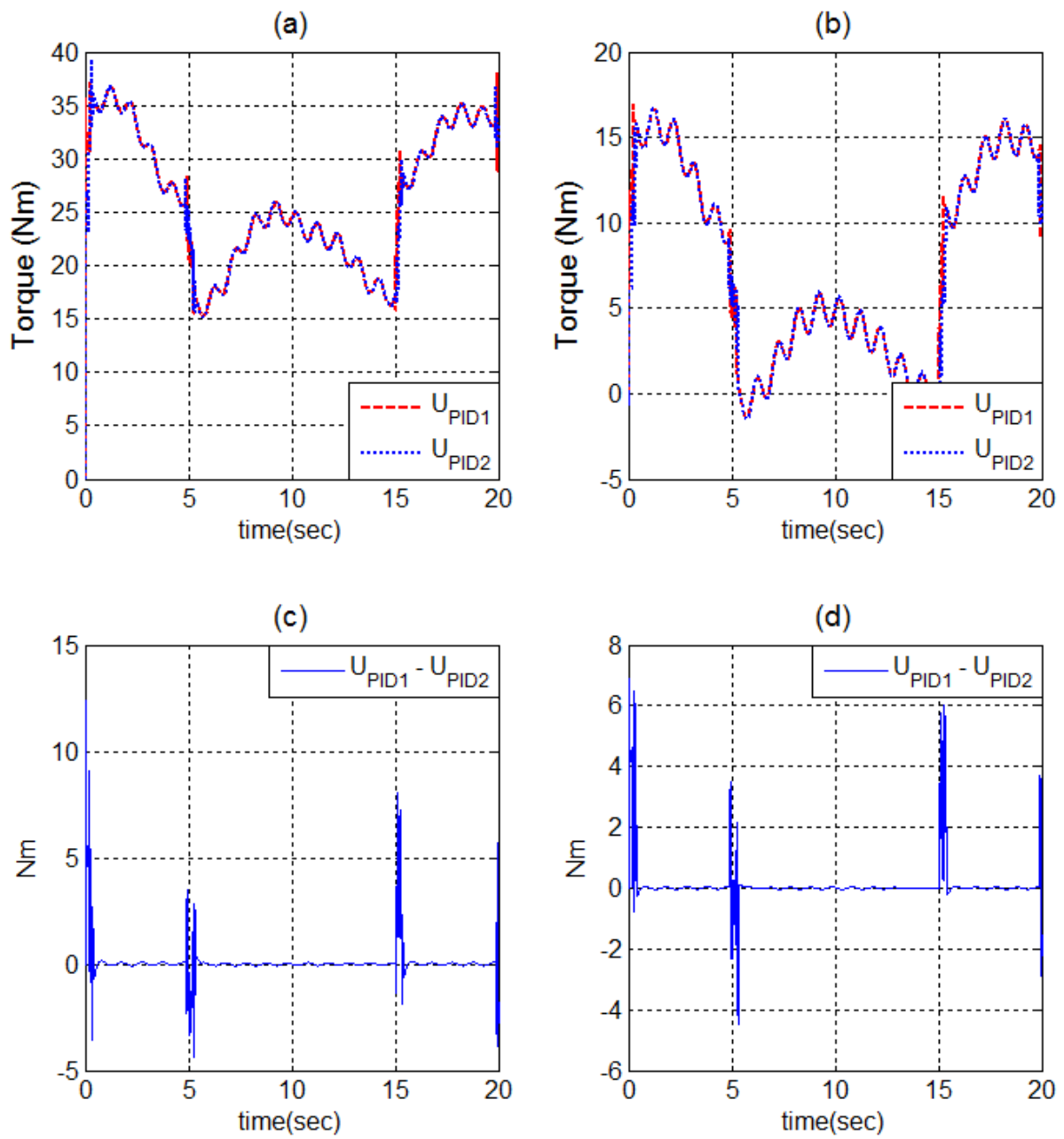


Fig. 4.15. (a) Control inputs of Joint 1, (b) Control inputs of Joint 2, (c) Control input difference of Joint 1, and (d) Control input difference of Joint 2 by the proposed PID control (PID1) and the previous PID control (PID2)

## 4.4 Conclusion

In this chapter, simulation was conducted to verify the equivalent relationship between the proposed PID control and backstepping control with TDE, nonlinear damping. The proposed method was identified through the equivalent relationship of the two controls. The control inputs, positions, and position errors of the two controllers were similar with each other. The range and patterns of PID gains could be anticipated by using nonlinear damping and (3.23). In addition, considering the proposed PID control without nonlinear damping, since the controller corresponds to TDC, a correlation between the previous study [4] and the proposed study was discovered. Then, robustness of the proposed PID controller was validated when comparing the proposed PID control and the previous PID control by TDC.

# Chapter 5. Experiment

## 5.1 Introduction

To validate the equivalent relationship between backstepping control with TDE, nonlinear damping, simulation and the proposed PID control was conducted. Then, relationship was proved in Chapter 4. To apply this relationship to the real systems, experiment will be implemented by using a conventional 6DOF PUMA type robot that is shown in Fig. 5.1.

## 5.2 Experiment

### 5.2.1. Experimental Setup

A 6-DOF PUMA robot (Samsung Faraman-AT2) was used for this experiment and is shown in Fig. 5.1. Only three joints are used from the base, however, it is enough to validate the equivalent relationships. AC servo motors are used to transmit power through a harmonic drive with gear ratios of 120:1, 120:1, and 100:1 for Joints 1, 2, and 3 respectively. The maximum continuous torque is 0.637, 0.319, and 0.319 Nm for Joints 1, 2, and 3 respectively. Each joint has an encoder with a resolution of 2048 pulse/rev attached at its shaft to sense the angular displacement. Thus, the resolution of each robot joint is  $3.66 \times 10^{-4} \text{ deg}$  (quadrature encoder).

The controller is operated in Linux-RTAI that is a real-time operating system environment with a sampling frequency of 1 kHz.

The desired trajectory of each joint is shown in Fig. 5.2 and is not applied to other joints.



Fig. 5.1.The 6 DOF PUMA robot (Samsung Faraman – AT2)

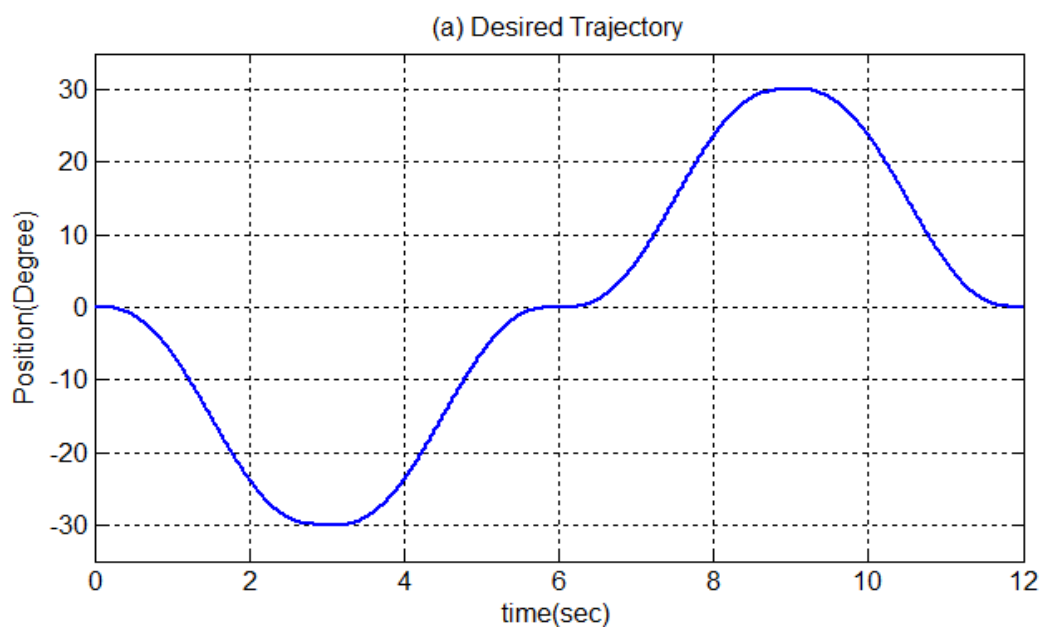


Fig. 5.2.The desired trajectory of Joints 1, 2, and 3

### 5.2.2. Design of Controllers

To prove the equivalent relationship between backstepping control with TDE, nonlinear damping and the proposed PID control, each controller will be compared. After designing backstepping control with TDE and nonlinear damping, the equivalent PID control is designed by using gains of backstepping control with TDE and nonlinear damping, and a sampling time in (3.22)

The sampling time is adopted as  $L = 0.002$  sec although the operation system environment has a sampling frequency of 1 kHz due to the effect of the sensor resolution and the numerical differentiation [20]. In practice, when the sampling time is 1msec in the experiment, control inputs changed rapidly at unspecific points because making control input require velocity states by numerical differentiation. In addition, the experiment was conducted for 12 sec.

First, backstepping control with TDE, nonlinear damping is designed to compare the proposed PID control.

The desired error dynamics are selected as considering damping ratio  $\xi = 1$  and natural frequency  $\omega = 10$  Hz.

According to the design method in [7],  $\mathbf{c}_1$  and  $\mathbf{c}_2$  are calculated as

$$\begin{aligned}\mathbf{c}_1 &= \text{diag}(10.0, 10.0, 10.0), \\ \mathbf{c}_2 &= \text{diag}(10.0, 10.0, 10.0)\end{aligned}\tag{5.1}$$

and nonlinear damping component  $\mathbf{w}$  is designed as

$$\mathbf{w} = \hat{\mathbf{F}} + \boldsymbol{\beta} + \boldsymbol{\rho} \quad (5.2)$$

where

$$\hat{\mathbf{F}} = \text{diag}(\dot{q}_1^2 + \dot{q}_2^2 + \dot{q}_3^2 + 1.0 \times 10^{-6}, \dots, \dot{q}_1^2 + \dot{q}_2^2 + \dot{q}_3^2 + 1.0 \times 10^{-6})$$

$$\boldsymbol{\beta} = \text{diag}(|\dot{\alpha}_1|, |\dot{\alpha}_2|, |\dot{\alpha}_3|)$$

$$\boldsymbol{\rho} = \text{diag}(|\hat{\mathbf{H}}_1|, |\hat{\mathbf{H}}_2|, |\hat{\mathbf{H}}_3|) \quad (5.3)$$

The bounding function  $\hat{\mathbf{F}}$  is determined by considering robot dynamics that are unknown, and  $1.0 \times 10^{-6}$  of

$\hat{\mathbf{F}}$  was used to keep  $\hat{\mathbf{F}}$  positive definite. Nonlinear damping component  $\mathbf{w}$  depends on feedback states.

Gains  $\bar{\mathbf{G}}, \mathbf{k}$  are tuned as

$$\bar{\mathbf{G}}^{-1} = \text{diag} ( 0.015, 0.012, 0.012)$$

$$\mathbf{k} = \text{diag} ( 50.0, 50.0, 50.0) \quad (5.4)$$

Second, considering PID control, the control input of PID control is denoted by the equivalent relationship

(3.18). Then, PID gains are represented as

$$\mathbf{K} = \text{diag}(150 + 375w_{11}, 120+300w_{22}, 120+300w_{33})$$

$$\mathbf{T}_I = \text{diag}\left(\frac{20 + 50w_{11}}{100+500w_{11}}, \frac{20 + 50w_{22}}{100+500w_{22}}, \frac{20 + 50w_{33}}{100+500w_{33}}\right)$$

$$\mathbf{T}_D = \text{diag}\left(\frac{1}{20 + 50w_{11}}, \frac{1}{20 + 50w_{22}}, \frac{1}{20 + 50w_{33}}\right)$$

(5.5)



where  $\mathbf{w} = \begin{bmatrix} w_{11} & \cdots & 0 \\ \vdots & \ddots & \vdots \\ 0 & \cdots & w_{33} \end{bmatrix}$  and  $\mathbf{w}$  is a positive definite diagonal matrix.

Third, time delay control (TDC) is designed to compare the proposed method. Relationship between proposed method and the previous study of [4] will be found through this step. Considering desired error dynamics and

(3.30),  $\mathbf{k}_v$  and  $\mathbf{k}_p$  are calculated as

$$\begin{aligned} \mathbf{k}_v &= \text{diag}(20.0, 20.0, 20.0) \\ \mathbf{k}_p &= \text{diag}(100.0, 100.0, 100.0) \end{aligned} \tag{5.6}$$

Gains  $\bar{\mathbf{G}}$  is determined as

$$\bar{\mathbf{G}}^{-1} = \text{diag}(0.015, 0.012, 0.012) \tag{5.7}$$

Fourth, PID control of the previous study is designed by considering TDC. Then, PID gains are denoted as

$$\begin{aligned} \mathbf{K} &= \text{diag}(150, 120, 120) \\ \mathbf{T}_I &= \text{diag}(0.2, 0.2, 0.2) \\ \mathbf{T}_D &= \text{diag}(0.05, 0.05, 0.05) \end{aligned} \tag{5.8}$$

### 5.2.3. Experimental Result

The desired trajectories assigned to the robot manipulator and the position trajectories generated by the system are shown in Fig. 5.3 (a), (c), and (e). The position trajectories follow the desired trajectories well as shown in Fig. 5.3 (a), (b), and (e). The position errors of each joint are represented and compared to confirm the equivalent relationship between the two controls in Fig. 5.3 (b), (d) and (f).

To validate the equivalent relationship of the two control inputs, the control inputs of each joint are compared and shown in Fig. 5.4 (a), (c), and (e). Although the results look similar, to investigate in detail, the difference between the two control inputs is calculated as defining difference of control inputs ( $\mathbf{u}_{Back} - \mathbf{u}_{PID}$ ) and shown in Fig. 5.4 (b), (d), and (f).

The difference was larger than the simulation results since the initial position is always changed by physical phenomena such as gravity when the robot manipulator is controlled. That difference occurred even if the same control methods were used twice in the experiment. To solve this phenomenon, control inputs and control input difference were transferred from discrete time domain to frequency domain by Fast Fourier Transform (FFT). Since control inputs are discrete and aperiodic signals, these can be considered in the frequency domain. The results were shown in Fig. 5.5. Control inputs were regarded as the same control inputs in the frequency domain since the range of control input difference is small. Thus, the equivalent relationship between backstepping

control with TDE, nonlinear damping and the proposed PID control was achieved.

Using variable PID control by proposed equivalent relationship, the gains  $\mathbf{K}$ ,  $\mathbf{T}_I$ , and  $\mathbf{T}_D$  are shown in Fig.

5.6. The gains  $\mathbf{K}$ ,  $\mathbf{T}_I$ , and  $\mathbf{T}_D$  are 3 by 3 diagonal matrices. Considering a range of gains with (3.24) in PID control, the range of each gain is arranged as

$$\text{diag}(150,120,120) < \mathbf{K} \leq \text{diag}(150+375w_{11}, 120+300w_{22}, 120+300w_{33})$$

$$\text{diag}(0.1, 0.1, 0.1) \leq \mathbf{T}_I < \text{diag} (0.2, 0.2, 0.2)$$

$$\text{diag}(0, 0, 0) \leq \mathbf{T}_D < \text{diag} (0.05, 0.05, 0.05)$$

(5.6)

These ranges of gains are identified in Fig. 5.6. Note that only diagonal elements of gains are expressed since other elements are zero. As already mentioned in Chapter 3, the patterns of variable PID gains depend on nonlinear damping component  $\mathbf{w}$ . The nonlinear damping component  $\mathbf{w}$  and its elements are shown in Fig. 5.7.

Comparing  $\mathbf{w}$  in Fig. 5.7 and PID gains in Fig. 5.6,  $\mathbf{K}$  has the similar pattern with  $\mathbf{w}$  and  $\mathbf{T}_I$ ,  $\mathbf{T}_D$  have similar patterns with  $\mathbf{w}^{-1}$  since it was mentioned in (3.23) that  $\mathbf{w}$  is proportional to  $\mathbf{K}$  and inversely proportional to  $\mathbf{T}_I$  and  $\mathbf{T}_D$ .

Note that  $\boldsymbol{\rho}$  is not dominant relatively when elements  $\hat{\mathbf{F}}$ ,  $\boldsymbol{\beta}$ , and  $\boldsymbol{\rho}$  of  $\mathbf{w}$  are compared. Its result is different with simulations since control inputs are small relatively. The diagonal term of  $\boldsymbol{\rho}$  is expressed as

$$\boldsymbol{\rho} = \text{diag}(|\widehat{\mathbf{H}}_1|, |\widehat{\mathbf{H}}_2|, |\widehat{\mathbf{H}}_3|)$$

$$|\widehat{\mathbf{H}}| = \left| \mathbf{u}_{(t-L)} - \bar{\mathbf{G}}^{-1} \dot{\mathbf{z}}_{2(t-L)} \right| \quad (5.7)$$

where  $\mathbf{u}_{(t-L)}$  is dominant in  $|\widehat{\mathbf{H}}|$ . If control input  $\mathbf{u}$  is small,  $\boldsymbol{\rho}$  will decrease. In this case, since it is difficult to predict the pattern of PID gains by control inputs, nonlinear damping component  $\mathbf{w}$  must be used to anticipate patterns of PID gains.

In the simulation and Chapter 3, the proposed PID control without nonlinear damping was compared with the previous study [4]. The results show that, when there is no nonlinear damping, the proposed PID control was the same as the previous PID control by the relationship between TDC and PID control.

To prove the results in the real system, when nonlinear damping is removed, PID gains are shown in Fig. 5.8 and expressed as constant matrices. The constant gain  $\mathbf{K}$  is smaller than the variable gain  $\mathbf{K}$  with nonlinear damping and the constant gains  $\mathbf{T}_I$ ,  $\mathbf{T}_D$  are larger than the variable gains  $\mathbf{T}_I$ ,  $\mathbf{T}_D$  with nonlinear damping.

The proposed PID control without nonlinear damping was compared with the original TDC in the same manner with the simulation. These results are shown in Fig. 5.9 and Fig. 5.10 respectively. That is, the proposed PID control without nonlinear damping is considered as TDC. That is, correlation between the proposed study and the previous study is discovered.

Control performance is compared by using each PID control in Fig. 5.11. Although the desired trajectory and

each controlled position trajectory is similar, position errors and control inputs have difference between two controllers. The proposed PID control is more robust than the previous PID control as considering position errors.

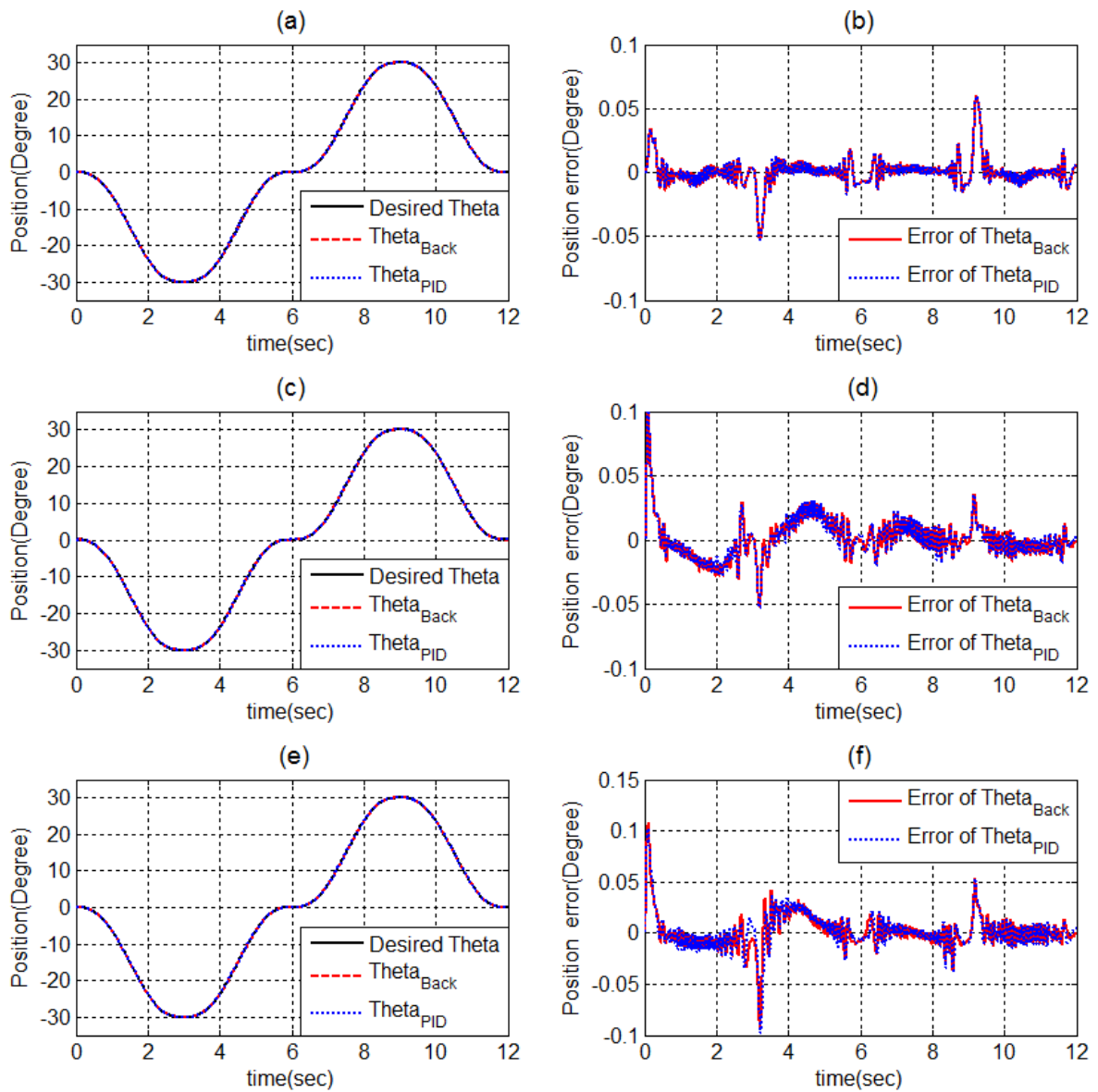


Fig. 5.3. (a) Position trajectories of Joint 1, (b) Position errors of Joint 2, (c) Position trajectories of Joint 2, (d)

Position errors of Joint 2, (e) Position trajectories of Joint 3, and (f) Position errors of Joint 3 by backstepping

control with TDE, nonlinear damping and the proposed PID control

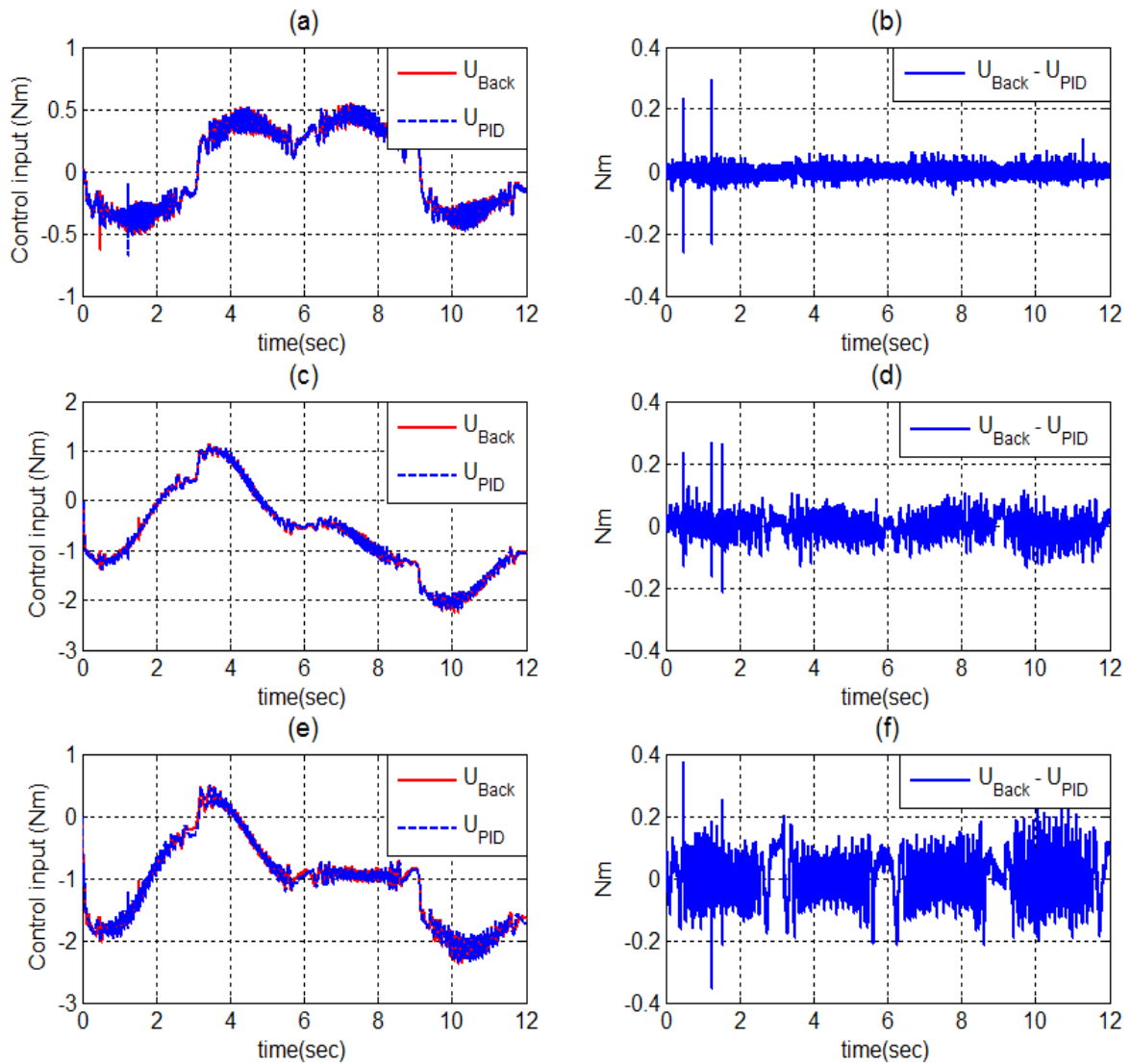


Fig. 5.4. (a) Control inputs of Joint 1, (b) Control input difference of Joint 1, (c) Control inputs of Joint 2, (d) Control input difference of Joint 2, (e) Control inputs of Joint 3, and (f) Control input difference of Joint 3 by

backstepping control with TDE, nonlinear damping and the proposed PID control in Time domain

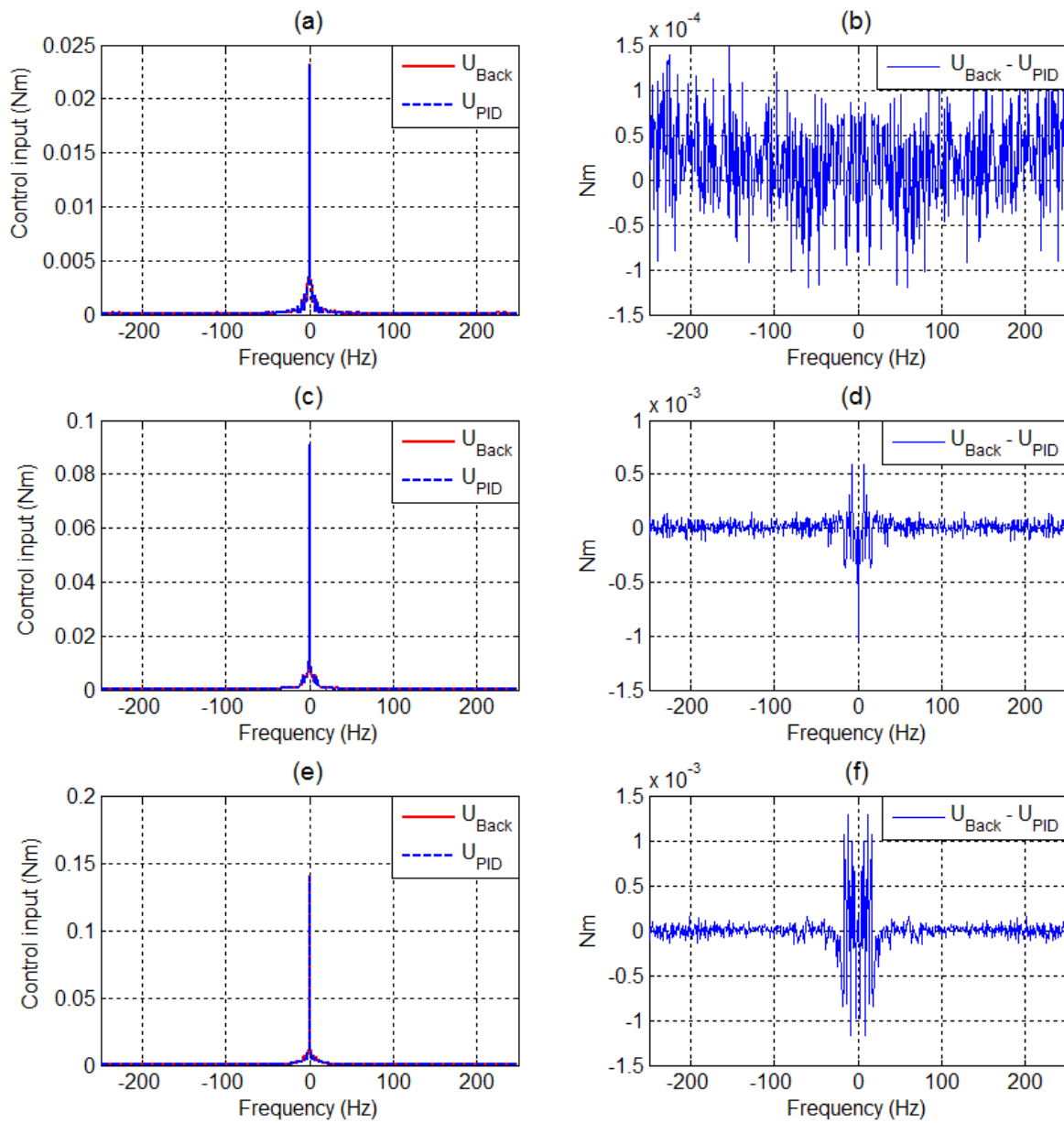


Fig. 5.5. (a) Control inputs of Joint 1, (b) Control input difference of Joint 1, (c) Control inputs of Joint 2, (d)

Control input difference of Joint 2, (e) Control inputs of Joint 3, and (f) Control input difference of Joint 3 by

backstepping control with TDE, nonlinear damping and the proposed PID control in Frequency domain



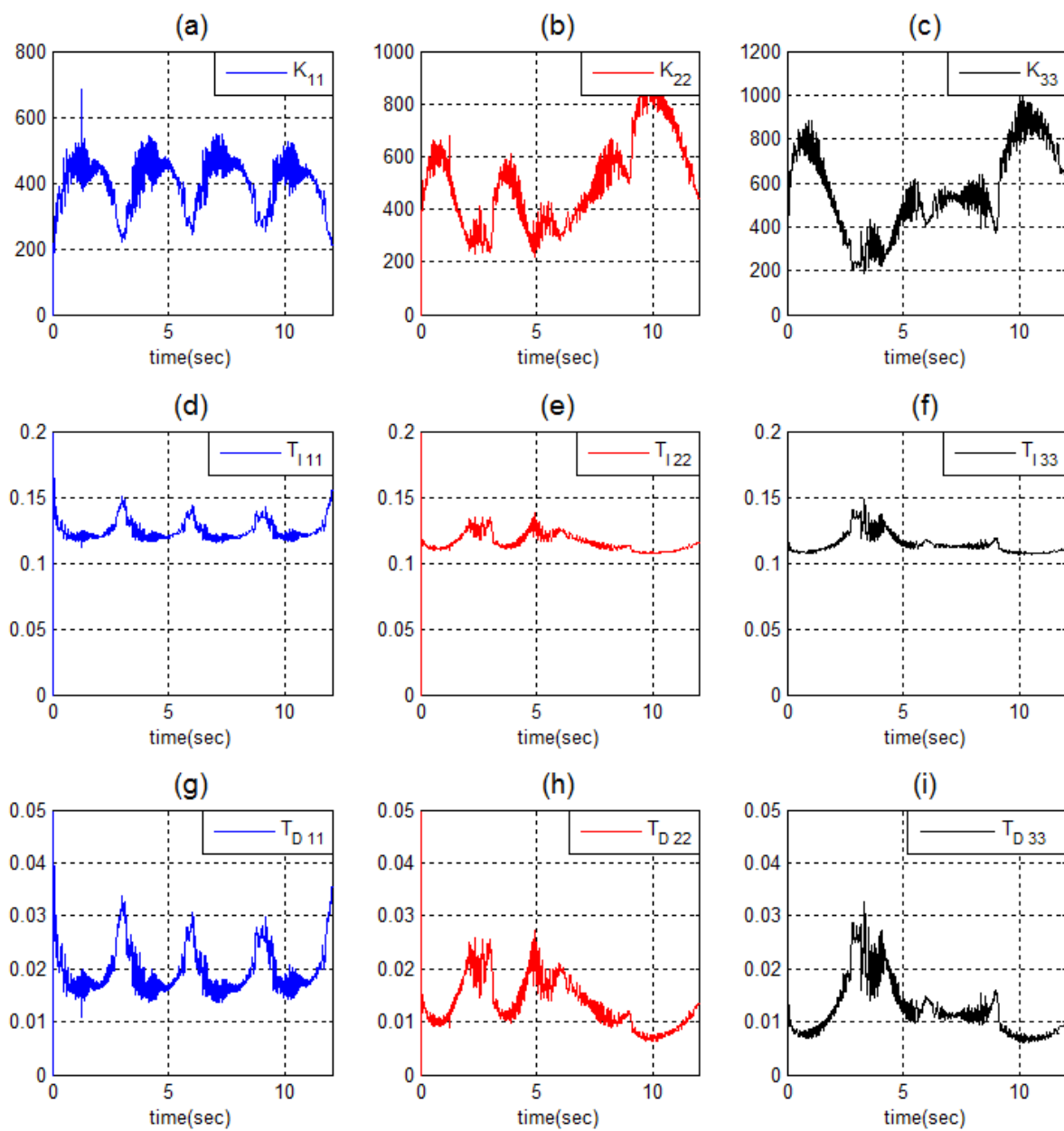


Fig. 5.6. (a),(b), and (c) Gain  $\mathbf{K}$ , (d),(e), and (f) Gain  $\mathbf{T}_I$ , and (g), (h), and (i) Gain  $\mathbf{T}_D$  of PID control.

The diagonal elements are only shown.

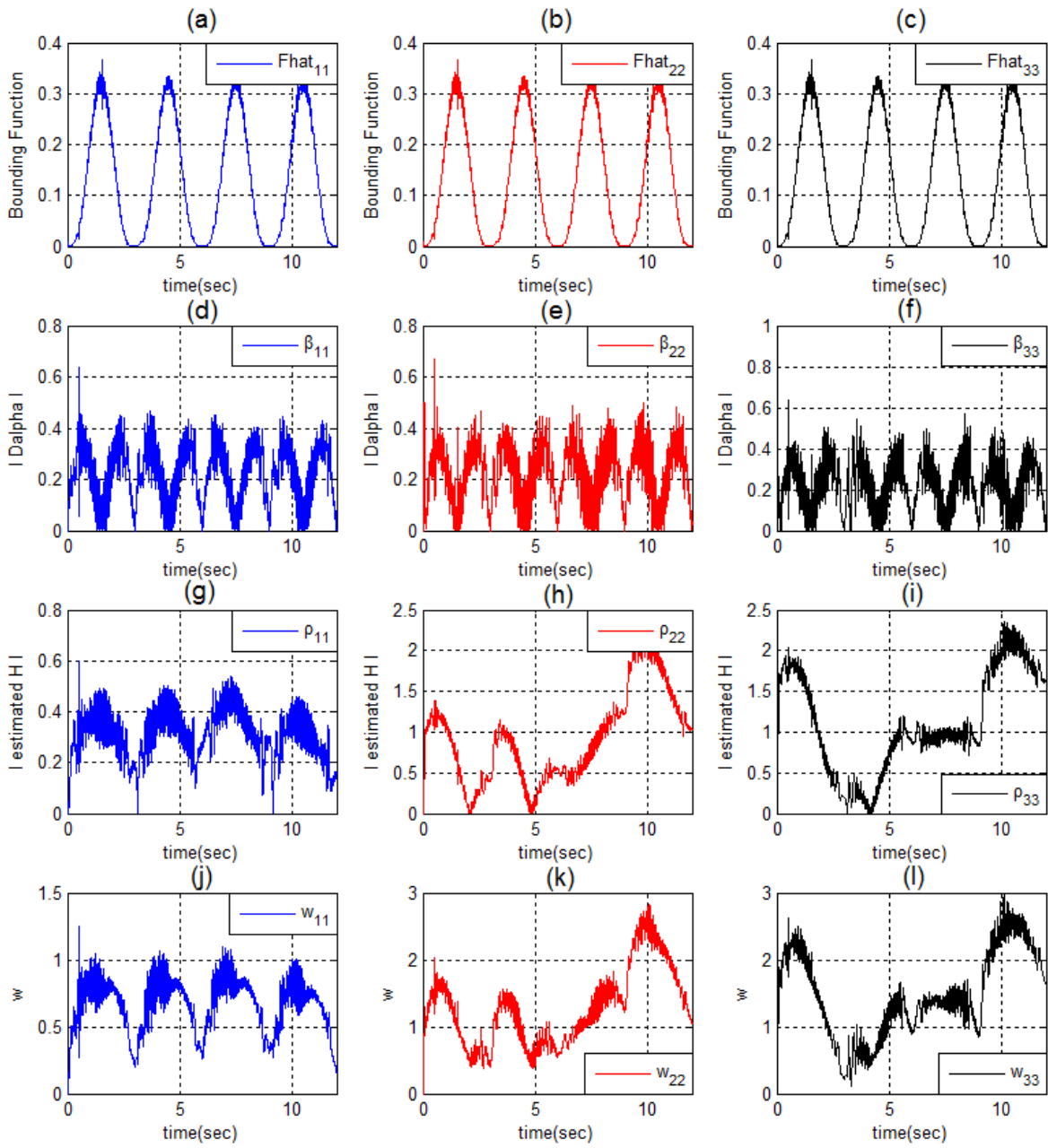


Fig. 5.7. (a), (b), and (c)  $\hat{\mathbf{F}}$ , (d), (e), and (f)  $\hat{\boldsymbol{\beta}}$ , (g), (h), and (i)  $\hat{\boldsymbol{\rho}}$ , and (j), (k), and (l)  $\hat{\mathbf{w}}$  of proposed PID

control. The diagonal elements are only shown.

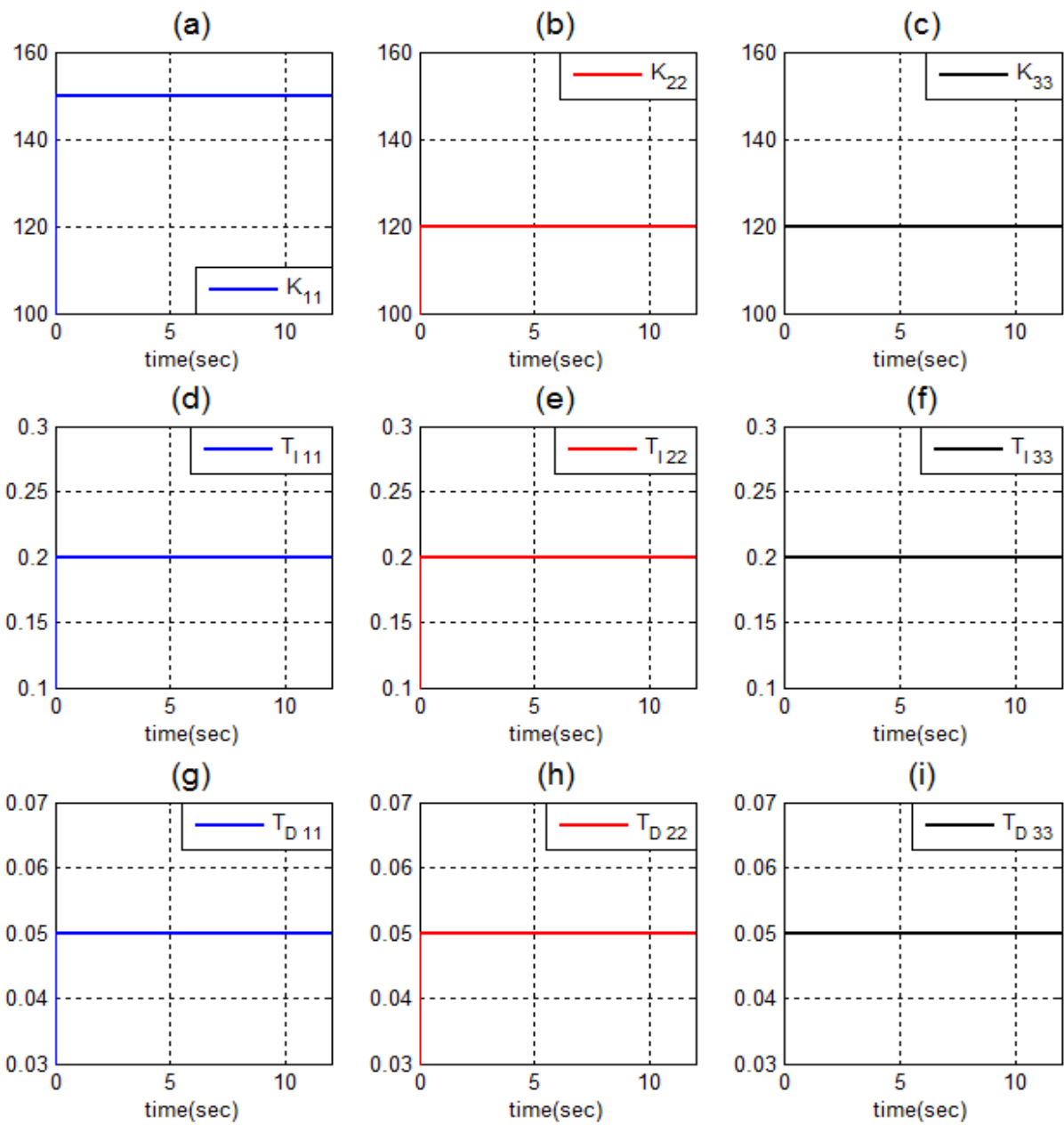


Fig. 5.8. (a),(b), and (c) Gain  $\mathbf{K}$ , (d),(e), and (f) Gain  $\mathbf{T}_I$ , and (g), (h), and (i) Gain  $\mathbf{T}_D$  of PID control without

nonlinear damping. The diagonal elements are only shown.

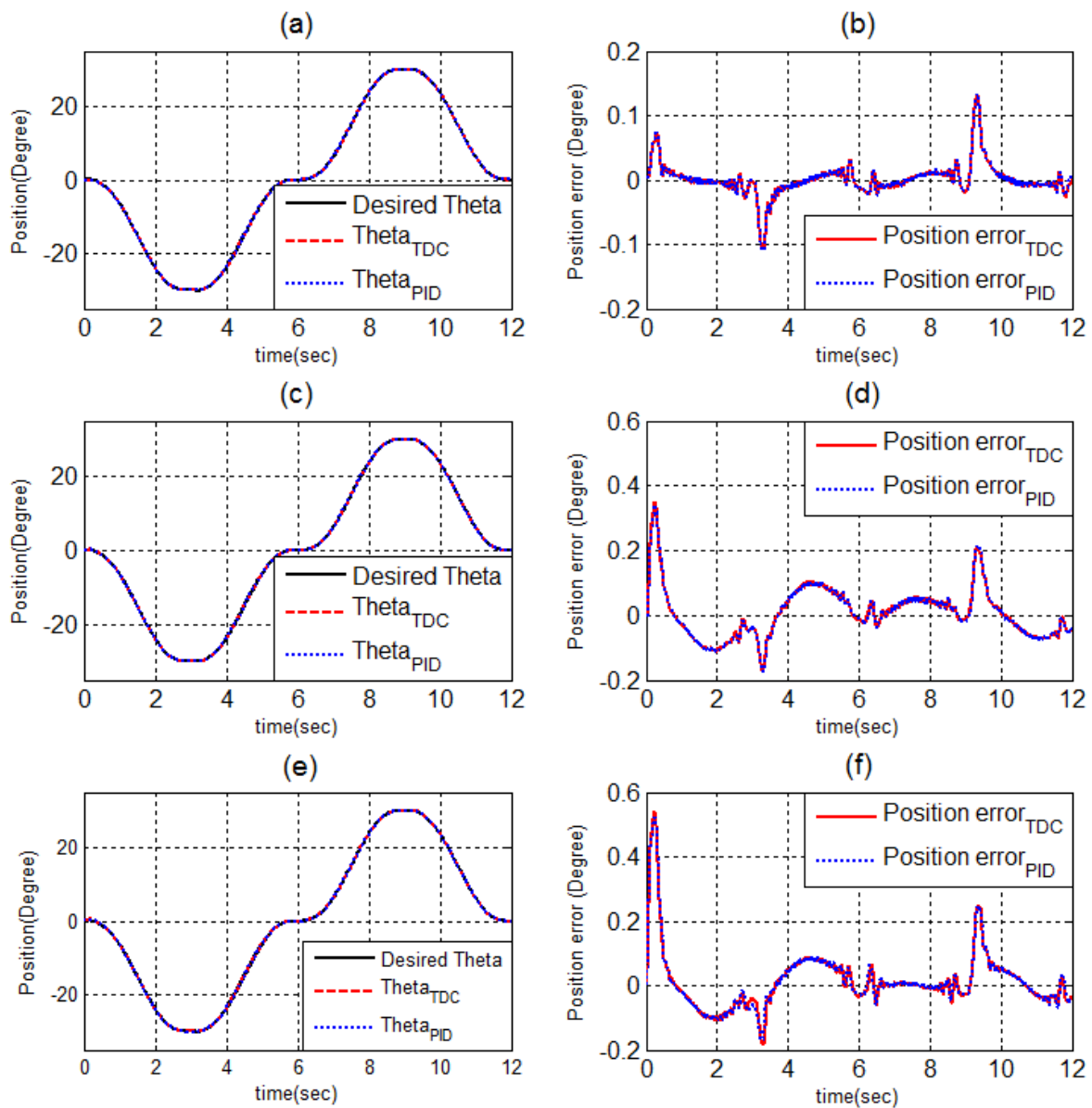


Fig. 5.9. (a) Position trajectories of Joint 1, (b) Position errors of Joint 2, (c) Position trajectories of Joint 2, (d)

Position errors of Joint 2, (e) Position trajectories of Joint 3, and (f) Position errors of Joint 3 by TDC and the

proposed PID control without nonlinear damping

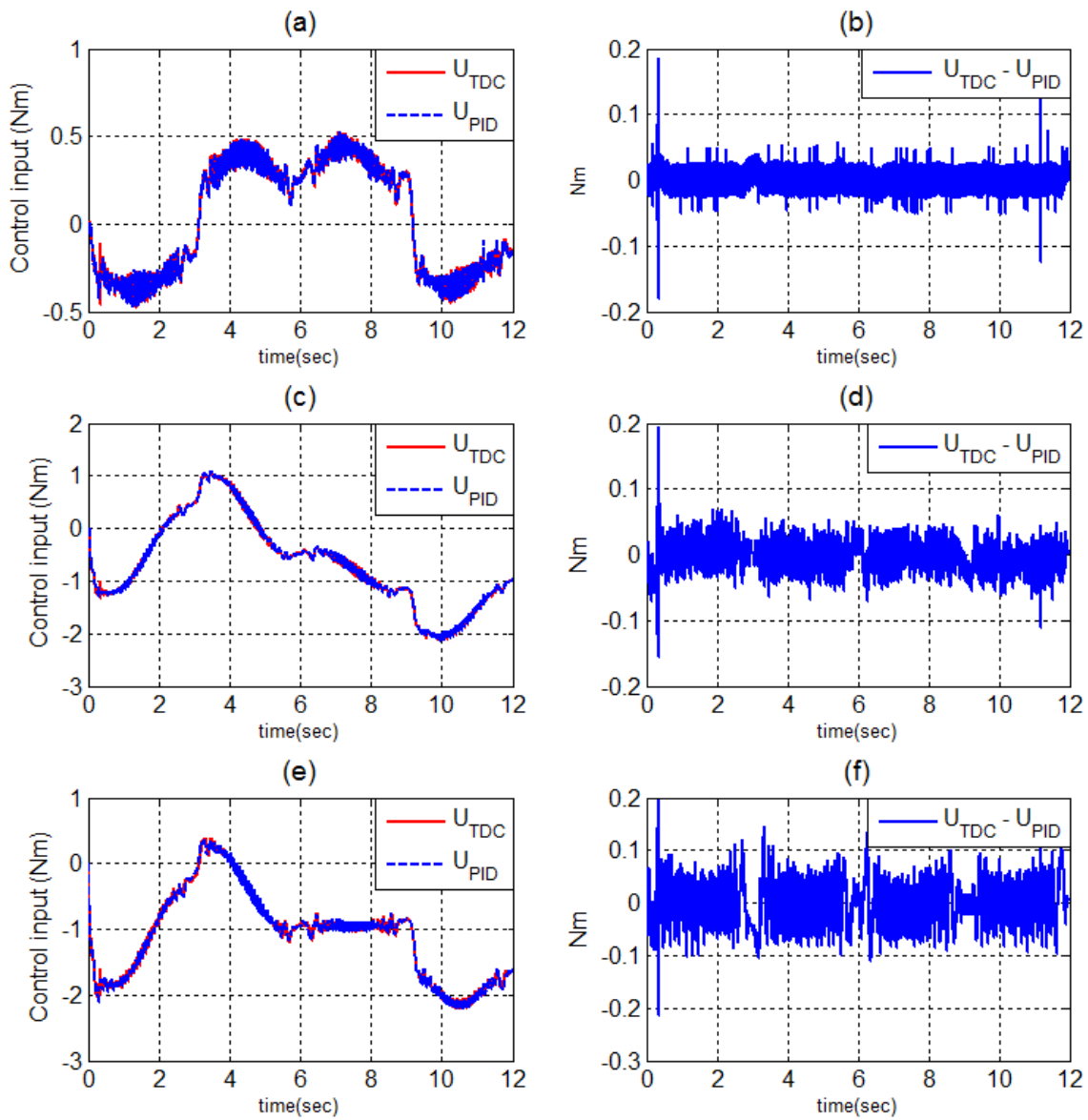


Fig. 5.10. (a) Control inputs of Joint 1, (b) Control input difference of Joint 1, (c) Control inputs of Joint 2, (d)

Control input difference of Joint 2, (e) Control inputs of Joint 3, and (f) Control input difference of Joint 2 by

TDC and PID control without nonlinear damping

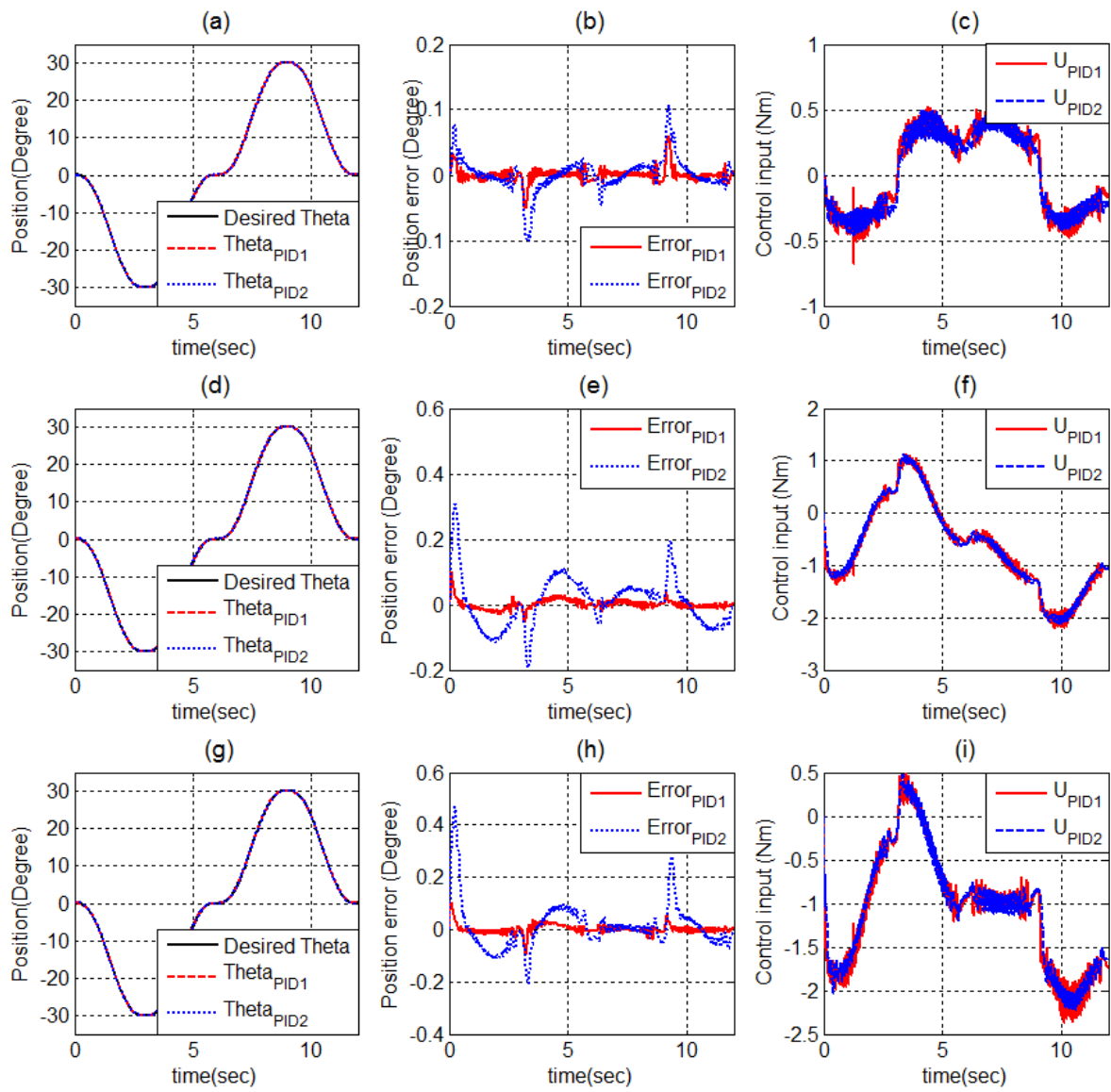


Fig. 5.11.(a),(d), and (g) Position trajectories of Joint 1,2, and 3, (b), (e), and (h) Position errors of Joint 1, 2, and 3, (c), (f), and (i) Control inputs of Joint 1,2, and 3 by the proposed PID control (PID1) and the previous

PID control (PID2)

### 5.3 Conclusion

In this chapter, the experiment was conducted to verify the equivalent relationship between backstepping control with TDE, nonlinear damping and the proposed PID control. The proposed method satisfied the equivalent relationship of the two controls. It was proved that control inputs, positions, and position errors of backstepping control with TDE, nonlinear damping correspond to positions, control inputs, and position errors of the proposed variable PID control. The range and patterns of PID gains could be anticipated by using nonlinear damping component  $\mathbf{w}$  and (3.23).

Considering the proposed PID control without nonlinear damping, the controller corresponded to the original TDC. Thus, the correlation between the previous study [4] and the proposed study was discovered. In addition, the proposed PID control was more robust than the previous PID control designed by TDC.

## Chapter 6. Conclusion

This thesis proposed the design method of robust PID control by using backstepping control with time delay estimation (TDE) and nonlinear damping. In the previous study by Chang et al. [4], a systematic design method of PID control for a class of nonlinear systems was presented by using time delay control (TDC). In this case, there was the inevitable problem of the so-called TDE error. Backstepping control with TDE, nonlinear damping solved this problem since TDE error is compensated by nonlinear damping [7].

In the proposal, it is considered that backstepping control with TDE, nonlinear damping would be related to PID control since PID control can be designed by TDC in the previous study. The equivalent relationship between the two controls is derived through theoretical analysis in the discrete time domain because many controllers are operated in digital devices.

The proposed PID control has the same characteristics with backstepping control including TDE, nonlinear damping. That is, the proposed PID control does not require exact information of robot dynamics and ensures closed-loop stability. Therefore, the proposed controller can be used in a nonlinear system, even one with hard nonlinearities such as the Coulomb friction and Stiction.



Considering the proposed PID control, PID gains derived from backstepping control with TDE and nonlinear damping are changed due to nonlinear damping during operation time. Thus, the proposed PID control has the advantages of variable structure controls such as variable structure PID control that use sliding modes. While variable structure PID controls with sliding modes have problems with chattering and complicated stability analysis, the proposed PID control does not consider these problems.

The equivalent relationship was proved through simulation and experiment. In the simulation, one-link and two-link robot models were used. Although there were nonlinear friction and continuous disturbance, the position trajectories tracked the desired trajectory well. In addition, comparing control inputs and position errors, each control has nearly similar results. In the experiment, a 6-DOF PUMA robot (Samsung AT2) was used to prove the proposed equivalent relationship between the two controls in the same manner.

After deriving the ranges of PID gains by using the equivalent relationship, characteristics of PID gains were discovered through simulation and experiment. As nonlinear damping was detected, the patterns of PID gains could be analyzed. Then, it was identified that the patterns and ranges of PID gains depend on nonlinear damping. Therefore, the pattern and range of PID gains can be anticipated by nonlinear damping.

When the proposed PID control without nonlinear damping was used, it was discovered that the control corresponds to TDC. That is, the correlation between the previous study [4] and the proposed study was

discovered. In addition, the proposed PID control and PID control of the previous study were compared in experiment. Then, it was verified that the proposed PID control is more robust than the previous PID control designed by TDC.

The proposed PID control has the same characteristics with backstepping control including TDE, nonlinear damping. It has high accuracy, counteracts TDE errors, and is theoretically stable. The proposed PID control can be used in industrial control systems. Consideration of tuning PID gains will be reduced and high accuracy and problems of stability will be solved by using the proposed PID control even if there is a nonlinear system that includes hard nonlinearities.

## Reference

- [1] Araki M, PID control, Control Systems, Robotics, and Automation, Vol.II, p.1-23(1995).
- [2] W. Li, X. G. Chang, F. M. Wahl, and J. Farrell, "Tracking control of a manipulator under uncertainty by fuzzy PID controller," Fuzzy Sets Syst., vol. 122, no. 1, pp. 125–137, 2001.
- [3] I. Cervantes and J. Alvarez-Ramirez, "On the PID tracking control of robot manipulators," Syst. Control Lett., vol. 42, no. 1, pp. 37–46, 2001.
- [4] P.H. Chang, J.H. Jung "A Systematic Method for Gain Selection of Robust PID Control for Nonlinear Plants of Second-Order Controller Canonical Form" in IEEE TRANSACTIONS ON CONTROL SYSTEMS TECHNOLOGY, VOL. 17, NO. 2, MARCH 2009
- [5] T. C. Hsia and L. S. Gao, "Robot manipulator control using decentralized linear time-invariant time-delayed joint controllers," in Proc. IEEE Int. Conf. Robot. Autom., 1990, pp. 2070–2075.
- [6] Z. H. Qu, "Robust control of nonlinear uncertain systems under generalized matching conditions," Automatica, vol. 29, no. 4, pp. 985–998, 1993.
- [7] Y. Jin, P. H. Chang, Y. S. Park., "Stability Analysis and Design of Time Delay Estimation Based Control for a Class of Nonlinear Uncertain Systems" in IEEE Conference on Decision and Control, pp.4084-4089, 2010.
- [8] P.H. Chang and S. H. Park, " On Improving Time-Delay Control under Certain Hard Nonlinearities," Mechatronics, vol. 13, no.4, pp. 393-412, 2003.
- [9] G.R. Cho, P. H. Chang, S.H. Park, and M Jin, "Robust tracking under nonlinear friction using time delay control with internal model," IEEE Trans. Control Systems Technology, vol. 17, no. 6, pp. 1406-1414, 2009.
- [10] M. Jin, S. H. Kang, and P. H. Chang, "Robust compliant motion control of robot with nonlinear friction using time-delay estimation," IEEE Trans. Ind. Electron., vol. 55, no. 1, pp. 258–269, 2008.
- [11] Pyung H. Chang and Jeong W. Lee, "A model reference observer for time delay control and its application to robot trajectory control", IEEE Trans. On Contl.. Vol 4, no.1, 1996
- [12] Z. J. Yang, H. Tsubakihara, S. Kanae, K. Wada, and C. Y. Su, "A novel robust nonlinear motion controller with disturbance observer," IEEE Trans. on Control Systems Technology, vol. 16, no. 1, pp. 137–147, 2008.

- [13] M. L. Krstic, Kanellakopoulos, and P.Kokotovic, Nonlinear and Adaptive Control Design. New York: Wiley, 1995.
- [14] Hassan k. Khalil, Nonlinear systems. Prentice hall, 1996
- [15] K. Youcef-Toumi and Osamu Ito, "A time delay controller for systems with unknown dynamics," Trans. Of ASME, J. Dyn. Sys. Meas., sontr, vol. 112, no. 1, pp. 133-142, 1990
- [16] H. K. Khalil, Nonlinear Systems (Third Edition). Upper Saddle River, NJ: Prentice-Hall, 2002.
- [17] Y. Jin, P. H. Chang, M. Jin, D. G. Gweon., "Stability guaranteed time delay control of manipulators using nonlinear damping and terminal sliding mode" in IEEE Trans. Industrial electronics, vol. \*, no.\*, 2012
- [18] M. Krstic, I. Kanellakopoulos, and P. V. Kokotovic, Nonlinear and Adaptive Control Design, New York, NY:John Willey & Sons, 1995
- [19] D.G. Zill nad M. R. Cullen, Advanced Engineering Mathmatics, PWS-KENT Publishing company, 1992.
- [20] E. Lee, J. Park, K.A. Loparo, C. B. Schrader and P.H. Chang. "Bang-Bang Impact Control Using Hybrid Impedance/ Time-Delay Control" , IEEE/ASME Transactions on Mechatronics, vol. 8, no.2,pp.272-277,2003.
- [21] J. H. Chung, P .H. Chang, "Backstepping using Time delay estimation", The Korean society of mechanical engineers, 춘계학술대회논문집, A, pp.577-582, 1998.
- [22] PID 2006, IEEE Contr. Syst. Mag., vol. 26, no. 1, Feb. 2006.
- [23] H. B. Kazemian, "The SOF-PID controller for the control of a MIMO robot arm," IEEE Trans. Fuzzy Syst., vol. 10, no. 4, pp. 523–532, Apr. 2002.
- [24] W. Li, X. G. Chang, J. Farrell, and F. M.Wahl, "Design of an enhanced hybrid fuzzy P+ID controller for a mechanical manipulator," IEEE Trans. Syst., Man, Cybern. B, Cybern., vol. 31, no. 6, pp. 938–945, Dec. 2001.
- [25] Y. L. Sun and M. J. Er, "Hybrid fuzzy control of robotics systems," IEEE Trans. Fuzzy Syst., vol. 12, no. 6, pp. 755–765, Dec. 2004.
- [26] J. Park and W. K. Chung, "Analytic nonlinear  $H_{\infty}$  inverse-optimal control for euler-lagrange system," IEEE Trans. Robot. Autom., vol.16, no. 6, pp. 847–854, Dec. 2000.
- [27] Y. Choi and W. K. Chung, "Performance limitation and autotuning of inverse optimal PID controller for lagrangian systems," ASME J. Dynam. Syst. Meas. Control, vol. 127, no. 2, pp. 240–248, 2005.
- [28] J. Park and W. Chung, "Design of a robust  $H_{\infty}$  PID control for industrial manipulators," ASME J. Dynam. Syst. Meas. Control, vol. 122, no. 4, pp. 803–812, 2000.

[29] T. C. Hsia, "A new technique for robust control of servo systems," IEEE Trans. Ind. Electron., vol. 36, no. 1, pp. 1-7, 1989.

[30] K.J. Astrom and T. Hagglund, PID controllers (Second edition), ISA,N. C., 1995.

## 요 약 문

### 시간 지연을 이용한 추정과 비선형 댐핑을 이용하는 백스테핑

#### 컨트롤을 기반으로 하는 강인 PID 컨트롤의 디자인 방법

논문은 시간지연을 이용한 추정(TDE)과 비선형 댐핑(nonlinear damping)을 이용하는 백스테핑 컨트롤(backstepping control)을 기반으로 하는 강인 PID 컨트롤의 디자인 방법을 제안한다.

PID 제어기는 귀환 제어기로서 많은 산업 컨트롤 시스템 분야에서 널리 사용되며 비례, 미분, 적분 이득으로 구성되어 있다. PID 제어기는 우리가 원하는 입력과 시스템 출력 사이의 오차를 이용하고, 시스템을 제어하기 위해 요구되는 이득 값을 선택해서 원하는 입력 값을 시스템의 출력 값이 되도록 한다.

PID 제어기의 이득 값은 시스템의 성능과 관련하여 물리적인 의미를 가지고 있으며, 이 이득 값들이 잘 조절 되었을 때, 과도응답과 정상상태 오차가 동시에 잘 개선됨으로써 만족할만한 성능을 가지게 된다. 만족할만한 성능을 가지는 PID 제어기를 얻기 위해서 이득 값을 조절하는 것에 대한 많은 과거 연구가 이루어 졌다. 그러나 이들 연구는 대부분 선형 플랜트에서 진행 되었으며 실제로 비선형 플랜트에서 이득 값을 선택하는 것은 어렵다. 비선형 플랜트에서도 PID 제어기를 구현하기 위한 많은 연구가 있지만 이들 연구에서 제안된 방법은 어렵고 이론적으로 복잡하며 때로는 안정성 분석에 대한 문제가 야기 된다. 그 결과, PID 이득 값은 체험적인 방법을 통하여 조절되는 것이 일반적이다.

이러한 문제에 대해, 디지털 시스템의 관점으로부터 비선형 플랜트에 대한 강건 PID 제어기의

이득 값을 선정하는 것에 대한 체계적인 방법이 제안되었다. 이 연구에서는, 플랜트의 모델을 정확히 알지 못함에도 불구하고, 플랜트가 이차 제어기 표준형으로 나타난다고 고려될 때, 제어기가 이산 시간 영역에서 실행된다면, 시간 지연을 이용한 제어기(TDC)를 이용해서 강건한 PID 제어기의 이득 값을 결정하는 방법이 제시되었다. 시간지연을 이용한 제어기와 PID 제어기의 등가 관계를 이용해서 PID 제어기의 이득 값이 결정 되었다.

시간지연을 이용한 제어기는 시스템의 비선형과 불확실성을 시간지연을 이용해 추정하는 간단하고 효율적인 제어기이다. 현재 시스템의 상태를 추정하기 위하여 한 단계 과거 시점의 시간에서 생성된 시스템 변수들의 정보를 이용하는 방법이다. 이 제어기는 시스템의 정확한 정보를 필요로 하지 않는 이점을 가지는 반면, 강한 비선형으로 인해 야기되는 시간 지연 추정에 의해 생기는 오차(TDE error)를 가진다는 단점 있다. 이 오차에 의해 시스템의 성능과 안정성이 저하된다.

문제는 강한 비선형을 가진 시스템에서 TDC 를 사용하여 PID 제어기의 이득 값을 구할 때, PID 제어기는 시간지연을 이용한 제어기(TDC)와 같은 특징을 가지게 되므로 시스템의 안정성과 성능이 보장되지 못하게 된다. 이러한 이유 때문에 이 연구에서는 시간지연 추정에 의해 생기는 오차(TDE error)를 상쇄시키고 제어기의 생성과정에서 안정성을 보장하는 시간 지연을 이용한 추정(TDE)과 비선형 댐핑(nonlinear damping)을 포함하는 백스테핑 제어기(backstepping control)를 이용한다. 이 제어기를 이용하여 우리는 등가의 PID 제어기를 구현하였고, 백스테핑 방법을 기반으로 하는 제어기의 파라미터를 이용하여 등가 PID 제어기의 이득 값들을 구성하였다. 따라서 PID 제어기는 강한 비선형에도 안정성이 보장되는 우수한 특징을 가지게

되었으며, 비선형 시스템에서 PID 제어기의 이득 값을 조절하는 것에 대한 문제를 해결하게 되었다. 또한, 제안된 PID 제어기는 비선형 댐핑에 의해서 가변 이득을 가지게 되며, 이는 시스템의 파라미터 변화와 외란에 강하다는 장점을 가지게 된다.

따라서 이 논문에서는 시간 지연 추정과 비선형 감쇠를 이용하는 백스테핑 제어기를 간단히 언급하고, 이를 이용해서 등가의 PID 제어기를 구성하고 제어기의 이득 값들을 구할 것이다. 또한, 제안된 PID 제어기에서 이득 값들의 크기와 형태를 분석할 것이며, 추가적으로 시간지연을 이용한 제어기(TDC)를 이용한 PID 제어기와 이 논문에서 제안된 PID 제어기를 비교할 것이다. 이러한 내용들은 모의실험과 실험을 통하여 증명 된다.

핵심어: PID 제어기, 시간 지연을 이용한 추정(TDE), 비선형 댐핑(Nonlinear damping), 백스테핑 (backstepping) 제어



## 감사의 글

논문을 이렇게 마무리하면서 어려운 환경 속에서도 부족한 저를 항상 붙잡아 주시고 더 큰 세상을 바라볼 수 있도록 학업을 꾸준히 해나갈 수 있도록 해주신 하나님 아버지께 감사 드립니다.

학문을 배움에 있어서 스승님으로써 때로는 부모님과 같이 저를 이끌어 주신 지도교수님이신 장평훈 교수님께 감사 드립니다. 교수님을 통해서 학문을 어떻게 해나가야 한다는 것과, 객관적이고 냉철하게 그리고 논리적으로 판단하는 능력을 키울 수 있었습니다. 부족한 저를 많이 깨닫도록 해주시고 이끌어 주셔서 감사합니다. 그리고 홍재성 교수님, 최홍수 교수님, 문상준 교수님 모두 감사 드립니다. 지도학생이 아님에도 불구하고 많은 관심과 격려에 많은 힘을 얻을 수 있었습니다. 모든 교수님들께서 주신 은혜 잊지 않고 살겠습니다.

로봇공학 1 기 입학생들, 병식이 형, 재영이 형, 상원이, 진호, 희진 모두 고맙습니다. 다른 학과 학생들에 비해서 비록 소규모의 그룹이었지만, 그 만큼 더 가까울 수 있었고, 친해 질 수 있었습니다. 작년 초에 같이 건물 뒤에서 족구 하던 것이 엇그제 같은데 벌써 졸업을 앞두고 있다니 시간이 빠른 것 같습니다. 힘들고 지친 순간에 도움을 주었던 병식이 형, 재영이 형 고맙습니다. 모두들 원하는 일이 다 이루시고 졸업 후 에도 가끔 모여 술 한잔 같이 기울일 수 있었으면 좋겠습니다.

연구실 선배님들 진오 형, 경빈이 형, Yi 형, 그리고 진호, 승희, 상래, 지혁, widya 모두 감사합니다. 부족한 후배들 때문에 고생하신 진오 형, 이탈리아에서 연구 잘 되시길 바랍니다. 연구하는데 많은 도움 주신 경빈이 형, Yi 형 감사합니다. 형들 덕분에 논문 잘 마무리 할 수 있었습니다. 그리고 동기 및 후배님들, 많은 도움 주지 못해 미안합니다.

연구 열심히 하고 초창기인 만큼 열정적으로 잘 해나가길 믿습니다. 모두들 더 성숙한 모습으로 미래에도 좋은 인연 잘 이어갔으면 합니다.

친구 및 가까운 지인 분들께도 감사 드립니다. 나의 오랜 벗 현명이, 재혁이, 군대 동기 문연이, 오래된 친구 같은 정만이, 나보다 더 시커먼 도엽이, 동네주민 동혁이 형, 같이 술 먹어주는 상우 형, 경현이 형, 돈 잘 버는 민균이 형, 내 말 잘 따라주는 좋은 동생들 종구, 창동, 경훈, 지호, 정웅, 앞으로도 좋은 인연 함께하고 하는 일이 모두 잘 되기를 바랍니다.

마지막으로 가족들에게도 감사 합니다. 가정이 어렵고 힘든 순간에도 믿음 안에서 동생과 저를 잘 보살펴주시고 항상 저를 믿어주신 어머니 고맙습니다. 그리고 집안의 막내로써의 역할에 충실한 착한 내 동생 준우야 고맙다. 주님의 은총 안에서 우리 가정이 늘 화목하고 행복했으면 합니다.

이 외에도 석사과정을 하면서 많은 이들의 도움을 알게 모르게 받았습니다. 다시 한번 모두에게 감사 드립니다. 이 논문은 하나의 논문일 뿐입니다. 하지만, 동시에 저의 인생에 있어서는 한 단계 더 성장할 수 있는 계기가 되었습니다. 미래에는 오늘보다 더 발전된 제가 있기를 바라며, 여러 방면에서 많은 도움을 주신 분들과 하나님께 이 영광을 돌립니다.

## **Curriculum Vitae**

**Name** : Junyoung Lee

**Birth Date** : Feb 3, 1985

## **Education**

2011.3 – 2013. 2: Master of Robotics Engineering, Daegu Gyeongbuk Institute of Science and Technology (DGIST), Korea

2003.3 – 2011. 2: Bachelor of Electronics Engineering, Keimyung University, Korea.